January 2019

Insights Into Nucleic Acid-Platinum(ii) Compound Interactions And Structural Impacts

Supuni Duneeshya Kamal Thalalla Gamage
Wayne State University, supunid6@gmail.com

INSIGHTS INTO NUCLEIC ACID-PLATINUM(II) COMPOUND INTERACTIONS AND STRUCTURAL IMPACTS

by

SUPUNI THALALLA GAMAGE

DISSERTATION

Submitted to the Graduate School

of Wayne State University,

Detroit, Michigan

in partial fulfillment of the requirements

for the degree of

DOCTOR OF PHILOSOPHY

2019

MAJOR: CHEMISTRY (Biochemistry)

Approved By:

_____

Advisor Date

_____

_____

_____

DEDICATION

To my parents, K. R. Hewapathirana, T. G. Kamal Ashoka and my husband Amila Maithriwardhane for their constant support, unconditional love, and blessings.

ACKNOWLEDGEMENTS

This thesis would have not been possible without the help of so many wonderful people whom I have been very fortunate to be around with. First, I would like to thank my doctoral advisor, Dr. Christine Chow for giving me the opportunity to work in her lab. The encouragement and support you provided during tough times in research is truly appreciable. I am thankful for providing me the space to grow into the person I am today: a scholar, a scientist, and a mentor. Thank you for guiding me to choose a career path that I am excited to follow. Next, I want to thank my committee members, Dr. Young-Hoon Ahn, Dr. Jennifer Stockdill, and Dr. Stephan Patrick for their valuable time and insightful comments in the committee meetings. I'm thankful to Dr. Ahn for allowing me to use his lab equipment to do my research.

The time in the lab would have been uneventful without the amazing colleagues I had the opportunity to work with. I thank previous Chow lab members, Dr. Gayani Dedduwa-Mudalige, Dr. Jun Jiang, Dr. Xun Bao, Dr. Danielle Dremann, Dr. Hyosuk Seo, and Dr. Nisansala Muthunayake for teaching me lab techniques and helping me during these years in numerous ways. I also want to thank the current Chow lab members, Prabuddha Madubashitha, Bett Kimutai, Evan Jones, Rabiul Islam, and Alan Mlotkowski. Specifically, I would like to thank Bett Kimutai and Dr. Nisansala Muthunayake for collaborating with me on projects and having many fruitful discussions. I consider myself lucky to be among such talented scientists who were great co-workers and friends. Many thanks to all the undergrads, Nathaniel Hardin, Brigid Jacob, Hassan Ramadan, and Titiana Gorges, with whom I had the opportunity to work with. I thank Dr. Amr Sonousi from Crich lab for synthesizing the carbohydrate-linked cisplatin analog for

my studies. I thank Fidelis Ndombera from Ahn lab for for the initial MTT studies and training me. Many thanks to all the past and present Ahn lab members and Bhagwat lab members for helping me in various ways and also for their friendship.

For the past year and a half, I worked as a staff scientist at the Lumigen instrument facility (LIC) where I got to expand my skills as an analytical chemist. I would like to convey my heartfelt gratitude to Dr. Judy Westrick for giving me the opportunity to work at the LIC. Dr. Westrick has been extremely understanding, supportive, and encouraging. I would also like to thank Dr. Johnna Birbeck for training me on mass spec instrumentation and supporting me with my projects. I am grateful for your friendship and it was a pleasure working with you. I would also like to thank all the LIC staff members for their friendship and support throughout my time working there.

I wish to express my gratitude to the Wayne State University and the Department of Chemistry, for giving me the opportunity to pursue a Ph.D. I appreciate the funding from the Thomas C. Rumble fellowship. There were many departmental and graduate school staff members who helped me with the administrative work. I thank all of them for their time. I warmheartedly remember all the professors and friends at my undergraduate institute, University of Colombo, Sri Lanka, where I lay the foundation to the Ph.D. journey. I thank all of my schoolteachers at Gothami Girls College and Sanghamitta Girls College, Colombo whose efforts have inspired me to follow my passion in science and research.

Finally, I would like to convey my gratitude to my family and friends. I would not be here today, if it is not for the dedication and sacrifices made by my parents, K.R. Hewapathirana and T. G. Kamal Ashoka. They took great efforts to provide me with the

best education in school and in life. I would like to thank my loving sister, Ama Shermila for her endless love and encouragement. Thank you for being my best friend growing up and sharing all the wonderful memories. Many thanks to my parents-in-law, Indra Kumari and H. M. G. Maithriwardhane for their love, continuous support, and understanding. You are the best parents-in-law a person could have and I am grateful for that. I was surrounded by a lovely group of people in Sri Lanka and in the USA who have become my lifelong friends. Specially, I want to thank my best friend Nadee Buddhiwickrama for always encouraging me to do my best. It is not easy to find a good friend who is always there for you and I am grateful to have you. None of this would be possible without the support from my loving husband, Amila Maithriwardhane. He is the reason behind all of my achievements and thank you for being so patient with me and staying by my side through thick and thin. Finally, I would like to acknowledge my son, Theja Thenandalu Mudalige for the joy he brings to my life. You give me strength to achieve my dreams.

TABLE OF CONTENTS

LIST OF TABLES

LIST OF FIGURES

LIST OF SCHEMES

LIST OF ABBREVIATIONS

DNA	deoxyribonucleic acid
RNA	ribonucleic acid
rRNA	ribosomal RNA
tRNA	transfer RNA
mRNA	messenger RNA
PTC	peptidyl transferase center
NER	nucleotide excision repair
TCR	transcription-coupled repair
GGR	global genomic repair
MMR	mismatch repair
BER	base excision repair
CSA/CSB	cockayne syndrome proteins
HR23B	UV excision repair protein RAD23 homolog B
XP	*Xeroderma pigmentosum* proteins (XPA, XPB, XPC, XPD, XPF, XPE, XPG)
RPA	replication protein A
TFIIH	transcription factor II H
ERCC1	excision repair cross-complementation group 1, a DNA excision repair protein
PCNA	proliferating cell nuclear antigen
RFC	replication factor C
ICP-MS	inductively coupled plasma mass spectrometry
HPLC	high performance liquid chromatography

LC-MS	liquid chromatography-mass spectrometry
NMR	nuclear magnetic resonance
PAGE	polyacrylamide gel electrophoresis
MALDI	matrix-assisted laser desorption ionization
EMSA	electrophoretic mobility shift assay
DMS	dimthylsulfate
DMSO	dimethylsulfoxide
DEPC	diethylpyrocarbonate
CMCT	1-cyclohexyl-(2-morpholinoethyl)carbodiimide metho-p-toluene sulfonate
NMIA	*N*-methylisatoic anhydride
MTT	3-(4,5-dimethylthiazol-2-yl)-2,5- diphenyltetrazolium bromide
MTS	3-(4,5-dimethylthiazol-2-yl)-5-(3-carboxymethoxyphenyl)-2-(4-sulfophenyl)-2H-tetrazolium
XTT	2,3-bis-(2-methoxy-4-nitro-5-sulfophenyl)-2H-tetrazolium-5-carboxanilide
WST	2-(2-methoxy-4-nitrophenyl)-3-(4-nitrophenyl)-5-(2,4-disulfophenyl)-2H-tetrazolium
3-HPA	3-hydroxypicolinic acid
GSH	glutathione
MRP2	multidrug resistance-associated protein 2
MVP/LRP	major vault/lung resistance-related protein
HSAB	hard-soft acid-base principle
CBDCA	1,1-cyclobutanedicarboxylato
DACH	*R,R*-diamminocyclohexane
OCT	organic cation transporters

GLUT	glucose transporters
FBS	fetal bovine serum
IC_{50}	half maximal inhibitory concentration
Ψ	pseudouridine

CHAPTER 1

INTRODUCTION

1.1 Abstract

cis-Diamminedichloridoplatinum(II), or cisplatin (**1**), is a widely used platinum-containing anticancer drug.[1] Cisplatin is only effective against certain cancers, including testicular and ovarian cancer.[2] Although cisplatin in its mono- or bis-aquated form can coordinate to RNA, enzymes, and other sulfur-containing proteins, its anticancer activity is attributed to DNA binding.[3] Despite its effectiveness against certain cancers, clinical usage of cisplatin is restricted by a number of dose-dependent side effects such as nephrotoxicity and neurotoxicity.[4] Additionally, certain cancers showed intrinsic or developed resistance to cisplatin therapy.[5,6] Over the past few decades, scientists have been trying to develop new platinum-based anticancer drugs that can overcome these problems. This chapter summarizes the mechanism of action, binding targets, and drawbacks of cisplatin and cisplatin analogs.

1.2 Cisplatin in cancer therapy

1.2.1 Discovery of cisplatin

Cisplatin (*cis*-diamminedichloridoplatinum(II)) is one of the most commonly used anticancer drugs in the world with a high success rate.[7] The serendipitous discovery of the antitumor activity of cisplatin in the 1960s opened up a field of metallodrug development for cancer treatment. Dr. Barnett Rosenberg, a physicist at Michigan State University, was interested in studying the impact of electric currents on cellular division in bacteria.[8] He carried out experiments using an apparatus with platinum electrodes immersed in ammonium chloride buffer, and he monitored *Escherichia coli* (*E. coli*) cell growth. After a period of time, *E. coli* cells were viewed under a microscope and found to have a long and filamentous shape instead of their normal length. This shape difference was found to be due to inhibition of cellular division.[8] With further experiments, the compound that causes the inhibition was found to be a platinum(IV) complex with the formula $[PtCl_4(NH_3)_2]$ in its *cis* form.[9] Because of the observed antiproliferative properties, it was of interest to test platinum compounds for their anticancer activity. Rosenberg and coworkers used the platinum(IV) complex *cis*-$[PtCl_4(NH_3)_2]$ and platinum(II) complex *cis*-$[PtCl_2(NH_3)_2]$ against Sarcoma 180 tumors in mice.[10] The *cis* form of the platinum(II) complex cisplatin (*cis*-$[PtCl_2(NH_3)_2]$) was found to be the active isomer; whereas, the *trans* complex was inactive **(Figure 1.1)**. The treatment of tumors was a success, with mice showing no signs of cancer after 6 months.[10] Following that result, cisplatin entered clinical trials and was approved for clinical usage in 1978.[11] Since then, it is been used to treat testicular cancer with over a 90% cure rate.[1]

Furthermore, cisplatin has been widely used to treat several other cancer types, including ovarian, cervical, head and neck, and non-small-cell lung cancer.[1]

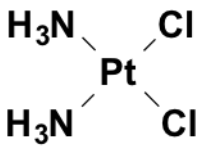

(1)

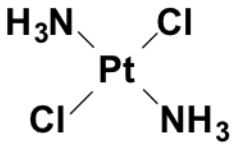

(2)

Figure 1.1. Structures of cisplatin (1) and transplatin (2). Both compounds have square planar geometry.

1.2.2 The structural components of cisplatin

The structure of cisplatin (**1**) (**Figure 1.1**) was first discovered by an Italian doctor, Michel Peyrone, in 1845.[12] It has a square planar geometry with two chlorido ligands and two ammine ligands coordinated to the platinum metal center in the *cis* form. The transition metal platinum is in the +2 oxidation state, giving an overall charge of zero to the complex. Based on the mechanism of action, the chlorido ligands are displaced by water (aqua ligand) and the ammine ligands remain coordinated to the platinum center. Therefore, chlorido ligands are referred to as the "leaving groups", whereas the ammine ligands are referred to as the "carrier ligands" or "non-leaving groups." As shown in **Figure 1.1**, two isomers exist, referred to as cisplatin (**1**) and transplatin (**2**).

1.2.3 Mechanism of action of cisplatin

The anticancer activity of cisplatin is generally believed to be derived from its interactions with DNA.[12] When cisplatin is administered intravenously, it encounters a relatively high Cl^- concentration (around 100 mM) in the blood. The higher Cl^- concentration (compared to cytoplasm) prevents displacement of the chlorido ligand on **1** by water, and the complex remains in the neutral state. Cisplatin can enter cells *via*

passive diffusion or *via* active transport using Cu-transporting proteins.[13,14] Inside the cell, the Cl^- concentration is lower (4-20 mM) than outside, causing the cisplatin to undergo aquation and yielding a positively charged species, $[PtCl(H_2O)(NH_3)_2]^+$.[15] The aquation is the rate-determining step of cisplatin coordination to DNA with a rate of 10.2 $\times 10^{-5}$ s^{-1}(**Figure 1.2**).[16]

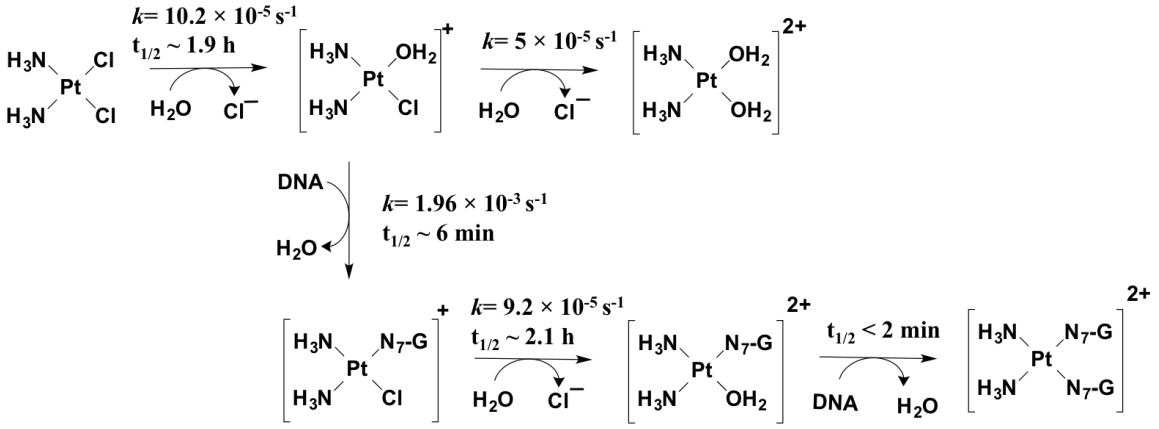

Figure 1.2. Ligand exchange equilibria for cisplatin. The chlorido ligands of cisplatin are displaced by one or two aqua ligands to produce cationic mono- and diaqua complexes, respectively. The monoaqua complex readily coordinates to the N7 position of a guanine base in DNA. A bifunctional DNA adduct is formed after the second chlorido ligand is replaced with an aqua ligand. The rates shown are from the literature.[16]

Monoaquation leads to generation of the charged reactive species of cisplatin (**Figure 1.3, 3**) and also prevents the molecule from diffusing out of the cell.[17] Electrostatic interactions favor attraction of the positively charged **3** to the negatively charged nucleic acid backbone. Upon interaction near a purine base, the aqua ligand is displaced from **3** and cross-linking to the nucleic acid occurs.[3] After subsequent displacement of the second chlorido ligand by a neighboring purine base, a stable adduct is generated.[15] Cisplatin preferentially coordinates to the N7 position of deoxyguanosine (dG) residues in DNA and makes 1,2-intrastrand d(GpG) adducts (**Figure 1.3**).[18] The compound is also known to make 1,2-intrastrand d(ApG) (dA is deoxyadenosine), 1,3-

intrastrand d(GpXpG), in which X is an intervening deoxynucleotide, and interstrand adducts with DNA.[3] The adduct formation distorts the DNA structure because of the structural constraints of the Pt atom. In particular, the 1,2-intrastrand adducts unwind and bend the DNA towards the major groove, exposing the minor groove.[1] Proteins, such as those belonging to the high-mobility group (HMG) class, repair enzymes, and transcription factors, preferentially bind to the exposed shallow and wide minor groove and initiate DNA repair processes or signaling cascades for apoptosis.[19,20]

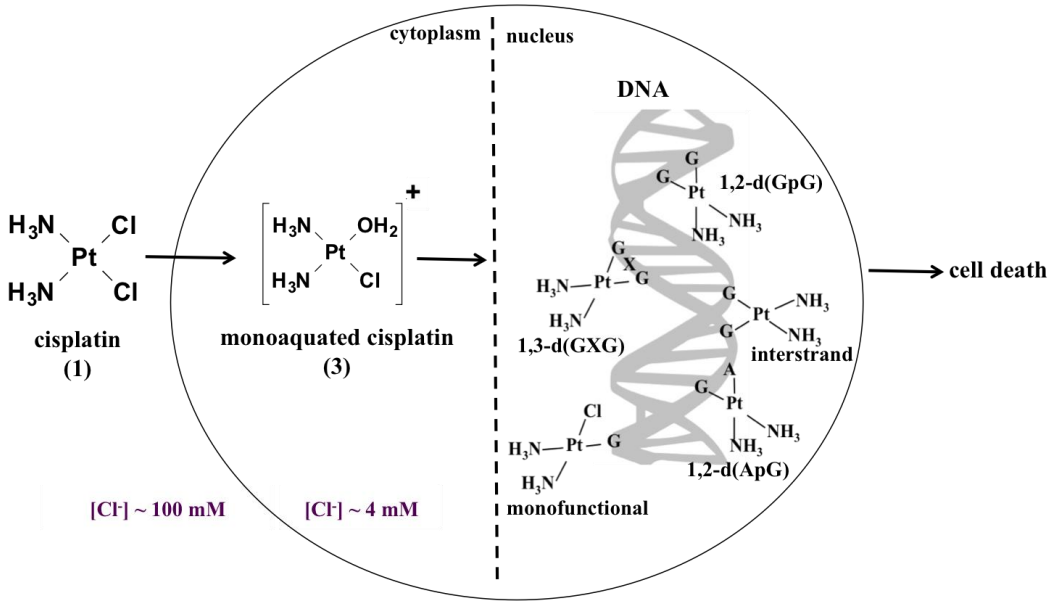

Figure 1.3. A general pathway of cisplatin mechanism of action.[17] Cisplatin (**1**) undergoes aquation and produces a positively charged species (**3**) inside the cell. Compound **3** coordinates to DNA and forms different adducts as shown. The adducts distort the DNA structure and initiate signaling cascades for cell death.

There is evidence to suggest that cisplatin reacts with many other cellular components in the cell other than DNA.[17] RNA, proteins, and other small molecules, particularly those that contain thiol groups such as glutathione, are some of the cellular targets of cisplatin (more details will be given in **Sections 1.3** and **1.4.2**). The nature of these reactions and their contributions toward the overall anticancer activity of cisplatin

are not fully understood due to the complexity of the intracellular environment and the lack of methodologies to investigate these processes.[17] Experiments are often carried out under *in vitro* conditions using activated cisplatin (aquated) and conditions that mimic the cellular environment to understand cisplatin accumulation on cellular components and how the resulting adducts affect normal cellular functions.[15]

1.3 DNA as a target of cisplatin

Numerous studies have focused on DNA as the main biological target of cisplatin that triggers the anticancer activity.[12] There is extensive evidence that points to DNA as the primary target of cisplatin. Bacteria treated with cisplatin have shown phenotypic characteristics that are similar to the effects caused by DNA-damaging agents.[21] Moreover, DNA repair-deficient cells have shown more sensitivity towards cisplatin, strongly supporting DNA as the major cellular target.[22]

Cisplatin enters the cell, undergoes mono- and/or bisaquation, and forms the activated species such as **3**. These species need to cross into the nucleus in order to react with DNA. Once inside the nucleus, due to the high nucleotide concentration, aquated cisplatin readily reacts with DNA. Isolated and purified DNA from leukocytes of cancer patients following cisplatin treatment showed the presence of approximately 65% of 1,2-d(GpG), 25% of 1,2-d(ApG), and 5-10% of 1,3-d(GpXpG) intrastrand cross-links.[19,23] Monofunctional adducts and interstrand adducts were also present in a smaller percentage. A significant structural effect on DNA was observed with the intrastrand adducts. The major 1,2-intrastrand cross-links unwind the DNA duplex and cause bending towards the major groove to generate a widened and shallow minor groove (**Figure 1.4a**).[24] The *cis*-GG bend angle caused by **3** coordination (1,2-adduct) has been

quantified to be 32° using a gel electrophoresis mobility shift assay, and the angle for c*is*-AG adducts is 34°.[24] Another study reported bending of 33-35° and an unwinding angle of 15-20° in a DNA double helix.[25] The interstrand cross-links also cause detrimental effects to the DNA structure by bending the helix towards the minor groove as shown in the X-ray crystal structure of a short DNA oligomer. (**Figure 1.4c**).[26] Overall, cisplatin binding impacts the duplex DNA structure to a level that significantly affects replication, transcription, and repair.[17] A variety of cellular proteins recognize and bind to the platinated DNA.[17] Depending on the recognition selectivity and processing of the platinum adducts by cellular proteins, cytotoxicity of cisplatin would be mediated.

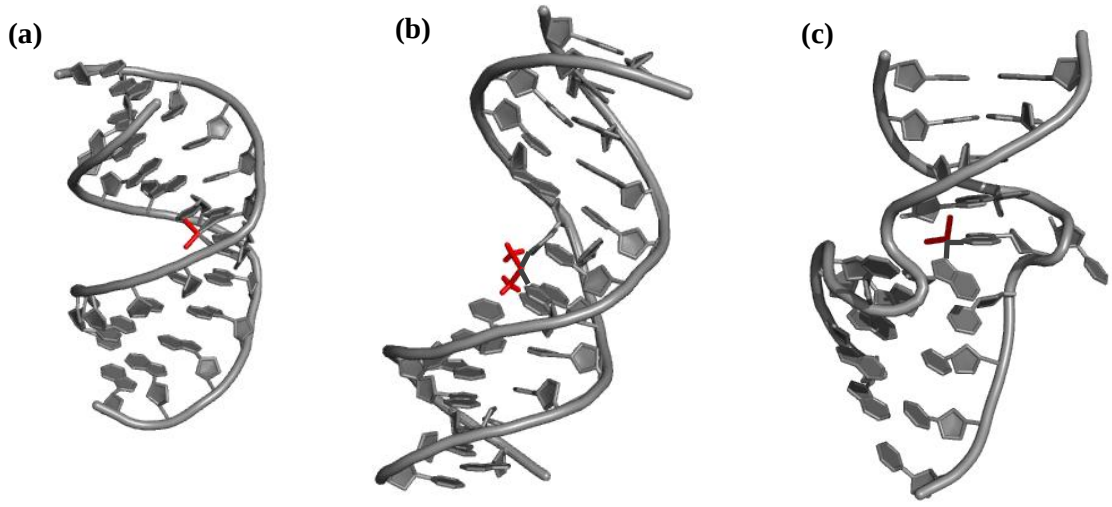

Figure 1.4. Different adducts of cisplatin on double-stranded DNA. A cisplatin 1,2-d(GpG) intrastrand cross-link on an 12-mer DNA (PDB ID: 1AIO) (a) is shown in comparison to a 1,3-d(GpTpG) intrastrand cross-link (PDB ID: 1DA4) (b), and an interstrand cross-link (PDB ID: 1A2E) (c). The DNA sequences (grey) for the 1,2-d(GpG) and 1,3-d(GpTpG) intrastrand adducts are d(CCTCTGGTCTCC) and d(CTCTAGTGCTCAC), respectively, with their complementary sequences. The interstrand cross-link is shown at the DNA duplex with the sequence (CCTCG*CTCTC)•d(GAGAG*CGAGG), where the adduct formation sites are indicated by asterisks. The C residues that are complementary to the Gs shown in asterisks are exposed to solvent in the crystal structure 1A2E. The cisplatin adduct is shown in red.

Inhibition of DNA replication by cisplatin was discovered by using partially purified human DNA polymerase α and β with template DNA.[27] Further experiments showed inhibition of activity of DNA polymerase I and III, as well as T4 DNA polymerase, caused by cisplatin adducts.[28] Both DNA and RNA polymerases are strongly blocked by the bifunctional adducts compared to monofunctional adducts. Inhibition of transcription by cisplatin adducts was shown in *in vitro* studies using wheat germ RNA polymerase II, *E. coli* T7, and SP6 RNA polymerases.[29,30] Since RNA polymerase II is an abundant protein in the cell and the main enzyme used to produce mRNA, it has been studied extensively with regard to cisplatin damage.[30] *In vitro* experiments done using purified RNA polymerase II, transcription factors, and DNA templates have shown that the elongation is blocked by cisplatin 1,2-(GpG) and 1,3-(GpTpG) intrastrand cross-links (**Figures 1.4a** and **1.4b**).[17] In addition, RNA polymerase II stalling at the platination site has been shown to act as a signal to initiate transcription-coupled repair or programmed cell death.[31]

In eukaryotes, DNA is associated with histone proteins and compacted into chromatin.[32] Cisplatin has shown preferred binding to the open form of chromatin.[33] Cisplatin binding also blocks transcription factor binding and chromatin remodeling,[34] as well as inducing phosphorylation and hyperacetylation in histone H3 and H4 proteins in HeLa cells, respectively.[35] Furthermore, a recent structural analysis of a nucleosome containing a site-specific 1,3-(GXG) intrastrand adduct showed that the adduct changes the rotational setting of the DNA wrapped around the histone proteins.[36]

Cisplatin adducts on DNA can be removed by different repair pathways. The primary process for cisplatin-damaged DNA repair is the nucleotide excision repair

pathway (NER).[17] Transcription-coupled repair (TCR) and global genomic repair (GGR) are the two key initial mechanisms of NER (**Figure 1.5**). *Xeroderma pigmentosum* proteins (XPA, XPB, XPC, XPD, XPF, XPE, and XPG) are involved in these mechanisms. As mentioned earlier, the signal to initiate TCR is RNA polymerase II stalling at the platination site and interactions with cockayne syndrome proteins, CSA and CSB.[37] For GGR, XPC-HR23B is the damage recognition protein.[17] After the initial recognition, both TCR and GGR follow the same path to repair the DNA. First, proteins XPA, replication protein A (RPA), and transcription factor TFIIH assemble on the DNA in a cooperative fashion.[17] XPB and XPD helicases, which are components of TFIIH, are responsible for DNA unwinding, and XPG binds to the unwound DNA. This step is followed by XPF-ERCC1 binding and removal of oligonucleotides containing the platinum adducts by a dual incision. RPA then recruits DNA resynthesis factors to fill the gap. This pathway of DNA repair has been well studied, and supported by the fact that *Xeroderma pigmentosum* cell lines lacking components of NER are more sensitive to cisplatin than normal cells.[38]

Overall, the significant effect and outcomes of cisplatin binding to DNA on replication, transcription, and repair processes are evidence to confirm that DNA is a major target of cisplatin. However, there are still many problems associated with the drug, which will be discussed later in **Section 1.4**.

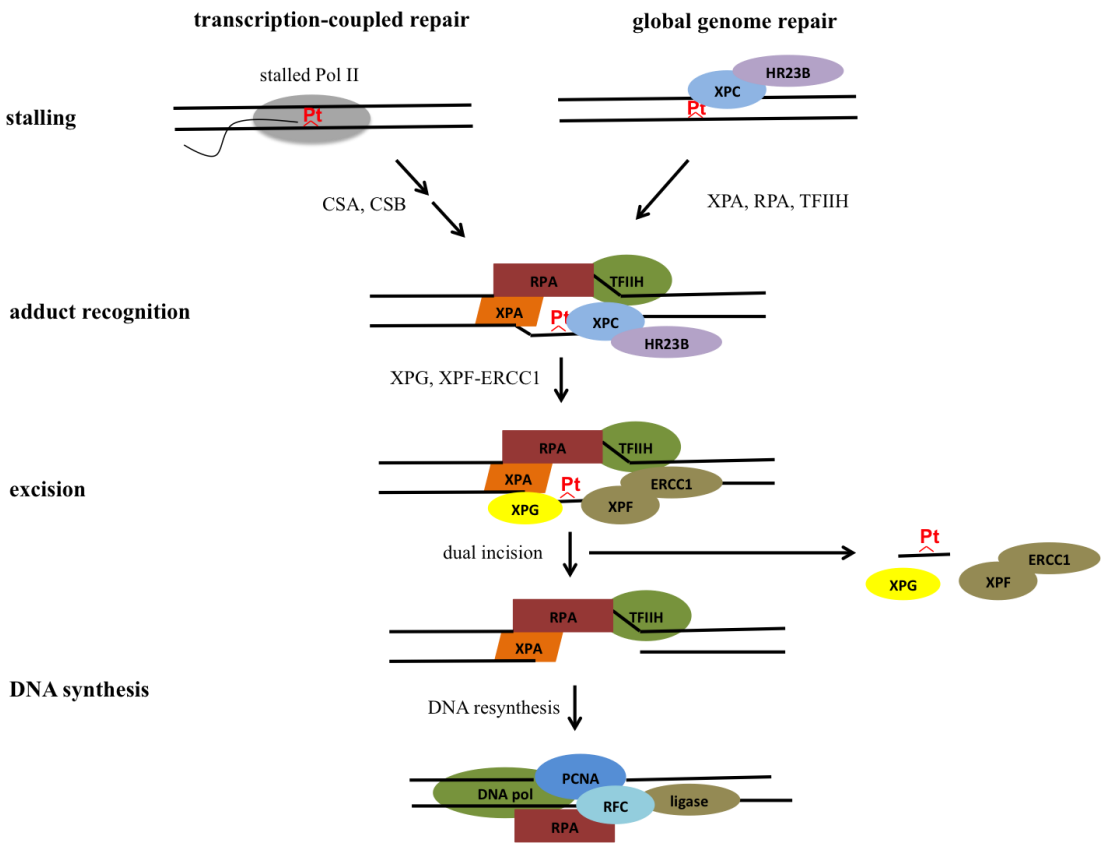

Figure 1.5. Nucleotide excision repair pathway for removing cisplatin lesions. The proteins involved in the transcription-coupled repair pathway or global genome repair pathway initially recognize the Pt lesion (red), which is then removed by the NER pathway. The Pt adduct is removed along with a flanking DNA region that is 24 to 32 nucleotides in length.

1.4 RNA as a target of cisplatin

The idea of cisplatin binding to DNA as the main driver for cancer cell apoptosis has been challenged by a variety of studies that show cisplatin binding to RNA, proteins, peptides, and lipids.[39-41] These studies point to cisplatin toxicity originating from multiple sources rather than solely from binding to DNA. Among these, RNA is a poorly characterized target considering its important regulatory roles in the cell. Particularly considering cisplatin coordination modes with purine bases, RNA could also be a target, possibly leading to some of the toxicity caused by the drug. Various regulatory roles of RNA suggest that its platination could have negative impacts on biological systems.

Experiments have been done to characterize cisplatin binding sites on RNA and determine rates of reactions with RNA compared to DNA. For example, cisplatin binding sites in ribosomal RNA hairpins were analyzed using radioactive labeling and enzymatic footprinting.[42,43] The binding preference of cisplatin for certain RNA secondary structures was analyzed by the Elmroth group using full-length $tRNA^{Ala}$ and hairpin models of its acceptor stem and anticodon loop, and the results showed that platinum coordination to RNA is highly sequence and structure dependent.[44,45] In a recent report by the DeRose lab, RNA-Pt adducts in cisplatin-treated *Saccharomyces cerevisiae* were quantified by using inductively coupled plasma mass spectrometry (ICP-MS).[46] These results suggested that cisplatin accumulates faster and is retained more on RNA compared to DNA. These studies also showed that cisplatin could interfere with several enzymatic activities, including exonuclease, endonuclease, and reverse transcriptase, even with a single adduct on the RNA strand. A number of studies focused on evaluating the reaction kinetics of cisplatin on DNA and RNA.[47-50] In one of those studies, cisplatin and its derivatives were reacted with RNA and DNA hairpins of similar sequence, namely r(CGCGUUGUUCGCG) and d(CGCGTTGTTCGCG), and found to have higher platination rates with the RNA hairpin.[51]

Very few crystal structures of platinum compounds bound RNA were available up to 2016. A low-resolution structure of yeast $tRNA^{Phe}$ showed two major cisplatin binding sites.[52] The first nearly atomic resolution crystal structure of cisplatin bound to the *Thermus thermophilus* 70S ribosome was reported in 2016.[40] This 2.6 Å-resolution X-ray structure reported nine cisplatin binding sites on the ribosome out of 2200 potential modification sites (**Figure 1.6**). Among these sites, two were found on the 30S small

subunit, six were on the 50S large subunit, and one was bound to the L9 ribosomal protein. When comparing the cisplatin coordination sites, three were located at the N7 position of adenosine nucleotides (A790 of 16S rRNA; A1848 and A2531 of the 23S rRNA), and five were at the N7 atoms of guanosines (G1300 of 16S rRNA; and G27, G425, G1606, and G2220-2221 of 23S rRNA). These crystal structure data shed light on our understanding of the RNA-cisplatin interactions and patterns, such as base preference and site of modification.

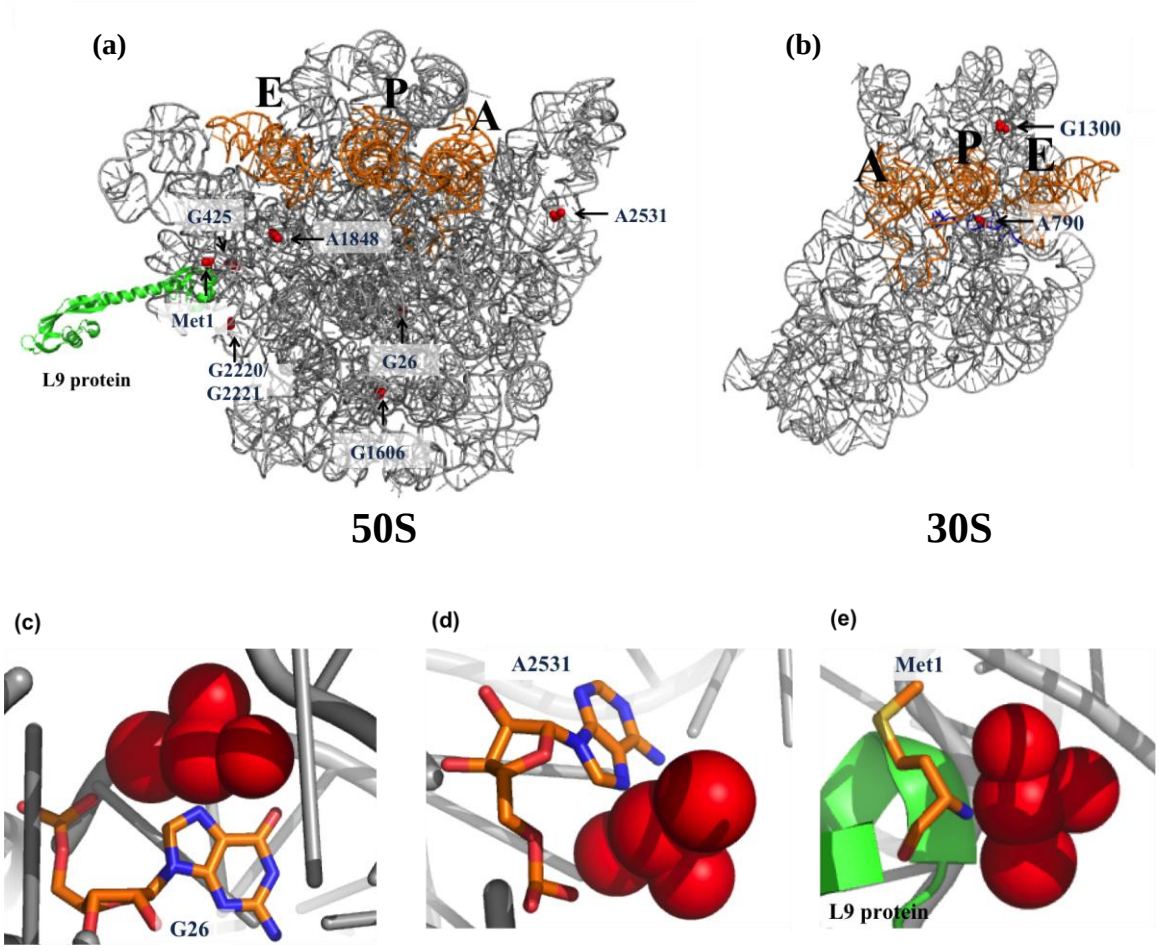

Figure 1.6. The crystal structure of *Thermus thermophilus* ribosomal subunits with cisplatin binding sites (PDB ID: 5J4B).[40] (a) The 50S subunit is shown with six cisplatin adducts (red) on 23S rRNA (grey) and one adduct on the L9 ribosomal protein (green). (b) The 30S subunit has two cisplatin binding sites. Examples of cisplatin binding at different residues, namely (c) G26, (d) A2531, and (e) Met1 of the L9 protein are shown. The A-, P-, and E-site bound tRNAs are shown in orange.

The previous work mentioned above led to the hypothesis that RNA-related processes may be inhibited by cisplatin and its derivatives. An earlier study done with platinated messenger RNA showed inhibition of *in vitro* translation activity.[53] Concentration and time-dependent inhibition of peptide synthesis were observed by cisplatin in this study, and maximum inhibition was detected after 30 min drug exposure. Furthermore, inhibition of peptide synthesis was observed at cisplatin concentrations as low as 3 μM. Another study showed that cisplatin is capable of making cross-links in structurally complex RNAs such as the internal loop region of spliceosomal RNAs.[54] Moreover, a cisplatin derivative was used to introduce a site-specific cross-link within the active site of a hammerhead ribozyme.[55] These studies showed that platinum compounds have the ability to introduce distance constraints for dynamic and complex RNA structures, therefore impacting the RNA function. Another study revealed inhibition of telomerase activity caused by cisplatin binding in human testicular cancer cells.[56] Telomerase is a ribonucleoprotein that adds TTAGGG tandem repeat sequences to telomeres using the RNA component of the enzyme. The telomere, the RNA component of the telomerase enzyme, and the gene encoding the RNA component all contain G-rich sequences; therefore, cisplatin is capable of making cross-links and inhibiting the telomerase activity through multiple mechanisms. Reduced telomerase activity is observed in a concentration-dependent manner by cisplatin; whereas, there weren't any effects from chemotherapy drugs known to target DNA, such as doxorubicin, bleomycin, methotrexate, and melphalan.[56]

As discussed above, cisplatin and platinum(II) compounds have been studied in order to identify their RNA binding sites and to determine their effects on RNA activity,

including the impact on mRNA, tRNA, rRNA, spliceosomal, and telomeric RNA function. However, the underlying mechanism of RNA recognition by cisplatin and thereby the inactivation of RNA is still not fully understood. Considering the fact that cisplatin and its derivatives are capable of inactivating a number of essential RNA-related functions, determining the link between RNA and cisplatin toxicity seems worthwhile.

1.5 Drawbacks associated with platinum-based anticancer drugs

Despite its significant success, cisplatin is not a perfect anticancer drug. The side effects caused by cisplatin are a significant limitation.[57] Common side effects include nausea, vomiting, diarrhea, temporary hair loss, signs of dehydration, neurotoxicity, nephrotoxicity, and ototoxicity.[57] The severe side effects of cisplatin result in part from its inability to distinguish tumor cells from normal cells. Therefore, a major concern for next-generation anticancer drug development is achieving selectivity for tumors over normal cells in humans.

On another note, cisplatin is successful for treatment of only certain cancers, and is therefore not universally employed for all cancers. For example, cisplatin cures testicular cancer with a rate of 90%, and nearly 100% if the cancer is found in the early stages.[17] With ovarian cancer, there is an initial cure rate of up to 70% with cisplatin; however, the five-year patient survival rate is about 15-20%.[58] With small cell lung cancer, the relapse rate could be as high as 95%.[58] This relapse occurs as cancer cells develop resistance to cisplatin therapy over time.[59] Some cancers could be intrinsically resistant to cisplatin and other platinum-based drugs, whereas others acquire resistance over time.[59] The cross-resistance of tumors to diverse antitumor drugs suggests that they could share common mechanisms of resistance.[58] Therefore, it is important to understand

these resistance mechanisms to refine therapeutic approaches to battle cancer. **Figure 1.7** summarizes the major pathways that cancer cells could use to develop resistance towards cisplatin and other platinum drugs. Such resistance mechanisms arise as a result of intracellular changes that prevent cisplatin from binding to DNA, activating the apoptotic signal pathway, or both. These pathways include changing the amount of cisplatin uptake and efflux, detoxification of the drug, platinum adduct repair in the cell, and inhibition of apoptosis. These mechanisms are discussed below in detail.

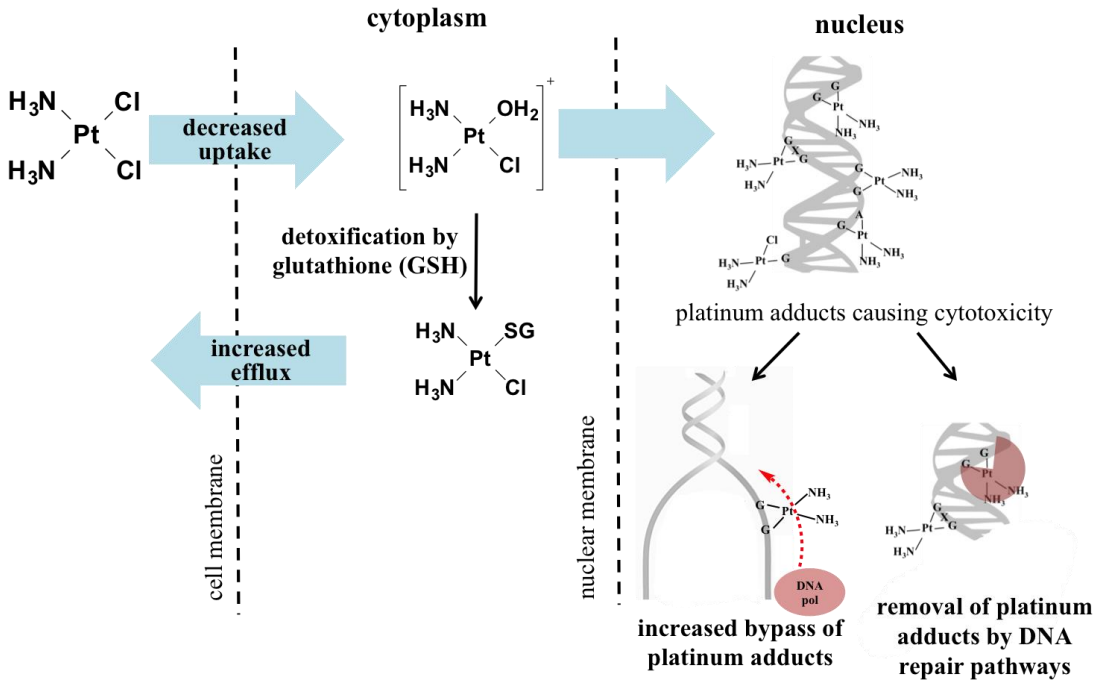

Figure 1.7. Cisplatin resistance mechanisms.[60] The level of cisplatin in the cell and how the cell responds to the drug in the cytoplasm and nucleus determine the anticancer activity of cisplatin.

1.5.1 Decreased uptake and increased efflux

The level of drug accumulation inside the cell determines the anticancer activity of the molecule. Drug accumulation changes as a result of reduced drug uptake, increased efflux, or both.[58] Tumor cells that are resistant to cisplatin have shown a higher expression of the MRP2 membrane protein, which is associated with cellular efflux of the

drug.[61] Cells overexpressing the MRP2 gene have demonstrated a 10-fold higher resistance to cisplatin than cells with normal levels of MRP2.[61] Cells overexpressing ATP7B, a copper-transporting P-type ATPase protein, demonstrated a 9-fold greater resistance to cisplatin due to higher efflux.[62] Some studies also showed that cells with increased levels of p-glycoprotein or the major vault/lung resistance-related protein (MVP/LRP) also have poor outcomes towards cisplatin therapy.[58] However, further work is required to confirm the role of these proteins in cisplatin resistance.

1.5.2 Detoxification by thiol-containing molecules

After activation in the cell, the aquated form of cisplatin is very reactive towards cellular components, particularly the abundant glutathione (GSH) and cysteine-rich metallothioneins.[58] Based on the hard-soft acid-base (HSAB) principle, Pt(II) is a relatively soft acid that can readily coordinate with soft bases such as RS^-.[63] Coordination of cisplatin with cellular thiol-containing molecules decreases the level of available complex to react with DNA, therefore promoting cisplatin resistance. This correlation between increasing levels of GSH and resistance was confirmed with a panel of resistant ovarian tumor models and in clinical studies.[64,65] Metallothioneins also have S-containing reactive centers that participate in cisplatin coordination; therefore, it is not surprising to see elevated metallothionein levels in cisplatin-resistant tumor cells.[66] Increased GSH expression level is a result of increased expression of the γ-glutamylcysteine synthetase (γ-GCS) gene, which is an important enzyme for GSH biogenesis.[67] Higher expression of GSH and metallothionine following cisplatin treatment could result from their involvement in controlling drug-induced oxidative stress in the cell.[68]

1.5.3 Increase in DNA damage repair

Cisplatin-induced DNA damage repair is explained in the **Section 1.2**. NER is the main mechanism used to remove the platinum adducts from DNA. Since DNA adduct formation is believed to be the lead mechanism for anticancer activity of cisplatin, removal of these adducts could be another pathway to acquire resistance. ERCC1 is one of the core proteins associated with the NER pathway, and up regulation of this protein is associated with cisplatin-based resistance due to increased DNA damage repair.[69] DNA mismatch repair (MMR) is another pathway for DNA damage repair in cells.[70] The down regulation or mutations in the MMR genes and the proteins (MutSα and MutSβ) in the MMR pathway are associated with cisplatin resistance.[71] Base excision repair (BER) has been proposed to play a role in cisplatin resistance in cells as well.[72] Low-fidelity DNA polymerase β, which is a part of the BER machinery, is capable of bypassing cisplatin intrastrand adducts, which might lead to cisplatin DNA-damage tolerance.[70] Overall, increased removal of cisplatin adducts in the NER pathway, reduced cytotoxicity due to poor recognition of the adducts, and bypassing cisplatin intrastrand adducts in the MMR and the BER pathways lead to cisplatin resistance in cancer cells. To overcome the cisplatin-associated resistance, new drugs need to be developed with different anticancer mechanisms.

1.6 Other platinum-based anticancer compounds

Since its introduction as a cancer therapeutic, cisplatin has made a major impact in cancer medicine as a successful drug and also as a model for platinum-based anticancer drug development.[7] Unfortunately, cisplatin is not universally effective on every cancer type and also has drawbacks as discussed in **Section 1.4**, thus emphasizing

the need for new drug development. The general structural features of the platinum compounds are shown in **Figure 1.8**.[73] Varying ligands contribute to the anticancer properties of the drug differently; therefore, it is important to understand these features to strategically modify or synthesize novel compounds. The non-leaving group, L, has the ability to interact with DNA and is usually a nitrogen donor. This group will determine the nature of the Pt adduct, structural impacts, and the resistance profile. The leaving group, X, will be removed upon aquation and governs the aquation kinetics and toxicity profiles. Typically, platinum(II)-based drugs have two L groups and two X groups in the *cis* configuration. By strategically modifying the ligands, the lipophilicity and solubility of the complex can be altered. Platinum(IV) complexes have additional axial ligands (R groups) that govern cell targeting, lipophilicity, and solubility.

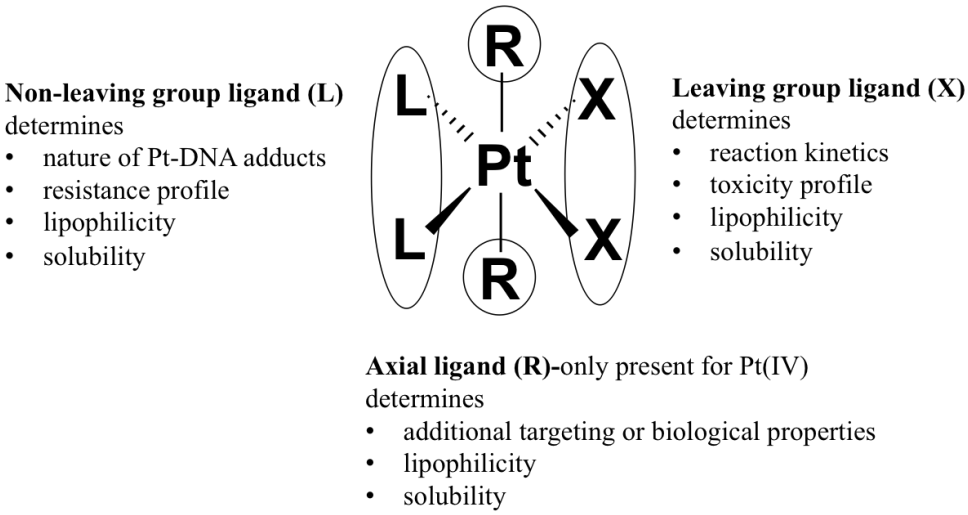

Figure 1.8. Different components of classical platinum anticancer drugs. The properties determine by each group are listed. Platinum(II) drugs have two X and two L groups in the *cis* configuration. Platinum(IV) compounds have two additional groups, R.

1.6.1 Clinically available platinum drugs

Out of more than thousands of molecules that have been synthesized and tested for anticancer properties, only two have been approved for clinical use worldwide along

with cisplatin. They are carboplatin and oxaliplatin (**Figure 1.9**).[73] Nedaplatin, lobaplatin, and heptaplatin are approved for regional use in Asia (**Figure 1.9**).[73] Overall, these molecules bind to DNA and have a similar mechanism of action as cisplatin leading to apoptosis. However, differences in the non-leaving group ligands result in different DNA adduct profiles, and therefore could be repaired at different rates.

The success of cisplatin led to a systematic development of new platinum-based drugs. Carboplatin is one such outcome that was approved for medical use in 1989.[74] It is widely used to treat ovarian cancers, but has also been used for brain, breast, testes, cervix, and lung cancers. It has a relatively stable 1,1-cyclobutanedicarboxylato (CBDCA) ligand as its leaving group that has a lower aquation rate (rate-determining step in the mechanism) and lower toxicity than cisplatin.[75] It therefore has lower reaction kinetics with cellular components compared to cisplatin, thus limiting off-target effects. Because of these reasons, higher doses of carboplatin can be administered.[76] On the other hand, it has the same ammine groups as non-leaving group ligands; therefore, carboplatin has a similar mechanism of action and resistance profile as cisplatin.[75]

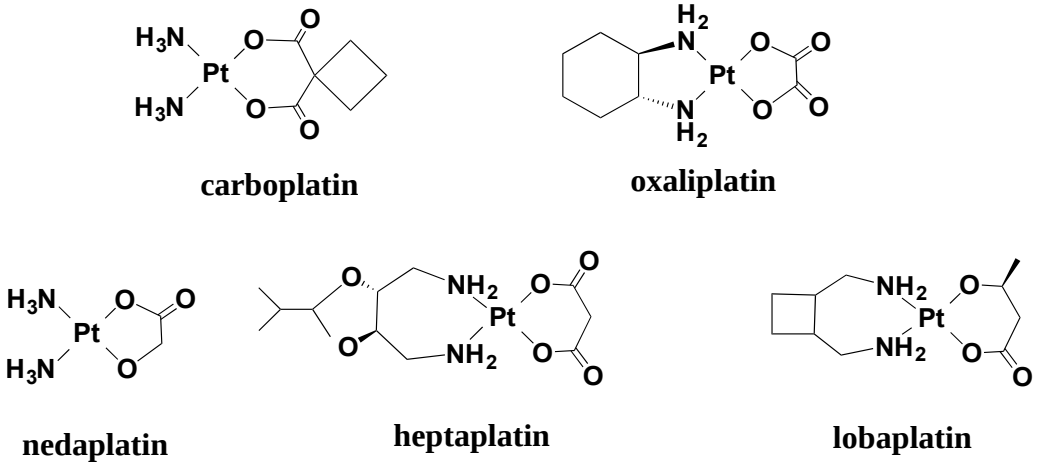

Figure 1.9. Structures of clinically approved platinum(II) drugs. Carboplatin and oxaliplatin are second-generation Pt(II) drugs, and nedaplatin, heptaplatin, and lobaplatin are third-generation drugs.

Oxaliplatin gained approval for international marketing in 1996 for combination chemotherapy for colon cancer.[77] It has an oxalate leaving group and *R,R*-diamminocyclohexane (DACH) non-leaving group ligand. Experimental data revealed that oxaliplatin utilizes organic cation transporters (OCT) for cell penetration, and the overexpression of OCTs in colon cancer provides a rationale for effectiveness of this drug against colon cancer.[77]

Nedaplatin was developed in Japan and approved for clinical use in 1995.[78] The glycolate leaving group confers higher water solubility to the molecule compared to cisplatin. Nedaplatin has the same non-leaving ammine ligands as cisplatin and carboplatin. It is primarily used to treat esophagus, head and neck, small cell lung cancers, and non-small cell lung cancers.[79]

Heptaplatin and lobaplatin are third-generation cancer drugs. Hepataplatin was developed in Korea to treat gastric cancer.[7] As shown in **Figure 1.9**, it has a malonate leaving group and 2-(1-methylethyl)-1,3-dioxolane-4,5-dimethanammine as the non-leaving group ligand, which forms a seven-membered chelate ring.[80]

Lobaplatin was initially developed in Germany, but only has regulatory approval for clinical use in China.[7] Initially it was used to treat chronic myelogenous leukemia, but is now used to also treat small cell lung cancers and metastatic breast cancer.[7] Lobaplatin is a heptaplatin derivative, but with different L and X ligands.

1.6.2 Other Pt(II) complexes

A large number of platinum(II) complexes has been developed and tested for their anticancer activity in both academia and industry. Conjugation of biologically available molecules is a common approach scientists are using in the hopes of lowering the toxicity

and achieving selectivity of platinum-based drugs. For example, glycoconjugation has been introduced to selectively target cancer cells with higher glucose transporter expression. Furthermore, these compounds have increased water solubility and reduced toxicity. There are a variety of platinum-containing molecules with sugar groups attached as non-leaving groups or leaving groups that are analogous to cisplatin and oxaliplatin (**Figure 1.10**).[81-83] Primarily, the work in this area has been limited to synthesis of the complexes and testing for cytotoxicity. The first Pt(II) complex with an attached amino sugar is shown in **Figure 1.10a.**[84] Recently, some effort has been made to establish a link between platinum-sugar conjugation and uptake using specific receptors in cancer cells.[83] The first experimental evidence of sugar-linked oxaliplatin analogs exploiting the glucose receptor was reported in 2013.[81]

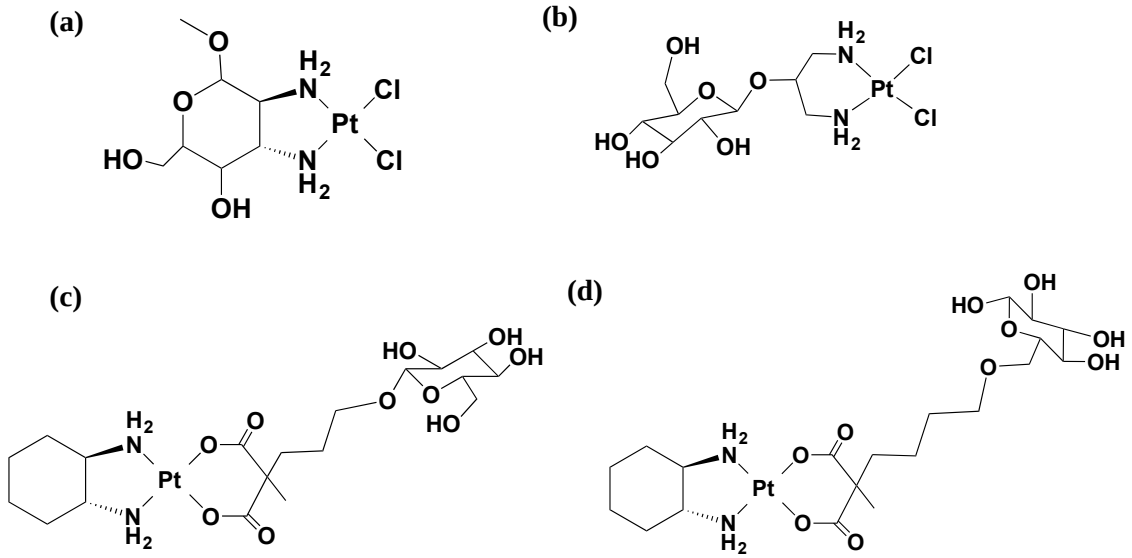

Figure 1.10. Structures of carbohydrate-linked Pt(II) complexes. (a) $PtCl_2$(methyl 2,3-diammino-2,3-dideoxy-α-D-mannopyranoside[84] and (b) *cis*-dichlorido[(2-β-D-glucopyranosidyl)propane-1,3-diammine]platinum(II)[82] are cisplatin derivatives with sugar groups attached as non-leaving group ligands. (c) (*trans*-R,R-cyclohexane-1,2-diammine)-malonatoplatinum(II)[81] and (d) glucose-Pt(II) complex[83] are oxaliplatin derivatives, in which sugar groups are attached to the leaving group.

Another class of Pt(II) complexes that has been synthesized contains a steroid

group (estrogen and testosterone) attached as the non-leaving group ligand (**Figure 1.11**).[85] Steroids have been used as targeting groups that utilize the overexpressed steroid receptors on certain cancer cells. For example, estrogen receptor is overexpressed in breast cancers to stimulate proliferation.[86] The rationale for attaching steroids is that they can kill the cancer cells by either enhanced uptake of the platinum drug or by blocking the steroid receptor from its biological function.

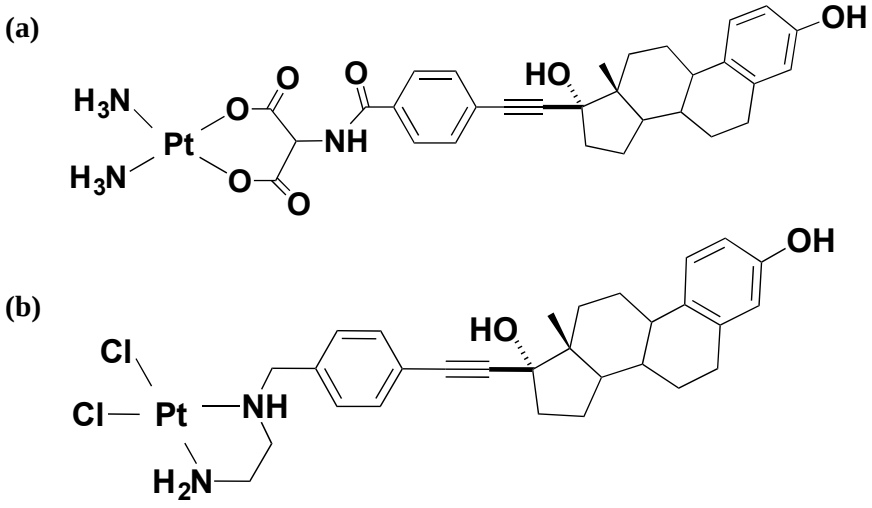

Figure 1.11. Structures of estrogen receptor ligands attached to Pt(II) complexes. (a) *cis*-dichlorido[*N*-(4-(17α-ethynylestradiolyl)-benzyl)-ethylenediammine]platinum(II) and (b) *cis*-diammino[2-(4-(17α-ethynylestradiolyl)-benzoylamino)-malonato] platinum(II) have the estrogen receptor group attached to the leaving group or the non-leaving group, respectively.[85]

Conjugating amino acids or peptides to make platinum(II) complexes is another idea that has been explored (**Figure 1.12**). Earlier studies showed that conjugation of netropsin and distamycin peptides, which are minor groove DNA binders, change the overall complex binding preference to poly(dA) over poly(dG).[87] Altered specificity for A residues on RNA was also observed for some amino-acid-linked cisplatin analogs with lysine, ornithine, and arginine as the non-leaving group ligands.[88]

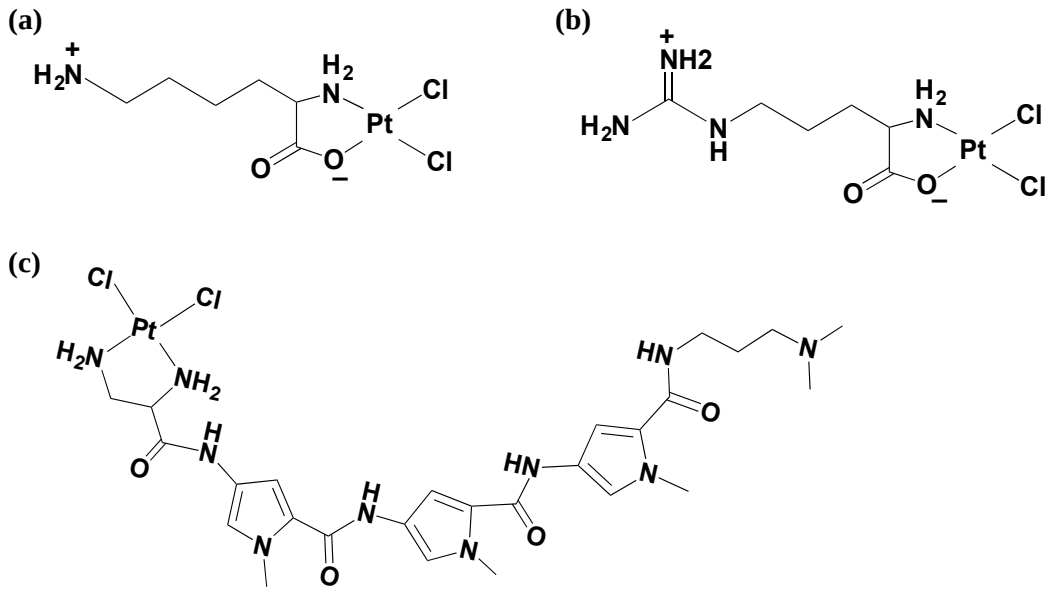

Figure 1.12. Structures of Pt(II) complexes attached to amino acids and peptides. (a) Lysine-Pt(II) or Kplatin, (b) arginine-Pt(II) or Rplatin, and (c) peptide-Pt(II) complexes are shown.[87,88]

In hopes of altering the spectrum of activity and thereby circumventing the drawbacks associated with clinically available drugs, researchers are introducing large changes to the general structure of platinum(II) compounds as shown in **Figure 1.12**. Another expectation of this search for new ligands is to find platinum drugs that are effective against other cancer types. Furthermore, *trans*,[89] monofunctional,[90] and polynuclear platinum(II) complexes[91,92] are some of the non-classical compounds being explored.

1.6.3 Platinum(IV) complexes

Platinum(IV) complexes have octahedral geometries, which differs from the square planar platinum(II) complexes. The two extra ligands in the complex can be used to tune cellular targeting, lipophilicity, uptake, and delivery.[7] Although the platinum(IV) complexes have been in discussion since the discovery of cisplatin activity, their clinical

significance was only recognized recently.[93] Platinum(IV) complexes are more resistant to ligand substitution than the platinum(II) complexes; therefore, they can be used as prodrugs to minimize unwanted side reactions before reaching target DNA. When reacting, Pt(IV) will undergo reduction to yield Pt(II) reactive species. Some of the Pt(IV) drugs that have reached clinical trials are tetraplatin, satraplatin, and iproplatin (**Figure 1.13).**[7] Out of these, satraplatin is the first orally active platinum complex to be synthesized.

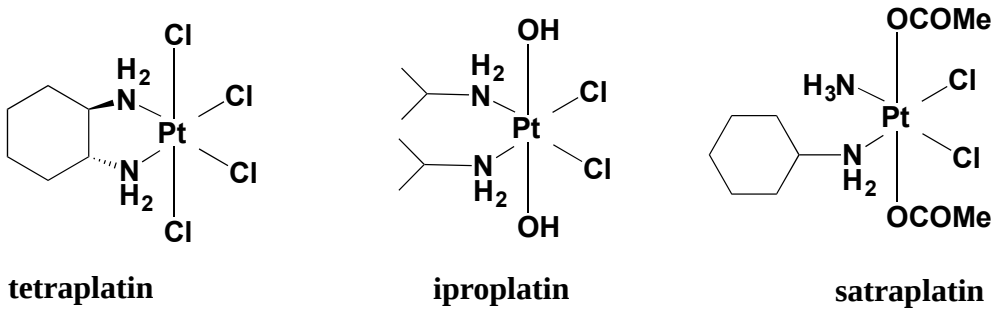

Figure 1.13. Chemical structures of Pt(IV) complexes. Structures of tetraplatin, iproplatin, and satraplatin are shown.

1.7 Platinum complexes as chemical probes

Cisplatin and a large number of platinum compounds have been synthesized and tested for their anticancer activity over the years.[7] The possibility of attaching different ligands to the platinum center as discussed in the above sections could be utilized to introduce new functionalities to the drug. While these modifications are introduced to improve the anticancer properties of the drug, there are some instances in which the modifications introduce other properties to the complex that allow for example visualization and purification.[94] Such properties allow the derivatives to be used as probes in biochemical studies. In this section, a new role of platinum complexes as chemical probes will be discussed.

A chemical probe is a small molecule that interacts with specific targets to provide information about that target. The reaction could also provide information about the environment, in which the target resides. Cisplatin forms stable and inert bonds with purine residues, allowing the adducts to be analyzed using a variety of techniques. For example at the nucleoside level, adducts can be detected and analyzed using high performance liquid chromatography (HPLC) and mass spectrometry (LC-MS).[95] In the context of nucleic acids, the adducts can be analyzed using gel electrophoresis techniques as well.[95] Cisplatin is a small molecule with a +1/+2 charge depending on aquation. As mentioned earlier, cisplatin's size, charge, and reactivity can be altered by changing the non-leaving group ligands. For example, fluorophores have been attached to detect the drug localization within complex cellular environments.[94,96] Furthermore, attachment of a reactive handle such as a "clickable" group to the Pt complex provides ways to incorporate a variety of functional groups (**Figure 1.14**).[94] This approach could be used for detection, isolation, and purification of Pt-bound targets.

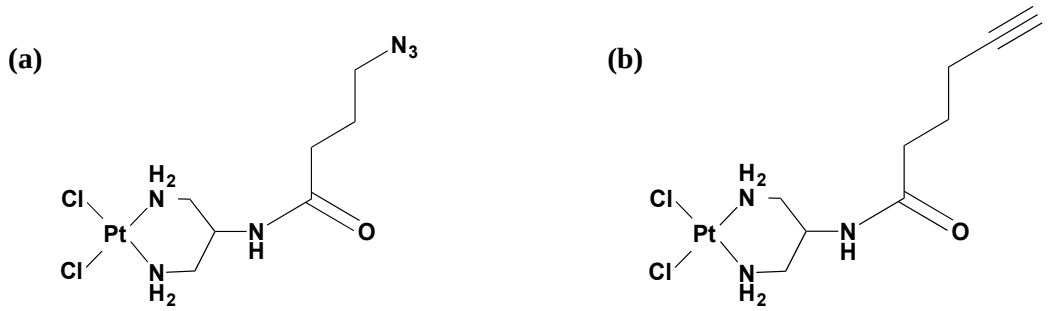

Figure 1.14. Chemical structures for cisplatin derivatives with "clickable" groups.[94] The (a) azide-appended and (b) alkyne-appended complexes can undergo click modification with another molecule with the counter-reactive part.

The information gained from cisplatin binding sites reflects how other small molecules find their targets, and could be used for novel drug development. Cisplatin can readily penetrate the cell membrane, allowing it to be used for *in vivo* probing as well.[43]

Additionally, cisplatin reactivity can be quenched using high chloride concentrations, which allows it to be used for monitoring binding kinetics. Differences in platination rates upon changes in the reaction medium (for example, salt, pH, and the presence of other ligands) give information about the microenvironment of the target and how those affect drug-target interactions.[50]

For the purpose of this thesis work, we were particularly interested in exploring cisplatin and its derivatives as probes for RNA structure. RNA plays important regulatory roles in the life cycle of a cell by modulating gene expression. Therefore, RNA has received much attention by scientists as a promising target for drug development. As the protein synthesis machinery in the cell, the ribosome has been a validated target for both anticancer and antibacterial drugs, and still has great potential for further exploration.[97] In order to find possible target sites, selective chemical reagents are needed to probe the structural details of rRNA *in vivo* and *in vitro.*[98] **Figure 1.15** shows some of the chemical probes that are available for RNA structure studies. Chemical probing techniques are useful in studying RNA structure at near physiological solution conditions and reveal information at the nucleotide level.[99] Compared to some other structure probing methods such as NMR spectroscopy and X-ray crystallography, only small amounts of sample (pmoles) are needed for chemical probing.[99,100] One limitation of this method is that only a few compounds have been applied to *in vivo* (dimethylsulfate (DMS), hydroxyl radicals, and Pb^{2+}) probing.[98] Additionally, these reagents are reactive at specific sites; therefore, they cannot detect some of the desired sites or need additional steps for detection at their reactive sites such as reverse transcription. For example, to detect N7-G

modification by DMS, aniline treatment has to be done, as methylation at this site doesn't directly inhibit reverse transcription.[101]

The use of cisplatin as a chemical probe for RNA has been reported previously by our lab previously.[43] By changing the non-leaving ligand to amino acids, the reactivity of the platinum complex has been altered, and this method has provided information about accessibility of rRNA towards various ligands.[88] Moreover, cisplatin has been used for both *in vitro* and *in vivo* probing, and adducts are identified by reverse transcription stops. Studies from our lab have also shown the feasibility of using cisplatin kinetics to investigate the impact of RNA microenvironments on drug binding.[50]

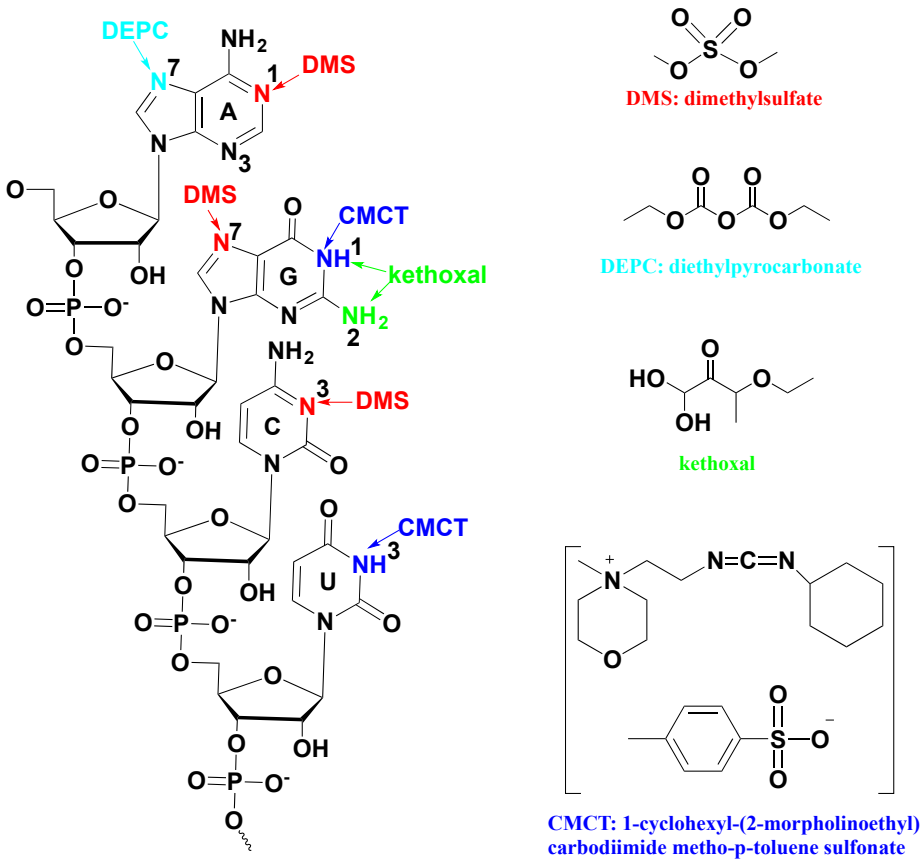

Figure 1.15. The chemical probes and their target sites. Certain modifications (*e.g.*, methylation or alkylation at N1-A, N3-C, N1-G, and N3-U) are detected by reverse transcription (RT) analysis. Modifications at the N7-G position by DMS are detected by aniline-induced strand scission and RT analysis.[98-100]

1.8 Aminoglycosides: RNA targeting antibiotics

Aminoglycosides are small molecule, broad-spectrum antibiotics that target bacterial ribosome and inhibit translation.[102] Commonly, aminoglycosides are composed of a 2-deoxystreptoamine (2-DOS) subunit that is connected to different amino sugar rings *via* glycosidic linkages (**Figure 1.16**). Streptomycin is an example of an aminoglycoside without a 2-DOS moiety.[102]

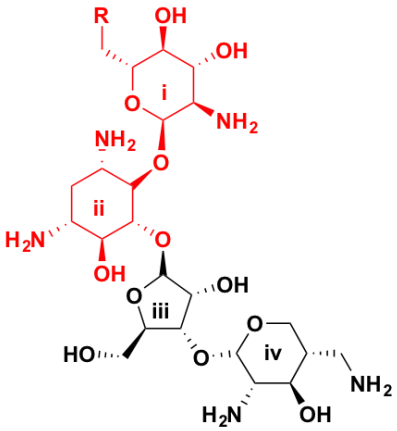

R = OH; paromomycin
R = NH_2; neomycin

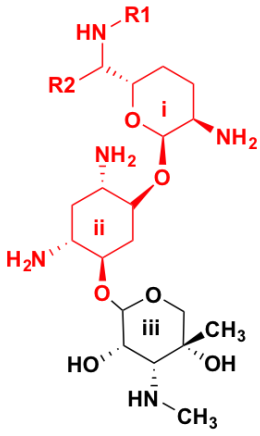

R1, R2 = CH_3, CH_3; gentamycin C1
R1, R2 = H, H; gentamycin C1a
R1, R2 = H, CH_3; gentamycin C2

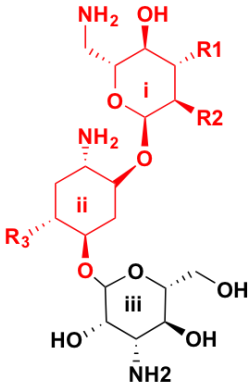

R1, R2, R3 = OH, OH, NH_2; kanamycin A
R1, R2, R3 = OH, NH_2, NH_2 H; kanamycin B

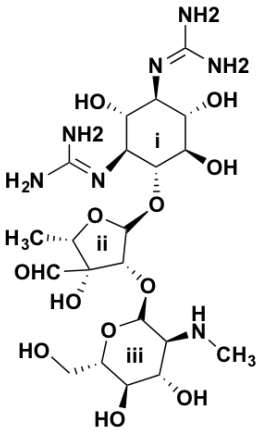

streptomycin

Figure 1.16. Chemical structures of aminoglycosides. Neomycin, paromomycin, gentamycin and kanamycin have the common 2-DOS moiety (red), whereas streptomycin does not.

Aminoglycosides inhibit protein synthesis by binding to the A site (helix 44, or h44) of the 16S ribosomal RNA with a moderate (μM) affinity.[103] Binding of the aminoglycosides induces or stabilizes an extrahelical conformation of residues A1492 and A1493.[104,105] These residues are important for aminoacyl tRNA recognition and mRNA translocation.[106,107] Aminoglycoside binding stabilizes the h44-mRNA-tRNA complex and induces codon misreading, translocation abortion, and decreased translation fidelity.[108,109] Crystal structures have also shown a secondary binding site for neomycin, paromomycin, and gentamycin at helix 69 (H69) of 23S rRNA as well.[106,110,111] The interactions in the H69 major groove can inhibit the recycling and translocation steps in protein synthesis.[112]

With the emergence of the antibiotic resistance, it is important to understand the underlying principles of drug-target interactions in order to develop novel drugs. Chemical tools are necessary to understand the electrostatics and salt-dependent properties in aminoglycoside-nucleic acid interactions. **Chapter 6** of this thesis describes the feasibility of using cisplatin kinetics to investigate these RNA-drug interactions.

1.9 Thesis overview and specific aims of the research

Serendipitous discovery of cisplatin opened up a field of metallodrug development for cancer treatment.[8] Strategic development of platinum and other metal-containing drugs has led to successful approval of treatments for several cancer types. Notably, platinum-containing drugs such as carboplatin and oxaliplatin, which were developed based on cisplatin, are prevailing in the treatment of cancer.[113,114] However, new platinum-based anticancer agents are only slowly being introduced to the clinic. With a deeper understanding of the mechanistic details of these drugs, many strategies

can be explored to develop next-generation platinum drugs that overcome the drawbacks associated with the parent drugs. In recent years, synthesis of platinum(II) complexes with biologically important ligands such as carbohydrates,[82,83,115] amino acids,[88] peptides,[87,116] steroids,[117] and folate[118] have been explored because of their reduced toxicity. Among these, glycoconjugation has received much attention. Carbohydrates are important elements in many drugs that target DNA and RNA.[119,120] There is recent evidence to suggest that carbohydrate motifs are utilizing glucose transporters for targeted delivery to cancer cells.[83,121] Despite the fact that glycoconjugation reduces overall toxicity of platinum drugs, leads to higher potency,[82] and facilitates targeted delivery[83], the impact of the sugar motif on the mechanism of cell death is still largely unknown. The ability of carbohydrates to form a number of hydrogen-bonding interactions and presence of the larger sugar group within the Pt coordination sphere can influence the reactivity of these molecules. To gain insight into the behavior of glycoconjugated platinum(II) complexes compared to cisplatin, I utilized a cisplatin derivative as a model compound as shown in **Figure 1.17** (compound **5**).[82]

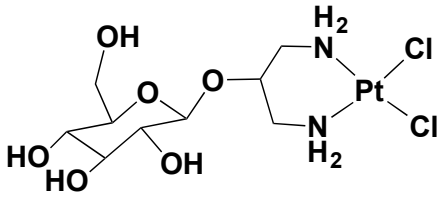

(5)

Figure 1.17. The structure of sugar-conjugated cisplatin derivative, compound 5.
The cisplatin derivative *cis*-dichlorido[(2-*β*-D-glucopyranosidyl)propane-1,3-diammine]platinum(II) is shown.

I also carried out experiments to reveal the feasibility of using cisplatin as a probe for RNA-ligand interactions. Aminoglycosides are cationic ligands that bind to RNA with

moderate affinity and poor selectivity. In order to develop new antibiotics, it is of importance to understand the structural mechanisms used by aminoglycosides to target RNA. It is challenging to experimentally determine the electrostatic environments that are involved in drug-RNA interactions; however, certain studies have shown the importance of the high number of positive charges on aminoglycosides in binding to RNA.[122,123] Isothermal titration calorimetric studies of neomycin B binding to a RNA stem loop revealed the contribution of hydrogen-bonding and electrostatic contacts.[122] Salt-dependent variations in binding were attributed to electrostatic contacts. However, there is still a lack of information on the relative contributions of electrostatic interactions for aminoglycoside binding and techniques to evaluate the electrostatic interactions. Experiments were carried out to achieve these goals with the following specific aims.

Aim 1: Determine the reactivity preferences, reaction rates, and the products formed for the reaction between compound 5 and nucleosides

Many known platinum(II) complexes prefer binding to the guanine base, but there are exceptions to this observation. For example, changing the non-leaving group ligand to amino acids such as ornithine and lysine has been shown to alter the binding preference to adenine.[88] The first aim of this thesis work was to determine the binding preferences of a carbohydrate-linked cisplatin analog (**5**) in the context of nucleosides. HPLC and LC-MS techniques were utilized to characterize the reaction products and to obtain reaction rates.

Aim 2: Investigate the reaction rates, binding sites, and structural impacts of compound 5 at the oligonucleotide level

Reactivity at the nucleoside level does not reflect influences of the nucleic acid backbone. Therefore, it is important to analyze drug reactivity at biologically relevant conditions to fully understand activity within the context of a cell. In this thesis work, kinetic experiments were carried out to determine the reaction rates and characterize DNA and RNA oligomers. Gel-based assays were used for the rate determination with mono- and bisactivated compound **5** in comparison to cisplatin. Additionally, reaction rates were obtained in the presence of varying salt conditions to understand the effect of electrostatics and the role of the sugar moiety on the overall binding kinetics. Moreover, the structural effects of binding were also evaluated using different gel-based assays in the context of plasmid DNA and DNA oligomer.

Cisplatin anticancer activity is mainly associated with DNA binding. However, with more mechanistic studies being done, this idea has been challenged and cisplatin was shown to bind to other cellular targets such as RNA and proteins, which could also disrupt cellular functions and lead to cell death.[39,53,56] In particular, cellular RNA has received increased attention in recent years.[40,46,124] My hypothesis was that an attached sugar group and overall positive charge would facilitate compound **5** accumulation on RNA. The chemical probing technique was used to detect reactive sites on the functionally important ribosome.

Aim 3: Evaluate the cytotoxicity of compound 5 against cancer cell lines compared to normal cells and quantify its accumulation levels

To explore the cytotoxicity of **5** towards various cancer cell lines, a series of MTT (3-(4,5-dimethylthiaxol-2-yl)-2,5-diphenyltetrazolium bromide) assays were carried out in this thesis work. Comparable cytotoxicity of compound **5** with cisplatin had previously been reported for ovarian and melanoma cancer cell lines, but my goal was to expand this study to other cancer cell lines (*e.g.*, prostate) as well as the corresponding normal cell lines. My hypothesis was that selective cancer cell targeting could be achieved by utilizing a characteristic feature of certain cancer cells, specifically enhanced uptake of glucose.[125] This idea was previously explored with glycoconjugated oxaliplatin derivatives, but not with cisplatin derivatives such as compound **5**.[83] Therefore, it was of interest to explore the differential accumulation of compound **5** in cancer cells compared to normal cells. As a proof of concept, the DU145 prostate cancer cell line was selected for this comparison based on the higher glucose transporter expression levels,[126] along with the normal prostate cell line-RWPE1.[83]

Aim 4: Probe RNA-aminoglycoside interactions using cisplatin kinetics as a tool

Based on a previous study from our lab that showed salt-dependent cisplatin coordination rates to RNA, we postulated that positively charged aminoglycosides could also impact the platination rates by competing with cisplatin for the target. Herein, I describe a kinetic method to monitor aminoglycoside interactions with RNA using cisplatin coordination rates. A gel-based assay was used to obtain the cisplatin coordination rates to RNA in the presence of various aminoglycosides.

CHAPTER 2

BIOCHEMICAL METHODS, CELL STUDIES, AND DATA ANALYSIS

2.1 Abstract

The work discussed in this thesis largely focuses on understanding the underlying mechanisms of platinum(II) complex activity and using certain features of these anticancer drugs for chemical probing. A variety of biochemical, bio-analytical, and molecular biology techniques were utilized for these purposes. Gel-based techniques were used to analyze product formation with DNA and RNA to observe, nucleic acid structural changes, and to obtain kinetic parameters for reactions between a carbohydrate-linked Pt(II) complex (**5**) and the parent compound cisplatin. These methods include agarose gel electrophoresis, as well as native and denaturing polyacrylamide gel electrophoresis (PAGE). Radioactive labeling was employed for visualization of the nucleic acids in the gels. In addition, high performance liquid chromatography (HPLC) and mass spectrometry (MS) techniques such as matrix-assisted laser desorption ionization (MALDI) and liquid chromatography mass spectrometry (LC-MS) were used for product characterization (*e.g.*, identity and quantity). Another goal of my thesis work was to understand the cellular toxicity and accumulation of the carbohydrate-linked Pt(II) compound (**5**) compared to the already known anticancer drug cisplatin. Cellular toxicity was assessed using an MTT (3-(4,5-dimethylthiaxol-2-yl)-2,5-diphenyltetrazolium bromide) assay, and Pt levels in the cell were determined by using inductively coupled plasma mass spectrometry (ICP-MS). The methods describe in this chapter were utilized to examine Pt-RNA or Pt-DNA interactions, but could also be employed with other small molecule-nucleic acid complexes.

2.2 Introduction

2.2.1 Reactivity and Pt(II) coordination rates with nucleosides and oligonucleotides

To evaluate the binding preferences of compound **5** with different RNA nucleosides (**Figure 2.1**), the reactions were analyzed by reverse-phase HPLC on a C18 column. Depending on the observed product formation, only certain nucleosides such as guanosine were selected for kinetic experiments. The rates of Pt(II) complex coordination to guanosine (G) and deoxyguanosine (dG) were determined by using HPLC-based assays as described in **Section 2.4.4**. The products were characterized by LC-MS.

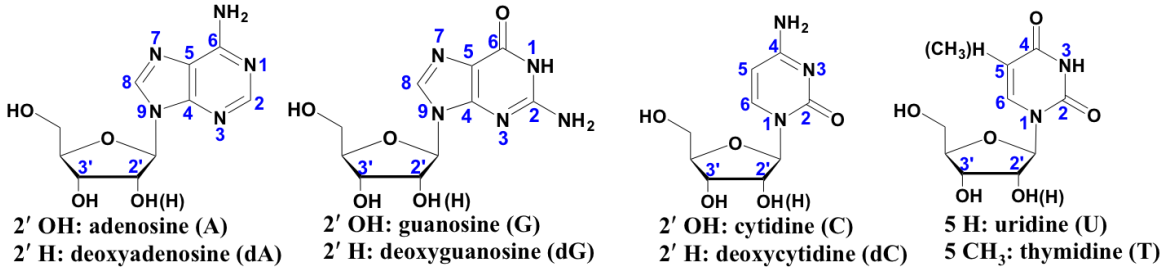

Figure 2.1. The chemical structures of RNA and DNA nucleosides. Adenosine, deoxyadenosine, guanosine, and deoxyguanosine have purine bases, whereas cytidine, deoxycytidine, uridine, and thymidine have pyrimidine bases.

Experiments were carried out to compare the reactivity of Pt(II) complexes at the oligonucleotide level (**Section 2.4.9**). Based on the reactivity at guanine bases, nucleic acid sequences with guanosine residues were employed. To determine the platination rate constants, an electrophoretic mobility shift assay (EMSA) technique was employed. The kinetic experiments were carried out using mono- or bis-activated Pt(II) compounds for comparison. Rates were obtained under different buffer conditions for the reactions between DNA/RNA and mono-activated Pt(II) compounds. All of the experiments were done in parallel to cisplatin reactions for comparison.

For all of the kinetic experiments carried out in this thesis work, pseudo-first-order conditions were maintained.[51] More specifically, the concentration of the Pt(II) complex was in large excess with respect to the other reactant (X= nucleoside, RNA or DNA). As such, the Pt(II) concentration was included in the rate constant, which is the pseudo-first-order rate constant or k_{obs}.[51] The reaction between Pt and X is second-order, but a ≥50-fold excess is used. Therefore, k_{obs} will be equal to the product of the Pt(II) concentration and the apparent second-order rate constant, $k_{2,app}$. The apparent second-order rate constant, $k_{2,app}$ is then obtained by varying the platinum concentration.

2.2.2 Cisplatin coordination rates to H69 RNA in the presence of aminoglycosides

Cisplatin binding to the H69 RNA hairpin loop is well characterized.[95] The H69 sequences with and without pseudouridine (ψ) modifications (**Figure 2.2**) were utilized in this experiment to determine the effect of the modification on aminoglycoside binding. Aminoglycosides such as neomycin and paromomycin (**Figure 1.16**) that are known to show interactions with the H69 region (19-mer) were used, and compared to the non-binding compound streptomycin.

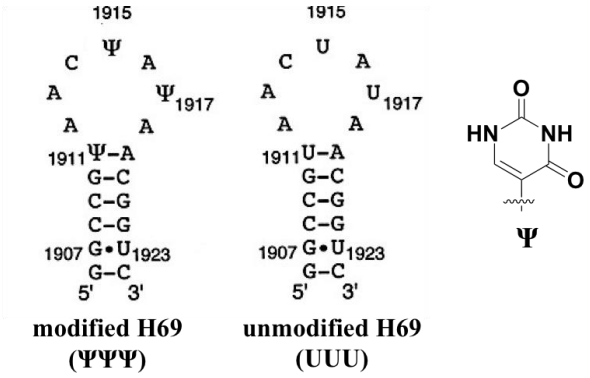

Figure 2.2. Structures of RNA constructs used in the kinetic study. Modified (ΨΨΨ) and unmodified (UUU) H69 rRNA constructs are shown, in which Ψ is pseudouridine (shown to the right).

2.2.3 Structural effects of platinum compounds on DNA

Structural effects caused by complex **5** were evaluated by reacting it with plasmid DNA and a duplex DNA oligomer (22-mer). As a comparison, reactions were done with cisplatin. By reacting with plasmid DNA, global structural changes caused by cisplatin and **5** were evaluated. The effect of a single platination event within a duplex DNA was also evaluated using the small oligomer DNA.

2.2.4 Structure probing of RNA

Single-stranded RNAs form many secondary structures and adopt complex scaffolds, which are important for its function.[97] There are various interactions that can occur between the bases, and with ions in the solution (*e.g.*, Mg^{2+}), that govern the structure and are important for drug binding.[127] Probing techniques are utilized to understand the key structural features of RNA at the nucleotide level. The two main probing techniques used for this purpose are chemical and enzymatic probing.[128] Some chemical probes are able to penetrate cell membranes and therefore can be used for *in vivo* probing (*e.g.*, DMS).[99] These small molecules provide information about solvent-accessible sites within complex, folded, tertiary structures of RNA.[128] In contrast, enzymatic probing provides less information about the folded RNA structure, due to the bulkiness of the probe. RNases can be utilized to determine ligand-binding sites in *in vitro* studies. **Table 2.1** shows some commonly used chemical and enzymatic probes and their targets. Depending on the size of the RNA, the detection method can vary. Modification or cleavage sites for small RNA can be directly detected by radiolabeling the RNA ends.[99] For larger RNAs (over 200 nucleotides), primer extension is used to determine the reactive sites.

Table 2.1. Chemical and enzymatic probes and their RNA targets[99,128]

probe	target
RNase T1	Unpaired G
RNase T2	Unpaired A>C, U, G
RNase V1	Paired or stacked nucleotides
RNase U2	Unpaired A>G>>C>U
RNase H	RNA only from DNA-RNA hybrids
Nuclease S1	Unpaired nucleotides
Mung bean nuclease	Single-strand regions
DMS	N7-G, N1-A, N3-C
CMCT	N7-G, N3-U
DEPC	N7-A
kethoxal	N1, N2-G
Fe-EDTA (•OH radicals)	Ribose C1′ and C4′
NMIA	2′-OH of flexible nucleotides
Pb^{2+}	Phosphodiester bonds in single-stranded regions and unstable helices
in-line probing	Phosphodiester bonds

DMS: dimethyl sulfate; DEPC: diethylpyrocarbonate; CMCT: 1-cyclohexyl-3-(2-morpholinoethyl) carbodiimide metho-p-toluene sulfonate; NMIA: *N*-methylisatoic anhydride.

The use of cisplatin as a probe for RNA structure was reported recently.[43] Reverse transcription-based primer extension followed by gel electrophoresis was employed to detect the cisplatin binding sites in RNA (**Figure 2.3**). The same method was exploited to

find compound **5** coordination sites on rRNA in this study. The ribosomes were isolated and platinated. Then, the rRNAs were extracted and used for primer extension reactions with DNA primers designed for specific regions of the ribosome.

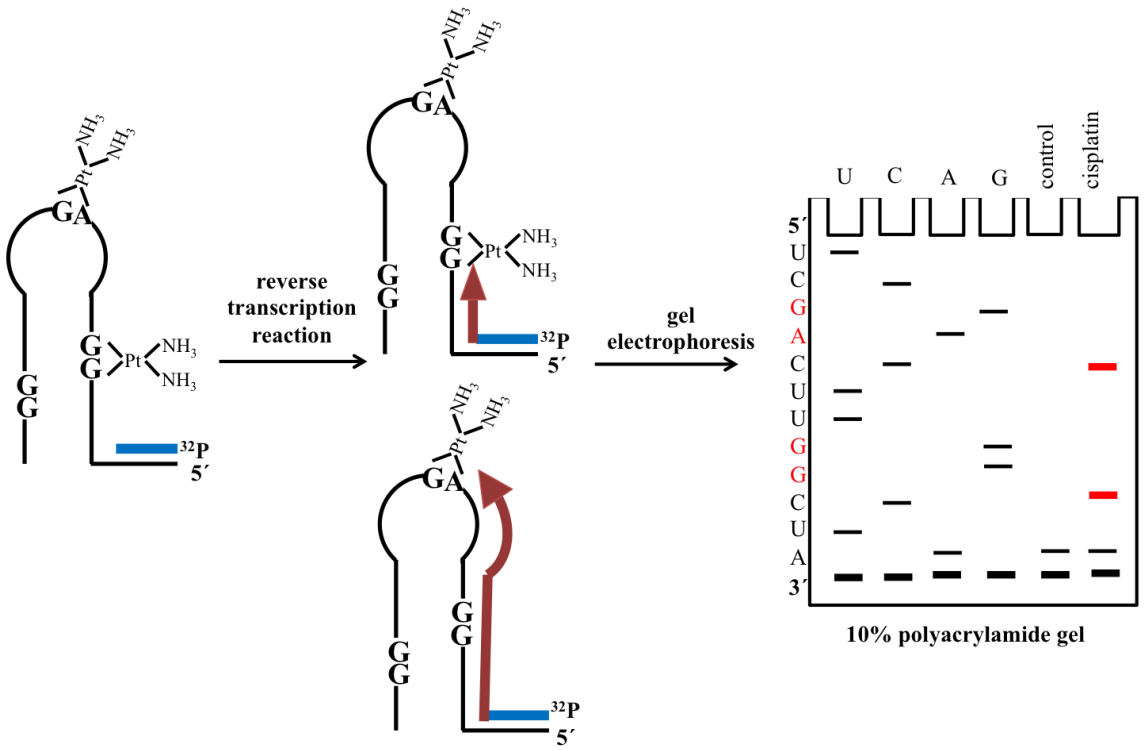

Figure 2.3. A schematic diagram showing the basic steps of cisplatin probing. Denaturing gel electrophoresis is carried out after the reverse transcription-based primer extension reactions. The resulting gel image will show the dideoxy sequencing lanes for each nucleotide control, and cisplatin reaction lanes. The red color bands in the cisplatin reaction lane depict the stop sites. The stop sites occur one nucleotide prior to the actual modification site on the RNA.

2.2.5 Potency and accumulation of platinum(II) compounds in human cancer and normal cell lines

The anticancer potency of **5** was tested by determining the IC_{50} values in several human cancer cell lines using the MTT colorimetric assay.[129] This assay relies on a color change in which viable cells convert the yellow-colored MTT (3-(4,5-dimethylthiazol-2-yl)-2,5-diphenyltetrazolium bromide) reagent into purple-colored formazan (**Scheme**

2.1).[130] The NAD(P)H-dependent cellular oxidoreductase enzymes in viable cells are responsible for the color change, as they reduce the MTT reagent to produce insoluble formazan.[130] The color change can be monitored by a multi-well scanning spectrophotometer/plate reader.

Scheme 2.1. The conversion of MTT to formazan. MTT is a yellow reagent and formazan is purple.

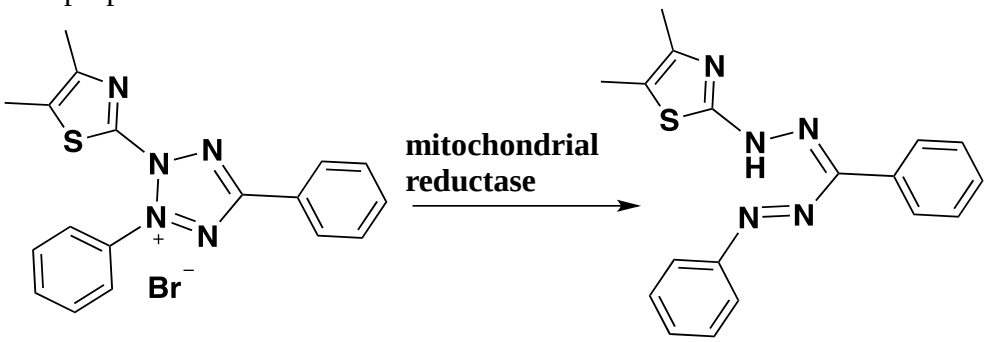

3-(4,5-dimethylthiazol-2-yl)-2,5-diphenyltetrazolium bromide
(MTT)

(*E*,*Z*)-5-(4,5-dimethylthiazol-2-yl)-1,3- diphenylformazan
(formazan)

2.3 Materials

2.3.1 Chemicals and supplies

Cisplatin (*cis*-diamminedichloridoplatinum(II)) was obtained from Alfa Aesar (Wardhill, MA). Anhydrous dimethylformamide (DMF) (99.8% purity) was obtained from EMD (Gibbstown, NJ). The HPLC grade acetonitrile, silver nitrate ($AgNO_3$), ammonium acetate (NH_4OAc), sodium dihydrogen phosphate (NaH_2PO_4), disodium hydrogen phosphate (Na_2HPO_4), KH_2PO_4, K_2HPO_4, magnesium chloride ($MgCl_2$), potassium chloride (KCl), sodium chloride (NaCl), agarose, bromophenol blue dye, dimethyl sulfoxide (DMSO), 2-amino-2-hydroxymethyl propane-1,3-diol (Tris), phenol-chloroform-isoamyl alcohol (25:24:1) (PCI), T4 DNA ligase, boric acid, phosphate buffer saline, pH=7.4 (PBS), and Dulbecco's Modified Eagle's (DMEM) cell culture media

from Fisher Scientific (Fair Lawn, NJ) were used. The chemicals potassium tetrachloroplatinate(II) (K_2PtCl_4), sodium perchlorate ($NaClO_4$), acrylamide, glycerol, xylene cyanol dye, *N*,*N'*-methylenebisacrylamide, urea, 4-(2-hydroxyethyl)-1-piperazineethanesulfonic acid (HEPES), 2-mercaptoethanol (2-ME), 3-hydroxypicolinic acid (3-HPA), ethylenediaminetetraacetic acid (EDTA), ammonium chloride (NH_4Cl), ethanol, neomycin B, paromomycin, streptomycin, penicillin-streptomycin (pen-strep), fetal bovine serum (FBS), tissue culture dishes, and 96-well plates were purchased from Sigma-Aldrich (St. Louis, MO). The chemicals Luria broth (LB) (BD medical Technology, Franklin Lakes, NJ), deoxynucleoside triphosphates (dNTPs) (Genscript, Piscataway, NJ), dideoxy nucleotide triphosphates (ddNTPs) (Roche, Indianapolis, IN), nuclease- and protease-free sucrose (MP Biomedicals, Solon, OH) were used. DNase I and ImPromII Reverse Transcriptase (RT) were purchased from Promega (Fitchburg, WI). The enzymes T4 RNA ligase and T4 polynucleotide kinase from New England Biolabs (Ipswich, MA) were employed in this study. The radiolabels [5'-^{32}P] pCp and [γ^{32}-P] ATP were purchased from Perkin-Elmer Life Sciences, Inc. (Waltham, MA). The Sep-pak C18 cartridges were purchased from Waters (Milford, MA). Keratinocyte-SFM media, 0.25% trypsin-EDTA (Gibco, Pittsburgh, PA), and 10 ppm platinum solution in 2% HNO_3 (High-purity standards, Charleston, NC) were used for the cell-based experiments. RNase-free distilled, deionized water (ddH_2O) was used for all experiments.

2.3.2 Nucleosides and oligonucleotides

Single RNA and DNA nucleosides were purchased from Sigma-Aldrich and stock solutions were prepared by dissolving them in ddH_2O to the desired concentration (The difference in UV absorbance between phosphate buffer and water is less than 0.15%).[131]

Concentrations of the nucleoside solutions were calculated by measuring the absorption at maximum wavelengths and using published extinction coefficients ($\varepsilon_{260\ nm}$ = 14,900 M^{-1} cm^{-1} for adenosine, $\varepsilon_{253\ nm}$= 13,600 M^{-1} cm^{-1} for guanosine, $\varepsilon_{271\ nm}$= 9100 M^{-1} cm^{-1} for cytidine and, ε_{262nm}= 10,100 M^{-1} cm^{-1} for uridine).[132]

DNA and RNA were purchased from Integrated DNA Technologies (Coralville, IA) and GE Dharmacon (Lafayette, CO), respectively. The DNA and RNA were gel purified as described in each method section. Concentrations of nucleic acid solutions were calculated by using the absorbance at 260 nm and single-stranded extinction coefficients (DNA1 ε_{260nm} = 176,500 $M^{-1}cm^{-1}$, RNA1ε_{260nm} = 190,700 $M^{-1}cm^{-1}$, H69 RNA_{ε} ε_{260nm} = 189,400 $M^{-1}cm^{-1}$, H69 primer ε_{260nm} = 192,000 $M^{-1}cm^{-1}$, A site primer ε_{260nm} = 165,500 $M^{-1}cm^{-1}$, 790 primer ε_{260nm} = 173,900 $M^{-1}cm^{-1}$, PTC (peptidyl transferase center) primer ε_{260nm} = 202,400 $M^{-1}cm^{-1}$).[133] The pUC19 plasmids were isolated and purified by using a plasmid maxi-prep kit from Qiagen (Germantown, MD).

DNA1: 5' TCTCCTTCTTGGTTCTCTTCTC 3'

DNA2: 5' GAAGAGAACCAAGAAGGAGAGA 3'

RNA1: 5' UCUCCUUCUUGGUUCUCUUCUC 3'

H69 RNA (UUU): 5' GGCCGUAACUAUAACGGUC 3'

H69 RNA (ΨΨΨ): 5' GGCCGΨAACΨAΨAACGGUC 3'

H69 primer: 5' CGACAAGGAATTTCGCTACC 3'

790 primer: 5' ACCAAGTCGACATCGTTT 3'

A-site primer: 5' GTTAAGCTACCTACTTCT 3'

PTC primer: 5' CACTTTAAATGGCGAACAGCC 3'

2.3.3 Cell lines

The human cancer cell lines HeLa, H1299, MDA-MB-231, and MDA-MB-453 were obtained from Dr. Young-Hoon Ahn's lab.[134-137] The human prostate cancer cell lines (DU145 and LNCaP) were obtained from Dr. K.V. Honn's lab in the Chemistry Department.[138,139] The normal prostate cell line, RWPE-1, was received from Dr. Zhihui Qin's lab in the Eugene Applebaum College of Pharmacy and Health Sciences, Wayne State University.[140]

2.3.4 Instrumentation

HPLC analysis was performed on a Waters 600 LC, with a 717 autosampler (Waters, Milford, MA), UV-detector, and a Supelco Discovery C18 column (5 μm particle diameter; 4.6 mm i.d. × 250 mm, Sigma-Aldrich, St. Louis, MO). The LC-MS analysis was carried out on a Shimadzu 8040 Nexera X2 Ultra High Performance/Pressure Liquid Chromatograph (UPLC) system with a quadrupole type tandem mass spectrometer (Shimadzu, Columbia, MD). An Acquity UPLC HSS T T3 C18 column was (1.8 μm particle diameter, 2.1 × 100 mm, Waters, Milford, MA) was used in LC-MS. The MALDI mass spectra were acquired on a Bruker UltrafleXtreme TOF (Bruker Daltonics, Billerica, MA). Whole cell platinum levels were quantified by using an Agilent 7700X ICP-MS, ASX-500 series ICP-MS autosampler with Agilent MassHunter software (Santa Clara, CA). The gel images were obtained on a Typhoon FLA 9500 instrument (GE Healthcare). The pH of the solutions was determined by using a Mettler Toledo (Columbus, OH) pH meter with an Inlab Versatile Pro pH electrode (electrolyte 3 mol/L KCl).

2.4 Methods

2.4.1 Preparation of activated cisplatin complexes

Cisplatin (1 mg, 3.3 μmol) and $AgNO_3$ (30 mg, 177 μmol) solutions were prepared by dissolving separately in 333.3 μL and 353.2 μL anhydrous DMF volumes to make 10 mM and 500 mM solutions, respectively.[48] To a 200 μL of prepared cisplatin solution 1 equivalent of $AgNO_3$ was added to give a 9.8 mM solution of mono-activated (aquated) cisplatin (compound **3**). To obtain bis-activated complex, the solutions were mixed in a 1:2 molar ratio. The reaction mixture was shaken at 37 °C for 16 h in the dark on a vortex mixer (**Scheme 2.2**). The resulting AgCl was precipitated by centrifugation at 14,000 rpm for 10 min, and the supernatant contained the desired mono-activated cisplatin (**3)**. Activated cisplatin was freshly prepared every time and diluted to intermediate stock concentrations with ddH_2O just prior to use.

Scheme 2.2. Generation of the mono-activated platinum species (3). One chlorido ligand will be removed as AgCl to yield the mono-activated species, compound **3**.

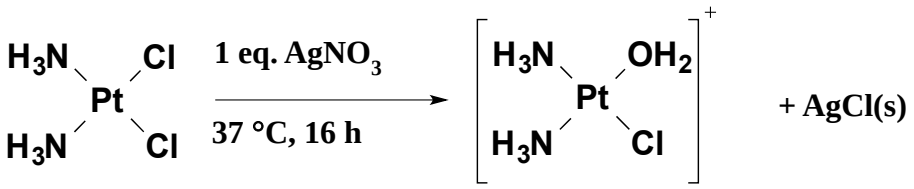

cisplatin **mono-activated cisplatin(3)**

2.4.2 Synthesis and purification of cis-dichlorido[(2-*β*-D-glucopyranosidyl)propane-1,3-diammine]platinum, compound 5

Synthesis of compound **5** was done as described previously from compound **4**.[82] Synthesis, purification, and NMR characterization of compound **4** (calculated mass 252 Da) was done by Amr Sonousi in Dr. David Crich's lab, Department of Chemistry, Wayne State University. Compound **4** (21 mg, 83 μmol) and K_2PtCl_4 (27 mg, 65 μmol)

solutions were prepared by dissolving in 1 mL of ddH_2O. To generate **5**, they were mixed (1:1 molar ratio, 65 μmol) and stirred at room temperature for 2 days in the dark. The color of the solution changed from orange to light brown. One μL of the crude product solution was mixed with 1 μL of saturated 3-hydroxypicolinic acid (3-HPA) matrix in 50% acetonitrile and analyzed by MALDI in the positive mode. The product was then purified by HPLC on C18 (5 μm particle diameter; 4.6 mm i.d. × 250 mm, Sigma-Aldrich, St. Louis, MO) on a Waters 600 LC with a 717 autosampler (Waters, Milford, MA) and UV-detector (**Figure 2.4a**). The mobile phases of 40 mM ammonium acetate, pH 6.5 (NH_4OAc) (buffer A), and 40% acetonitrile (buffer B) were used. The column was equilibrated with 95% (v/v) buffer A and 5% (v/v) buffer B, and then the percentage of buffer B was increased in a linear gradient from 5 to 35% over 30 min. The product peak was collected, dried, and characterized by MALDI-MS (**Figure 2.4b**) and ^{1}H-NMR (D_2O solvent, Agilent DD2-600 MHz NMR with Agilent (^{1}H-^{19}F/^{15}N-^{31}P) 5 mm PFG One NMR Probe). The total dry weight of purified **5** (calculated mass 518 Da) was about 25 mg (~75% yield) and it was light yellow in color.

Scheme 2.3. Chemical synthesis, structure of the carbohydrate-linked cisplatin analog (*cis*-dichlorido[(2-*β*-D-glucopyranosidyl)propane-1,3-diammine]platinum (5)), and activation step.

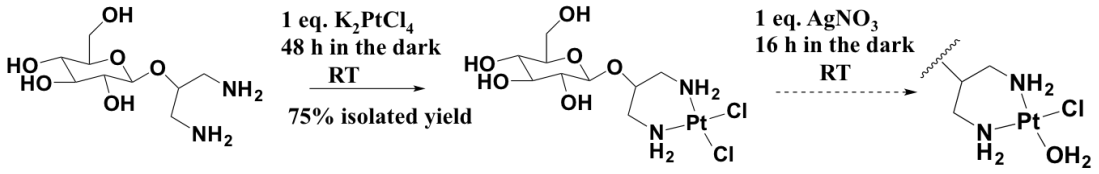

(4) **(5)** **mono-activated 5**

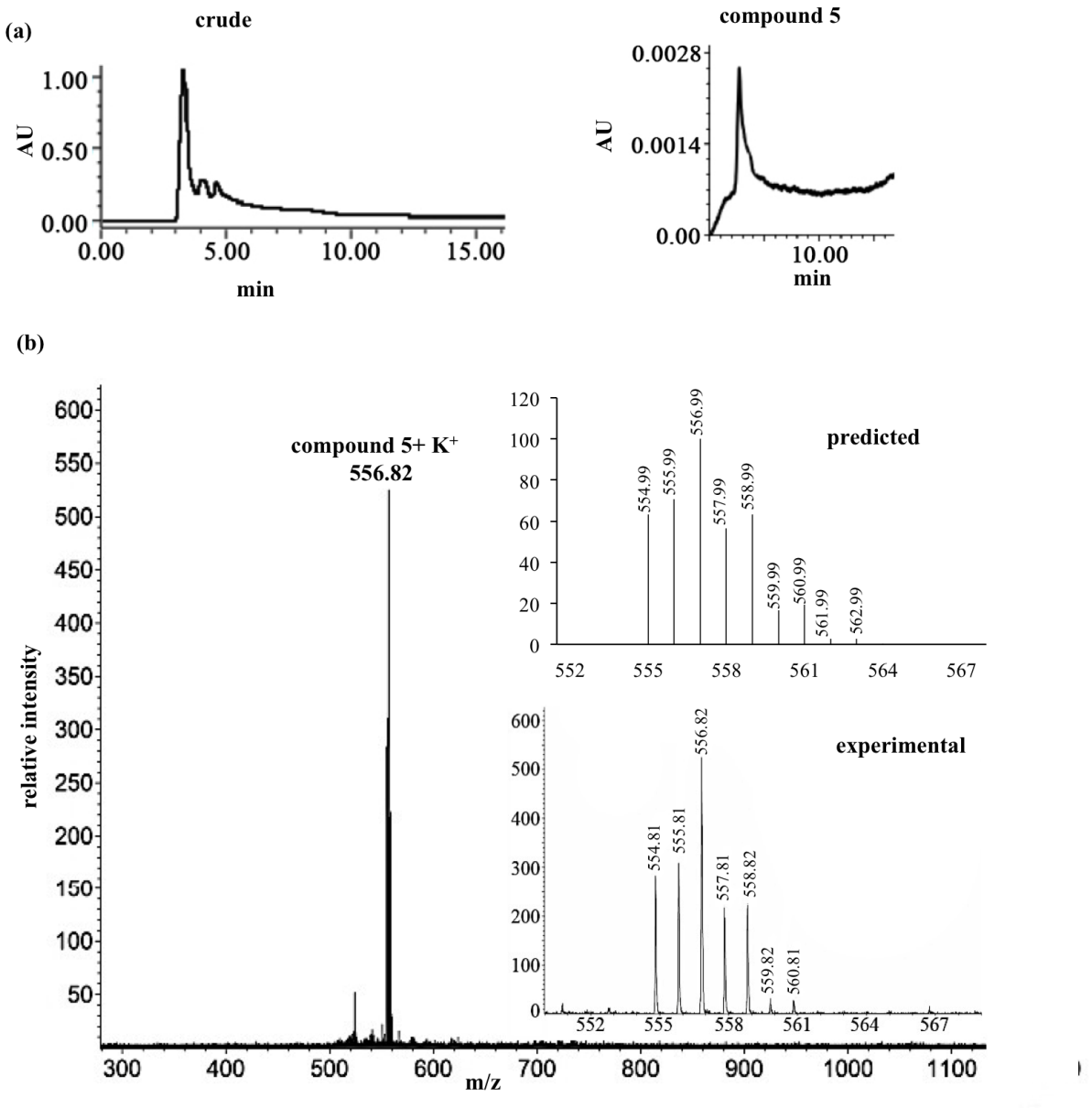

Figure 2.4. Isolation and characterization of compound 5. (a) The HPLC trace (C18 column, eluted at 3.5 min with linear gradient of B from 5 to 35% over 30 min, flow rate 1 mL/min) for crude and purified **5**. (b) The MALDI-MS spectrum for purified **5**. The calculated mass for [compound **5**+K^+] is 556.99 Da and the observed (3-HPA matrix, positive detection mode) was 556.82 Da. The inset shows the isotopic distribution for predicted and observed complex.

MALDI-MS spectrum showed a peak at 557 Da, which is the mass for **5** (518 Da) associated with K^+. The isotopic distribution observed on MALDI-MS as shown is the inset of **Figure 2.4b** matched the predicted pattern as shown. Platinum has five stable

isotopes, ^{192}Pt (0.7%), ^{194}Pt (32.8%), ^{195}Pt (33.7%), ^{196}Pt (25%), and ^{198}Pt (7%) and Cl has two stable isotopes, ^{35}Cl (75.8%) and ^{37}Cl (24.2%). Compound **5**: ^{1}H NMR (600 MHz, D_2O): δ 4.36 (d, *J*(H1,H2) = 7.7 Hz, 1H;H1), 3.57 (m, 1H; H7), 3.72 (dd, *J*(H6a,H6b) = 12.5 Hz, *J*(H5,H6a) = 2.4 Hz, 1H; H6a), 3.54 (dd, *J*(H6a, H6b) = 12.1 Hz, *J*(H5, H6b) = 5.3 Hz, 1H; H6b), 3.10-3.33 (m, 4H; H2, H3, H4, H5), 2.51-2.61 (m, 2 × 2H; H8, H9) (**Appendix A, Figure A4**).

Mono-activation of **5** was carried out in ddH_2O. A 9.8 mM solution of **5** was prepared by dissolving 6 mg (11.6 μmol) in 1.16 mL of ddH_2O. The $AgNO_3$ solution (500 mM) was prepared by dissolving 30 mg in 353.2 μL of ddH_2O. To obtain the mono-activated complex, one equivalent of $AgNO_3$ (11.6 μmol, 23.2 μL) was added to the solution of **5** (**Scheme 2.3**). The activated complex was divided into 50 μL aliquots, dried in a speed vac concentrator, stored in -80 °C, and redissolved in ddH_2O just prior to use.

2.4.3 Reaction of mono-activated 5 with nucleosides

Adenosine, guanosine, cytidine, and uridine nucleoside solution stocks were prepared by dissolving about 2 mg in 500 μL of water, and the exact concentrations were determined by measuring the UV absorbance.[131,132] The reactions were carried out by mixing nucleoside (0.1 mM): mono-activated **5** (0.5 mM) in a 1:5 ratio at 37 °C for 16 h in the dark. The reaction mixtures were quenched by adding 3 μL of 3 M NaCl and vortexing. The quenched reaction mixtures were analyzed by reverse-phase HPLC on a Supelco Discovery C18 column (5 μm particle diameter; 4.6 mm i.d. × 250 mm) on a Waters 600 LC with a 717 autosampler and UV-detector. The mobile phases of buffer A and buffer B were used. The column was equilibrated with 95% buffer A and 5% buffer

B, and then the percentage of buffer B was increased in a linear gradient from 5 to 35% over 30 min.

2.4.4 Kinetic parameters for the reaction between G and dG nucleosides with Pt(II) complexes

For the kinetic measurements mono-activated cisplatin (**3)** and mono-activated compound **5** were used. Reactions were carried out by mixing sodium phosphate buffer, pH 7.0 (final concentration 25 mM) with freshly prepared and diluted nucleoside solution (final concentration 0.1 mM) and mono-activated Pt(II) (final concentration 5 mM) in a 1:50 molar ratio. The total volume of the master reaction mixture was adjusted up to 300 μL by adding ddH_2O. The reactions were vortexed and incubated at 37 °C in the dark up to 6 h. At varying time points, 45 μL of sample was removed from the reaction mixture and quenched by adding 3 μL of 3 M NaCl (final concentration 188 mM) and vortexing. The quenched samples were immediately frozen on dry ice and stored at -80 °C until further analysis. The quenching time points were 0.5, 1, 2, 3, 4 and 6 h. This procedure was repeated three times for each nucleoside reaction. The samples were centrifuged at 10,000 rpm for 10 min before injection onto the HPLC. The same HPLC method described in **Section 2.4.3** was used, and 35 μL from each sample was injected onto the column. The retention times for the nucleosides were confirmed by comparing to standards and the peak areas (unreacted nucleoside and products) were calculated using Empower software (Empower Software Solutions, Inc., Orlando, FL). The pseudo-first-order rate constants were calculated by plotting the ratio of unreacted nucleotides over quenching times. HPLC standard calibration curve for G (from Bett Kimutai) is shown in **Appendix A, Figure A1**.

Scheme 2.4 shows the kinetic model for a reaction between X (nucleoside, RNA, or DNA) and Pt(II) under pseudo-first-order reaction conditions. The reaction between the Pt(II) complex and X was considered to be a second-order reaction as shown in **Equation 2.1**.[51] To maintain pseudo-first-order conditions, high Pt(II) concentrations were used, in which a ≥50-fold excess over X was used (the specific concentrations are mentioned in the Methods section for each experiment).[47] Therefore, k_{obs} was equal to the product of the Pt(II) concentration and apparent second-order rate constant, $k_{2,app}$ **(Equation 2.2)**. To experimentally obtain k_{obs}, the unreacted RNA ratio $[X_t]/[X_0]$ and time were plotted to fit an exponential decay (**Equation 2.3)**, in which the m2 corresponded to k_{obs}.

Scheme 2.4. Kinetic model for the reaction between Pt(II) complexes and X, in which X can be nucleosides, RNA or DNA.

Pt(II) + X $\xrightarrow{k_{app}}$ Pt-X X= nucleoside, RNA, or DNA

$-d[X]/dt = k_{app}[Pt(II)][X]$ **Equation 2.1**

Under pseudo-first-order conditions,

$k_{obs} = k_{app}[Pt(II)]$ **Equation 2.2**

$-d[X]/dt = k_{obs}[X]$

$\ln[X_t]/[X_0] = -k_{obs}t$

The unreacted X ratio is $[X_t]/[X_0]$, and

$[X_t]/[X_0] = A e^{-k_{obs}t}$ **Equation 2.3**

Y= m1 exp (-m2X)+m3, in which Y= $[X_t]/[X_0]$, m2= k_{obs}, m1= amplitude of the reaction, m3= extent of the reaction

2.4.5 Product characterization by LC-MS

The dG or G and mono-activated **5** reaction mixtures from **Section 2.4.4** (after 16 h reaction) were analyzed on LC-MS or by direct injection onto a mass spectrometer

(details below). The analysis was carried out on a Shimadzu 8040 Nexera X2 Ultra High Performance/Pressure Liquid Chromatograph (UPLC) system with a quadrupole type tandem mass spectrometer (Shimadzu, Columbia, MD). The sample was introduced and ionized by using an electrospray ionization (ESI) probe (nebulizing gas flow 3 L/min, drying gas flow 15 L/min, interface 4.5 kV, heat block temperature 400 °C). An Acquity UPLC HSS T T3 C18 column (1.8 μm particle diameter, 2.1 × 100 mm, Waters, Milford, MA) was used, and the column oven was maintained at 40 °C. For the LC buffers, 10 mM NH_4OAc, pH 5.2 (buffer C), and 10 mM NH_4OAc (10%) in 10% acetonitrile (buffer D) were used. Elution was carried out with a flow rate of 800 μL/min, from 100 to 67% buffer C and increase in D from 0 to 33% over the course of a 17 min gradient. For direct injection, 2 μL of the reaction mixture was introduced to the mass spectrometer with a flow rate of 300 μL/min using buffer D. Peaks were identified by using LabSolutions software.

2.4.6 Ethanol precipitation of nucleic acids

To a centrifuge tube containing nucleic acid solution (V volume), 2.5 V of 100% ethanol and 0.1 V of 3 M NH_4OAc were added and the sample was placed on dry ice for 45 min. The sample was then centrifuged at 14,000 rpm for 45 min at 4 °C. The supernatant was carefully removed and 100 μL of 70% ethanol was added to the pellet. The sample was placed on dry ice for 15 min and centrifuged at 14,000 rpm for 15 min at 4 °C. The supernatant was removed and the remaining pellet was dried in a speed vac concentrator. The dried nucleic acid pellet was dissolved in 50 μL of ddH_2O by vortexing.

2.4.7 Radiolabeling of the RNA at the 3' end and purification

The 3' end of each H69 RNA (UUU and ΨΨΨ) was radiolabeled using [5'-^{32}P]-pCp and T4 RNA ligase.[141] For the radiolabeling RNA (50 pmol per reaction), 10 μCi of [5'-^{32}P]-pCp, 30 units of T4 RNA ligase enzyme, 3 μL of 10× ligase buffer (50 mM Tris-HCl, pH 7.5, 10 mM $MgCl_2$, 1 mM dithiothreitol), 4 μL of DMSO, and ddH_2O (total volume is 30 μL) were used. Following a 16 h incubation time at 4 °C, the labeled RNA was ethanol precipitated and gel purified on a 20% denaturing polyacrylamide gel (0.8 mm thick, acrylamide: bisacrylamide 19:1, 1× TBE). Following PAGE, the RNA bands were visualized by autoradiography, excised, and eluted by the crush-and-soak method in 350 mM NaOAc, pH 5.3, 0.1 mM EDTA buffer overnight at 4 °C.[142] Desalting of the purified RNAs was carried out using Sep-pak C18 columns.[132] The eluted RNA was dried in a speed vac concentrator. The dried nucleic acid pellet was dissolved in 50 μL of ddH_2O by vortexing.

2.4.8 Radiolabeling of nucleic acids at the 5' end[143]

For the labeling of 50 pmol DNA or RNA, 10 μCi [γ-^{32}P] ATP and 10 units T4 polynucleotide kinase were reacted in 3 μL of 10× T4 polynucleotide kinase buffer (50 mM Tris·HCl, pH 7.6, 10 mM $MgCl_2$, 5 mM DTT, 0.1 mM spermidine, and 0.1 mM EDTA). The total volume was adjusted to 30 μL with ddH_2O and the sample was incubated at 37 ^{o}C for 45 min. The labeled nucleic acid was isolated by gel purification as described for 3' labeling followed by desalting.

2.4.9 Platination rates for the reactions with oligonucleotides

The DNA1 and RNA1 strands were used for kinetic experiments. The unlabeled DNA or RNA (0.7 μM) and corresponding 5'-radiolabeled DNA or RNA (50,000-60,000

cpm) were mixed with buffer (final concentration of 12 mM K^+ and 20 mM Na^+, pH 6.2) and ddH_2O to a volume of 50 μL in an 0.6 mL centrifuge tube, placed in a boiling water bath for 2 min, and then on ice for 5 min. The reaction was then spun down and allowed to reach room temperature before adding the Pt(II) compound. The sample was then incubated with mono-activated Pt(II) complex (final concentration of 94 μM) at 37 °C in the dark. The total volume of the reaction mixture was 60 μL. The reactions were quenched at different time points by taking 5 μL aliquots and putting into a tube containing 1 μL of 2 M NaCl, followed by freezing of the samples on dry ice. A control reaction was also carried out by adding water instead of the platinum compound. To each reaction 0.4 μL of loading buffer that contains 0.1% bromophenol blue, 0.1% xylene cyanol, 1× Tris base, boric acid, EDTA, and 8 M urea was added, and the solutions were loaded onto a 20% polyacrylamide gel (0.4 mm thick, acrylamide: bisacrylamide 19:1, 1× TBE) and run at 48 V/cm for about 3 h. The gel image (illustrated in **Figure 2.5a**) was analyzed and the unreacted nucleic acid was quantified using ImageQuant™ software (GE Healthcare) using the following **Equation 2.4**.

Equation 2.4:

Fraction of unreacted RNA ($[X_t]/[X_0]$)

$$= \frac{(\text{unreacted RNA counts} - \text{background (bkg)counts})}{(\text{unreacted RNA counts} - \text{bkg counts}) + (\text{product RNA counts} - \text{bkg counts})}$$

Kaleidograph 4.1 software was used to plot the fraction of unreacted nucleic acid over time to obtain the platination rates (**Figure 2.5b**). Each reaction rate was obtained by averaging three trials. For comparison, experiments were carried out with bis-activated platinum complexes as well. To compare the salt-dependent reaction rates, reaction rates

were obtained in a 12 mM K^+ and 5 mM Na^+, pH 6.2 buffer. Each reaction rate was obtained as an average from three trials.

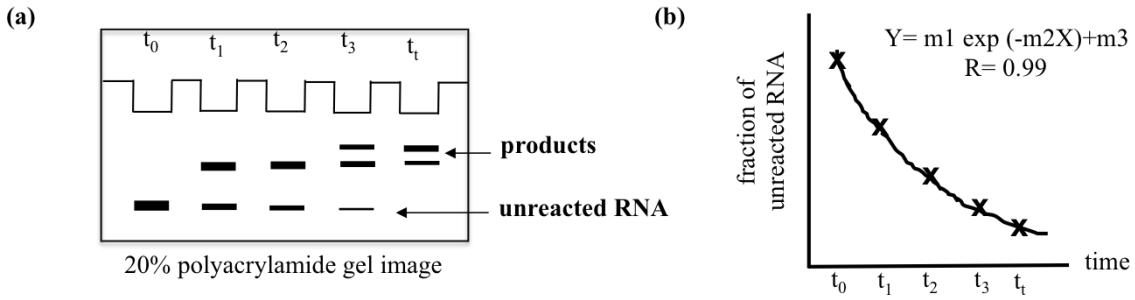

Figure 2.5. Schematic diagram of the gel and graph for kinetic experiments. (a) A schematic of the electrophoretic mobility shift assay is shown. The quenched reactions are loaded onto a 20% denaturing polyacrylamide gel and the products and reactants are separated and quantified. The concentration of unreacted RNA decreases over time from t_0 to t_t. (b) A representation of the exponential decay of the reactant over time.

2.4.10 Cisplatin coordination rates to H69 RNA in the presence of aminoglycosides

The basic kinetic experiment protocol described in **Section 2.4.9** was followed for this experiment. The labeled (50,000-60,000 cpm) and unlabeled H69 hairpins (final concentration of 0.7 μM) were incubated with freshly prepared aminoglycoside (final concentration 1, 3, or 6 μM) at 37 °C for 30 min in buffer (final concentration of 12 mM K^+ and 20 mM Na^+, pH 6.2) and water. This step was followed by incubation with mono-activated cisplatin (final concentration of 188 μM) at 37 °C in the dark as described above. The final volume of the reaction mixture was 60 μL. The experiment was repeated three times to obtain each rate for neomycin, paromomycin and streptomycin at 1, 3, and 6 μM concentrations.

2.4.11 Platinum complex reaction with plasmid DNA

The pUC19 plasmids were isolated by QIAGEN Plasmid Maxi Kit following the user protocol. Reaction tubes were prepared containing 0.5 μg of DNA plasmid, 10 mM sodium phosphate buffer (pH 7.4), and water (final volume 10 μL). The plasmid was

platinated with either freshly mono-activated cisplatin (final concentration of 160 μM) or compound **5**, separately. The reactions were incubated at 37 °C in the dark for 24 h. At varying time points, reactions were quenched by adding 3 μL of 3 mM NaCl and 1 μL of loading dye (0.25% bromophneol blue, 0.25% xylene cyanol, 30% glycerol). A control reaction was also prepared without adding Pt(II) compound. The quenched reactions were then loaded on to a 1.2% agarose gel and ran at 75-80 V until the xylene cyanol dye band has migrated off the gel.

2.4.12 Platinum complex reaction with duplex DNA oligomer

A model DNA was chosen to examine the impact of platination on DNA bending.[24] The DNA1 (3 nmol) was platinated with bis-activated cisplatin, or **5** (6 nmol), by reacting in a 1:2 ratio, then the products were purified and desalted by using 20% polyacrylamide gel electrophoresis and ethanol precipitation as described earlier. Platinum adduct formation was confirmed by MALDI-MS. For that, 2 μL (300 pmol) of platinated DNA was mixed with 1 μL of saturated 3-hydroxypicolinic acid (3-HPA) matrix in 50% acetonitrile, spotted on a MALDI plate, and allowed to dry. The mass spectra were acquired on a Bruker UltrafleXtreme TOF (Bruker Daltonics, Billerica, MA) instrument in the positive-ion reflector mode.[95]

The 5' end of the DNA2 strand (50 pmol) was radiolabelled using [γ-^{32}P] ATP, gel purified, and desalted as described in **Section 2.4.8**. For the annealing reaction, 60,000-100,000 cpm from the radiolabelled DNA2 strand and 20 pmol from platinated DNA1 strand were used. A control reaction was done with unplatinated DNA1 as well. The total reaction volume was adjusted to 10 μL with deionized water and the reaction was brought to 90 °C in a water bath. It was allowed to cool slowly to room temperature

over 6 h, and then the temperature was further reduced to 4 °C and held constant for an additional 2 h by keeping in the cold room. To the annealed oligomer (10 µL), 1 µL of 10 mM ATP, 2 µL of 10× T4 DNA ligase buffer (400 mM Tris-HCl, 100 mM $MgCl_2$, 100 mM DTT, 5 mM ATP, pH 7.8), and 1 unit of T4 DNA ligase were added. After adjusting the total volume to 20 µL with water, the ligation reaction was allowed to proceed for 1 h at room temperature. The ligation reactions were loaded onto an 8% native polyacrylamide gel (0.8 mm thick, mono:bisacrylamide ratio of 29:1, 1× TBE, 10 min pre-run) and run (89 mM Tris-borate, 89 mM acid, 2 mM EDTA) at approximately 10 V/cm for 5 h until the bromophenol blue dye marker had migrated off the gel. A water-cooled electrophoresis apparatus was used to maintain the temperature of the gel at room temperature. Migration of all the DNA bands in the original autoradiogram was measured manually and used for the bend angle calculations. A calibration curve for distance migrated over the length (bp) was plotted for the unplatinated control. Using the calibration curve, calculated lengths were obtained for the platinated oligomer bands with reduced mobility. The relative mobility (R_L) of the platinated DNA (the ratio between the calculated length of the oligomer and actual length (L)) was calculated for the 110 or 132 bp sized oligomers. Determination of the DNA bend angle was performed using the equation $R_L - 1 = (9.6 \times 10^{-5} L^2 - 0.47)(RC)$, in which L represents the length of a particular oligomer with relative mobility R_L and RC is the curvature relative to DNA bending of an A tract (A DNA with a known bend angle).[24,144,145] The detailed calculations with the results are discussed in **Chapter 4**.

2.4.13 Isolation of 70S ribosomes and ribosomal subunits

Bacterial ribosomes or ribosomal subunits were isolated from the *E. coli* DH5α

strain by using the sucrose gradient method.[146] *E. coli* was grown to 0.4 OD and the culture was centrifuged at 6,000 g for 20 min to pellet the cells. The pellet was resuspended in buffer A (20 mM HEPES-KOH, pH 7.5, 100 mM NH_4Cl, 10 mM $MgCl_2$, and 0.5 mM EDTA) and lysed on a French Press. After adding DNase I (5 μg/mL), the lysate was incubated on ice for 15 min. The lysate was centrifuged twice at 15,000 rpm for 30 min and the supernatant was collected. After adjusting the NH_4Cl concentration in the supernatant to 500 mM, the sample was centrifuged at 42,000 rpm for 4 h to pellet the crude ribosomes. The pellet was washed and resuspended in buffer B (20 mM HEPES-KOH, pH 7.5, 200 mM NH_4Cl, 1 mM $MgCl_2$). The concentrations of the crude ribosomes were determined by using a Nanodrop UV-visible spectrometer. About 30 OD of crude ribosomes were layered on 40 mL of a 10-30% sucrose gradient in buffer B with 1 mM $MgCl_2$ and centrifuged in a swinging bucket rotor on a Sorvall WX 80 ultra centrifuge at 19,000 rpm for 19 h. The ribosomes and subunits were collected separately. Fractions of the same type were combined and the Mg^{2+} concentration was raised to 10 mM. Ribosomes were pelleted by centrifugation at 42,000 rpm for 24 h at 4 °C. Pure ribosomes were redissolved in storage buffer (ribosome subunit stock buffer: 20 mM HEPES-KOH, pH 7.5, 10 mM $MgCl_2$, 30 mM KCl; full ribosome stock buffer: 20 mM HEPES-KOH, pH 7.5, 6 mM $MgCl_2$, 30 mM NH_4Cl) and stored at -80 °C.

2.4.14 Platination of ribosomal RNA and rRNA purification

For each reaction, 15 pmol of ribosomes/subunits were used. Platination was carried out by reacting mono-activated platinum(II) compounds with ribosomes/subunits in 1:200 pmol ratio for 16 h at 37 °C in the dark (72 mM HEPES, pH 6.5, 3.6 mM $MgCl_2$, 88 mM KCl). Excess platinum(II) compound was removed by ethanol

precipitation. Phenol-chloroform extraction with 10 mM EDTA was done to extract the reacted rRNA followed by ethanol precipitation. Isolated rRNA was dissolved in ddH_2O and the concentration was determined using a Nanodrop UV-visible spectrometer (1 OD= 23.5 pmol of 70S rRNA, 1 OD= 69 pmol of 30S rRNA).

2.4.15 Reverse –transcription and primer extension reactions

The appropriate DNA primers were radiolabeled with [γ-^{32}P] ATP at the 5' end as described earlier. Platinated rRNA (500 ng) and 1 μL of radiolabeled primer (60,000-100,000 cpm) were incubated together at 80 °C for 3 min and then allowed to cool down to room temperature for 5 min. The master mixture for a reverse transcription reaction was prepared by mixing 24 units of ImProm-II reverse transcriptase enzyme, 1 μL of 5× reverse transcriptase reaction buffer, and 0.4 μL of 50 mM $MgCl_2$. To the primer-annealed platinated rRNA, 1.65 μL of the master mixture, 1 μL of dNTP (stock concentration 10 mM), and ddH_2O (total volume 5 μL) were added. Primer extension was carried out at 43 °C for 1 h. For sequencing, total RNA was used with the corresponding radiolabeled primer. For the sequencing reverse transcription reaction 1 μL of dNTP:ddNTP 1:4 (0.5 mM:2 mM) was used instead of the dNTP mixture. Termination of the reactions was done by heating the reaction mixture at 95 °C in a water bath for 2 min after adding 2 μL of denaturing loading dye (80% formamide, 1× TBE, 0.02% bromophenol blue, 0.02% xylene cyanol) and quickly placing on ice. Reactions (50,000 cpm per lane) were loaded into 10% denaturing polyacrylamide gels (0.4 mm thick, acrylamide:bisacrylamide 19:1, 0.5× TBE, 7 M urea). Gels were run at 33 V/cm, for approximately 3 h. Gels were exposed to a phosphor screen overnight and imaged on a Molecular Dynamics Phosphorimager and analyzed using ImageQuant software.

2.4.16 Initiate cell growth from a frozen stock

Autoclaved tips and tubes were used at all experiments. The experiments were carried out in a Laminar floor hood under aseptic conditions to avoid contaminations. Sterile media and solutions were used for the cell growth and assays and 70% ethanol was used to wipe the surfaces. Cancer cells were grown in Dulbecco's Modified Eagle's (DMEM) medium with heat inactivated 10% FBS and penicillin (5 units/mL) and streptomycin (5 units/mL) as antibiotics. For the normal cells, keratinocyte media containing prequalified human recombinant epidermal growth factor 1-53 (EGF 1-53) and bovine pituitary extract (BPE) was used. The media, solutions, and the enzymes were stored at 4 °C and thawed at 37 °C water bath prior to use. All of the cultures were incubated in a humidified, 37 °C, 5% CO_2 incubator.

Frozen vials containing the cells were removed from the liquid nitrogen freezer and immediately thawed by placing in a 37 °C water bath for 1-2 min. The thawed cells were transferred to a sterile centrifuge tube containing 1 mL medium and centrifuged for 5 min at 200 × g. The supernatant was discarded and the pellet was resuspended by adding 1 mL medium. It was then transferred to a culture plate that contains appropriate amount of medium and incubate at 37 °C to let the cells attach to the plate. The cells were monitored and the medium was changed after 5-6 days. The cells were grown until they reach confluency.

2.4.17 Trypsinizing and subculturing cells from a monolayer

After reaching 80-90% confluency, cells were dispersed by trypsin treatment and reseeded onto new plates. The medium was removed from the primary culture and PBS was added to wash the cells. Trypsin-EDTA solution (0.25% for cancer cells and 0.05%

for normal cells) was added and incubated at 37 °C for about 10 min to dislodge the adhered cells. Tapping on the culture dish facilitated dislodging as well. Cells were observed under the microscope to ensure that the cells are detached. For cancer cells, small volume of medium containing FBS was added to the plate to inactivate trypsin, and mixed by pipetting to make a homogenous cell suspension. For normal cells, after adding FBS containing medium, cells were transferred to a centrifuged tube and centrifuged for 2 min at 200 × g. Supernatant was removed and the pellet was resuspended in keratinocyte media. Equal volume of the cell suspension was added to fresh plates with media and incubated at 37 °C in a 5% CO_2 incubator. The media was changed as needed and the cells were grown to confluency.

2.4.18 The anticancer potency of compound 5 using MTT assay

After reaching the confluency, the cells were trypsinized and collected in a 15 mL centrifuge tube. The total volume was adjusted to 5 mL by adding medium and mixed well by pipetting. From the cell suspension 10 μL was taken and placed on the hemocytometer to count the cell number under the microscope. Cancer cells (10,000/well) were seeded in a transparent flat-bottom 96-well plate with medium. Cells were grown for 24 h to allow them attached the plate. After that, the media was removed and fresh media and varying concentrations of the platinum compounds were added to the wells. Two controls were done with each experiment. A growth control well had cells and media, but no platinum compounds, whereas blank control wells had only media. After 72 h of incubation, 10 μL of MTT stock (5 mg/mL) was added to all the wells and incubated for additional 4 h. Then media was removed and 200 μL of DMSO was added to dissolve the formazan product formed by viable cells. After 10 min incubation, the

optical density of each well was measured at 520 nm using a microplate reader (BioTek synergy H1 hybrid reader BioTek instruments, Winooski, VT). For each drug concentration, % cell viability was calculated using the following equation.

Equation 2.5:

$$\%\ \text{cell viability} = \frac{\text{OD per drug concentration} - \text{OD of the blank control}}{\text{OD of the growth control} - \text{OD of the blank control}}$$

The IC_{50} value was obtained by plotting the % viability against the drug concentration, in which IC_{50} is the drug concentration that gives the 50% cell viability. Each experiment was repeated two or more times in parallel to obtain the IC_{50} values.

2.4.19 Quantify the platinum levels in the cells by ICP-MS

Accumulated Pt in the human cells was quantified by using an Agilent Technologies 7700 series ICP-MS instrument (Santa Clara, CA). Platinum levels in human prostate cancer cell line, DU145 and normal prostate cell line, RWPE-1 were quantified for comparison. The cells were grown in a monolayer until confluency, trypsinized, and homogenized. From the cell suspension, an equal number of cells (460,000) were seeded onto 6 cm culture dishes and grown for 18 h. The media was removed and the cells were washed with PBS. To each plate, platinum compound solution (final concentration of 50 μM) and keratinocyte media was added to give a volume of 3 mL. The cells were incubated for 2 h at 37 °C. The media was removed, cells were collected into centrifuge tubes by trypsinizing, and washed with PBS. Homogenized cell solutions were prepared by mixing, and cell number in each tube was counted by using a hemocytometer. Then, the cells were digested by adding 300 μL of concentrated nitric acid and incubating at room temperature for 16 h. The samples were diluted by adding ddH_2O up to 3 mL prior to the analysis. A standard series of Pt

solutions with 0.5, 1, 5, 10, 25, 50, 100, 200 ppb concentrations was prepared in 2% HNO_3 and 0.5% HCl solution for calibration. Two independent trials for each cell line were carried out simultaneously for cisplatin and compound **5**. The digested cell samples were analyzed in the ICP-MS along with solvent blanks, no-drug blank, and standards (plasma gas flow 15 L/min, nebulizer pump speed 0.3 rps, spectrum acquisition mode, 100 sweeps per sample, 3 replicates per sample, general purpose plasma mode). The instrument was calibrated with 10 ppb internal standard solution that contains ^{209}Bi. The recommended platinum isotope with the least polyatomic interferences for ICP-MS, ^{195}Pt was detected.[147,148] The data were obtained under high energy He tune mode in which the internal standard signal was stable and the R value for the calibration curve was 1. Furthermore, 10 ppm validation standard was run after the samples for quality control.

CHAPTER 3

CARBOHYDRATE-LINKED PLATINUM COMPOUND: PRODUCT CHARACTERIZATION AND KINETIC STUDIES WITH NUCLEOSIDES

3.1 Abstract

When it comes to new drug development, an understanding of the mode of action is needed to refine the therapeutic approaches to further enhance efficacy. This thesis work focuses on a novel class of cisplatin-derivatives, carbohydrate-linked platinum complexes, due to their reported higher cell potencies, tumor selectivity, and low toxicity. To get insight into the behavior of glycoconjugated platinum(II) complexes compared to cisplatin, *cis*-dichlorido[(2-*β*-D-glucopyranosidyl)propane-1,3-diammine] platinum(II) (compound **5**) was utilized. First, the binding preference of compound **5** was established by reacting it with DNA and RNA nucleosides and analyzing the products by HPLC and LC-MS. The compound reacted more with guanosine (G) and deoxyguanosine (dG) over other nucleosides. To further characterize the differential reaction rates, HPLC-based kinetic experiments were carried out with dG and G nucleosides and mono-activated **5** and compared to mono-activated cisplatin. Overall, 2.5-fold or lower reaction kinetics for compound **5** were observed compared to cisplatin. The reduced coordination rates of **5** compared to cisplatin are likely the result of steric hindrance from the bulkier sugar group at the site of reaction. Perhaps surprisingly, compound **5** showed a higher coordination rate with the RNA nucleoside G compared to the corresponding DNA nucleoside dG. This preference of **5** for G over dG is opposite of the preference of cisplatin for dG.

3.2 Introduction

Chemotherapy along with radiation therapy is the most common way to treat cancer.[149] Chemotherapeutics include alkylating agents (*e.g.*, busulfan, chlorambucil, carmustine), hormones, antitumor antibiotics, and metal complexes such as cisplatin.[150] Among them, cisplatin and platinum-based drugs have received much attention due to their successful cure rates.[7] As a result, a large number of Pt-based and other metal-containing complexes have been synthesized in the hope of finding better drugs.[7] Most studies are focused on finding drugs with low side effects, and compounds with higher cytotoxicity, efficacy, and selectivity towards tumors compared to normal cells. A characteristic feature of platinum-based complexes is that the leaving- and/or non-leaving group ligands can be replaced with a variety of functional groups. These ligands determine different aspects of the compound.[73] Careful selection of the ligands facilitates tuning of cytotoxic characteristics of the complex. Carbohydrates are a class of tunable molecules that can serve as ligands and introduce a variety of favorable chemical properties to platinum complexes.[150,151]

Carbohydrate moieties are components of antibiotics (*e.g.*, aminoglycosides, vancomycin), antivirals (*e.g.*, ribavirin, stavudin), as well as antitumor (*e.g.*, doxorubicin, bleomycin) drugs.[152,153] One of the reasons these functionalities are widely used in drugs is that they help reduce toxicity and improve molecular targeting.[150] The hydrogen-bonding capability of carbohydrates leads to improved water solubility of the molecules. Carbohydrates are essential molecules in biological systems and therefore tend to be nontoxic. Carbohydrate attachments facilitate drug binding to specific targets such as ribosomes.[153] Additionally, cells have specific carbohydrate transporters that can

facilitate drug uptake.[154] Glucose and other monosaccharides in the body are transported through cell membranes *via* facilitated diffusion by using a family of 14 transport proteins called GLUTs.[155] These transporters are highly expressed in metabolically active cells such as cancer cells.[126,156] Therefore, sugar pendants can direct the drugs to tumor cells for higher uptake.[83] One phenomenon that is crucial for tumor growth and progression is cell-cell recognition through carbohydrate-protein interactions.[157] Modified carbohydrates can interfere with these interactions and inhibit cancer growth.[157] Moreover, carbohydrates have functional groups that can be easily modified to introduce amino, thiol, and carboxylato groups. Modifications allow carbohydrates to serve as strong donor ligands that are capable of coordinating to metals. Specifically, in platinum-based anticancer agents, the non-leaving group ligands are usually N-donor ligands (**Figure 3.1**). Thus, if the carbohydrates are to be attached as non-leaving groups, often they are modified with an amino group that can be used to coordinate to a platinum center.[151] The nature of the ligand influences the activity of the drug against different types of cancer, which will be briefly discussed in this section in regards to binding preferences.

Interest in exploring sugar conjugation for platinum-based anticancer drug development began about a decade after cisplatin was approved as a drug by the FDA.[84] Tsubomura and co-workers synthesized the first amino sugar-platinum complexes with promising anticancer activity against Sarcoma 180 in mice (**Figure 3.1a**).[84] **Figure 3.1b** shows simple diaminosugar-platinum complexes with a 2,3-diamino-2,3-dideoxy-D-glucose non-leaving group and different leaving groups. The cytotoxicity of these derivatives was mostly in the low micromolar range as determined by MTT assays with

CH1 (ovarian), HeLa (cervical), SW480 (colon), and U2OS (bone) human cancer lines, however the cytotoxicities were not significantly improved compared to clinically available Pt-based drugs.[158] More recently, polynuclear Pt(II) complexes with higher water solubility and cytotoxicities compared to cisplatin have been reported (**Figure 3.1c**).[159] The concept of attaching a known drug to sugar-platinum complexes has also been explored to generate multifunctional drugs.[160] This strategy was developed to overcome resistance problems by linking two anticancer drugs such as doxorubicin and a cisplatin derivative (**Figure 3.1d**); however, no advantage over the individual drugs was observed in that case. To improve the drug-receptor interactions, sugars have also been attached to the Pt center *via* linkers.[161] Oxaliplatin derivatives with various linkers attached to the 6th position of glucose (**Figure 3.1e**) have been shown to be taken up selectively by GLUT1.[83] In this study, longer linkers were shown to inhibit cell uptake, as they could restrict the transporter conformational changes.[83]

Another class of carbohydrate-Pt complexes that were recently developed and tested were Pt(IV) complexes. These complexes are kinetically inert and therefore more stable for oral administration.[162] With the axial ligands, more functionalities can be introduced to the drug to increase cellular accumulation, reduce side effects, and drug resistance.[162] Recently, several glycoconjugated Pt(IV) complexes have been reported in which sugar derivatives were introduced as axial ligands for targeted cancer therapy (**Figure 3.1f**).[163,164] For an example, the compound shown in **Figure 3.1f** has shown GLUT1 and OCT transporter-dependent selective accumulation in cancer cells over normal cells and a significantly higher antitumor activity (over 150-fold) compared to cisplatin, oxaliplatin, and satraplatin.[164]

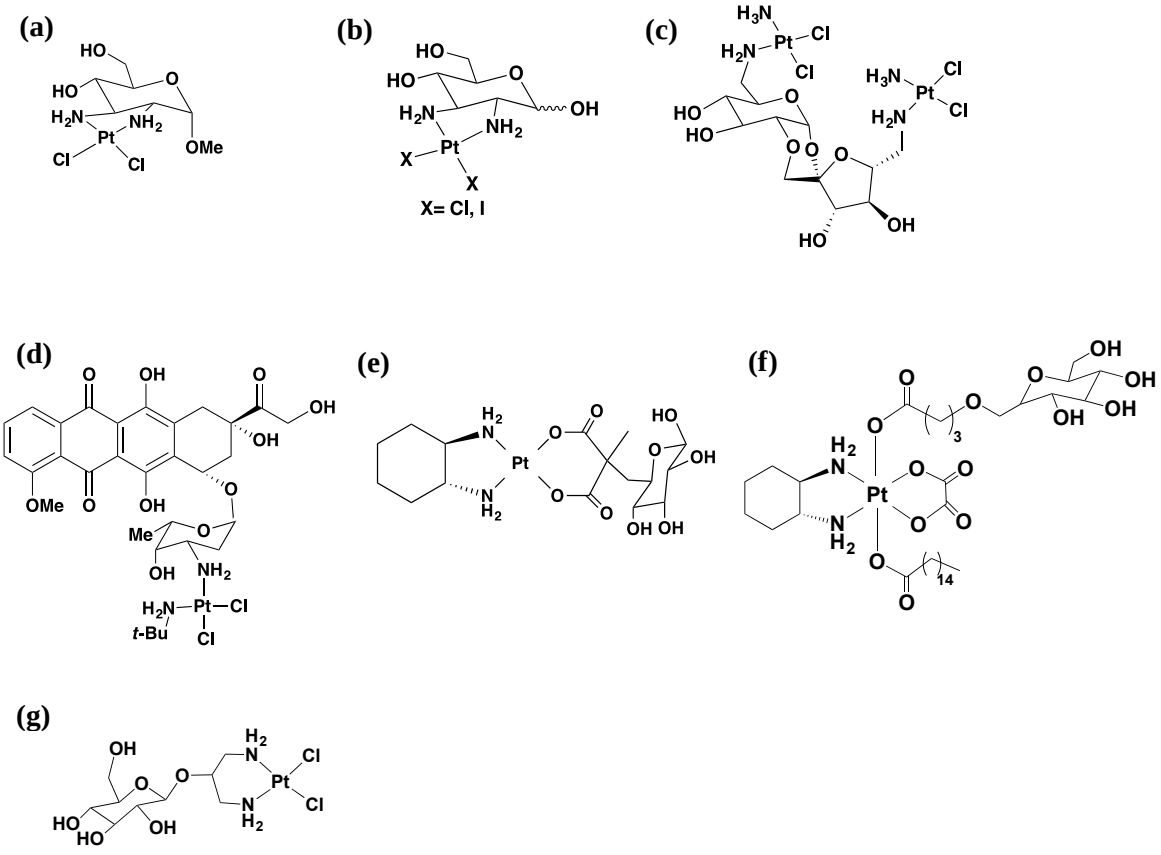

Figure 3.1. Examples of different types of sugar-platinum complexes. Structures of diaminosugar-Pt(II) complexes (a and b), a polynuclear Pt(II) complex (c), Pt(II)-doxorubicin complex (d), an oxaliplatin derivative with glucose attached to the Pt(II) center *via* a methylene linker (e), a sugar-Pt(IV) complex (f), and compound **5** (g) are shown.

As explained with some examples in this section, a variety of glycoconjugated-Pt complexes have been synthesized and studied extensively. These studies are mainly confined to cellular cytotoxicity assays and have shown promising activity. A few attempts have been made to elucidate the transporter dependence and cancer cell selectivity of the glycoconjugated-Pt(II) complexes.[81,83,115,121,165] Although these studies show a promising strategy for cancer treatment, detailed reactivity and structural impacts of a glycoconjugated-Pt complex with nucleic acids are mostly unknown. Therefore, the

work described in this thesis attempts to understand the behavior of a glycoconjugated-Pt(II) derivative in terms of the reactivity preferences with nucleosides, reaction rates with nucleosides and oligonucleotides, and structural effects on DNA.

The carbohydrate-linked cisplatin derivative, *cis*-dichlorido[(2-*β*-D-glucopyranosidyl)propane-1,3-diammine]platinum(II) that is been explored in this thesis work has a short 2-propane-1,3-diamine linker between the sugar and the platinum center (compound **5, Figure 3.1g**).[82] As observed in a crystal structure, the complex has a normal square planar geometry for the Pt(II) center with usual (compared to cisplatin) Pt−Cl and Pt−N distances (231 and 202 pm, respectively).[82] Both the glucopyranose ring and the chelate ring adopt a chair conformation. In another study, the solution structure of **5** was determined by NMR in D_2O,[161] revealing similar structures in both the solid and solution states. Furthermore, the NMR study showed that the carbohydrate moiety is in the axial position of the six-membered chelate ring.[161] Compound **5** has a solubility of >20 mg mL^{-1} at 25 °C, which is higher than that of cisplatin (2.5 mg mL^{-1}).[82]

3.3 Objectives

Although many examples of platinum complexes bound to sugars are known,[150,151] only a few reports focus on the role of the carbohydrate moiety on the reaction kinetics with nucleosides and target site identification on larger oligonucleotides. In general, platinum(II) complexes show preferences towards guanine bases. However, there are a few variants with known preferences towards the adenine base.[88] One objective of the work in this chapter was to conduct a study with nucleic acid building blocks to evaluate the reactivity of compound **5** compared to cisplatin. After determining the reactivity preference for G nucleosides, a kinetic study was done to compare the

reaction rates of mono-activated **5** towards DNA and RNA nucleosides, dG and G, respectively. Another objective was to compare mono-activated compound **5** reaction rates with that of cisplatin. Finally, the platination products were characterized by using mass spectrometry to determine the adduct types (*i.e.*, monoadducts vs. biadducts). Overall, in this work I investigated the kinetics and binding stoichiometry of a carbohydrate-linked platinum(II) complex (**5)** with the nucleic acid building blocks.

3.4 Results and discussion

Compound **5** was synthesized and characterized as described previously (**Chapter 2, Section 2.4.2**). The MALDI-MS spectrum show a peak at 557 Da, which is the predicted mass for **5** (518 Da) associated with K^+. The peak patterns in the ^{1}H-NMR spectra for the ligand (compound **4**) and Pt(II) complex (**5**) are consistent with the literature (**Figure 3.2, Appendix A, Figure A2-A4**).[82,161] Clear peak shifts are observed after coordination for protons at C7 (4.20 to 3.57 ppm), and C8 and C9 (2.96-3.20 to 2.55 ppm), which correspond to a shift of 0.63 ppm and 0.41-0.65 ppm, respectively. In the six-membered chelate ring, the C7, C8, and C9 protons are closer to the Pt center; therefore, electron localization causes the protons to be shielded more in **5** than in the free ligand, **4**, leading to the observed upfield shifts and supporting complex formation. Minor peak shifts are observed for the other protons.

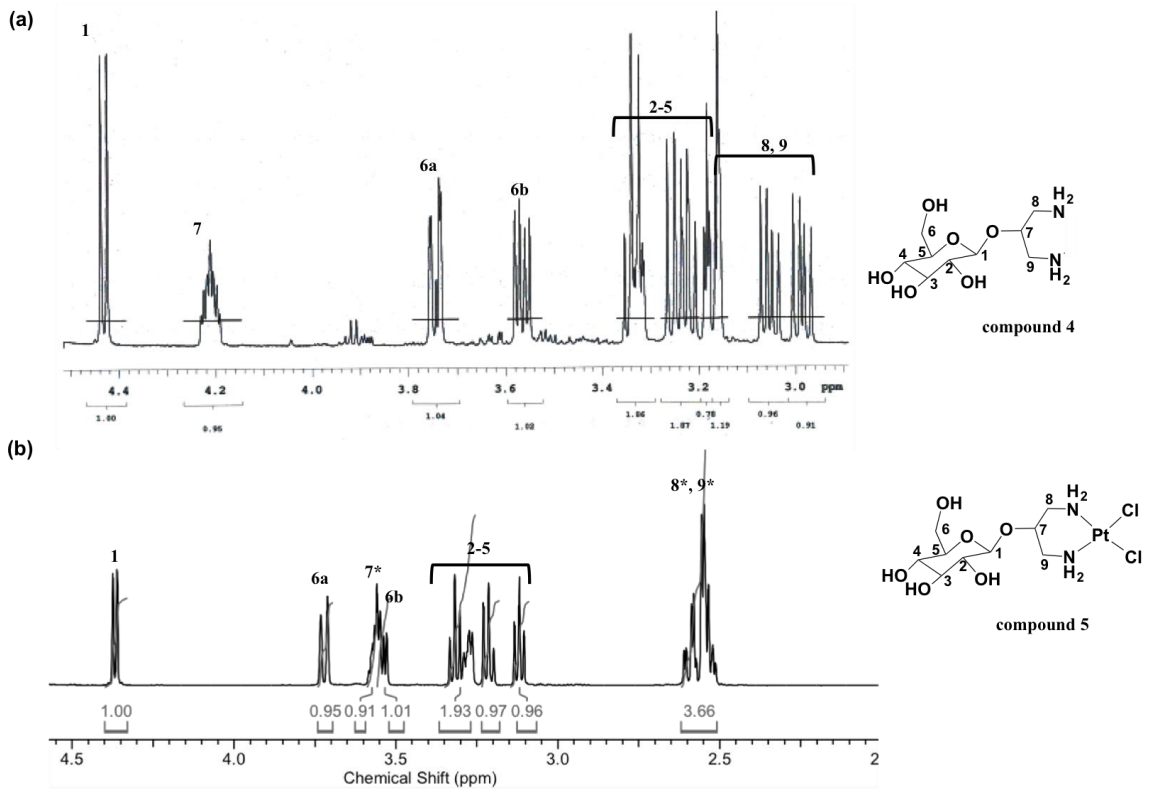

Figure 3.2. The ^{1}H-NMR spectra of (a) compound 4 and (b) compound 5 in D_2O (600 MHz). The C atoms are numbered in the chemical structures (left) and the corresponding proton signals are shown in the spectra. Signals that show significant peak shifts are marked with an asterisk (*).

3.4.1 Reactivity with nucleosides

Cisplatin and many other platinum-based drugs are known to react with purine bases, adenine and guanine.[166] Higher reactivity is usually observed with guanine. Initially G and dG were reacted with a 5-fold excess of mono-activated **5** for 5 h at 37 °C in ddH_2O, pH 7.6 to detect the reactivity, and a higher peak intensity (compared to when buffer was used) with G was observed compared to dG. Therefore, RNA nucleosides were used to identify the reactivity preference; mono-activated **5** was reacted with adenosine (A), guanosine (G), cytidine (C), and uridine (U) under identical conditions. The nucleoside solutions were reacted with 5-fold excess of mono-activated **5** and

quenched with NaCl after 16 h, and then the products were analyzed by HPLC (**Figure 3.3)**.

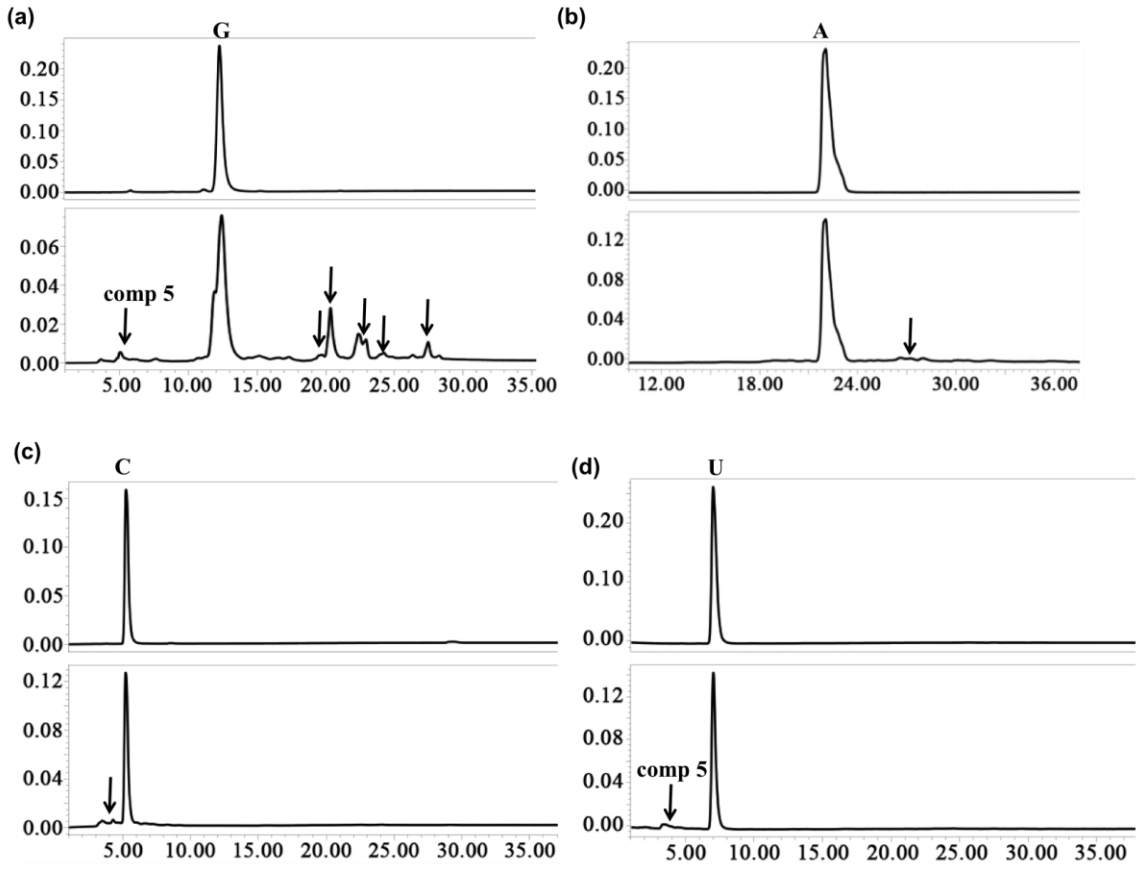

Figure 3.3. HPLC analysis of RNA nucleoside reactions with mono-activated compound 5. HPLC spectra (C18 column; buffer A: 40 mM ammonium acetate, pH 6.5; buffer B: 40% acetonitrile; linear gradient of B from 5 to 35% over 30 min; flow rate 1 mL/min) for control (top) and reactions (bottom) with (a) guanosine, (b) adenosine, (c) cytidine, and (d) uridine nucleosides are shown. Arrows show the possible adducts for the reactions.

Additional peak formation at higher retention times is mainly observed with G but not with other nucleosides, A, C, and U. For the reaction with G, four major peaks corresponding to possible platinum adducts are detected with 20.4, 22.4 (two unresolved peaks), and 27.5 min retention times with minor peaks at 19.7 and 24.2 min. Product formation with **5** is observed with A (27-28 min) and C (4.2 min) to a minor extent, but not with U. Based on the overall results, compound **5** appears to form multiple adducts

with G to a higher level than with other nucleosides. The presence of multiple adducts could be the result of mono-substitution ($[Pt(C_9H_{20}O_6N_2)G(Cl)]^+$, or $[Pt(C_9H_{20}O_6N_2)G(H_2O)]^{2+}$), or bis-substitution. For cisplatin, the dG binding preference at the N7 position was explained by the ability to form a hydrogen bond between the ammine-NH of cisplatin and the O6 of guanine base, which stabilizes the adduct.[167] The bidentate sugar ligand of compound **5** has two H-donor ammine groups that can engage in hydrogen bond formation with the O6 of guanine. Therefore, as with cisplatin, we propose that compound **5** binding to the N7 position of guanine would be preferred over other nucleosides based on the potential hydrogen-bonding interaction with the O6 of guanine.

3.4.2 Kinetic experiment with G and dG nucleosides

Cisplatin is well known to bind to DNA, and the direct coordination step is under kinetic control.[15] Preference in reactivity may be governed by the non-leaving ligand, size, and charge. As shown by the initial reactions, compound **5** appears to have preferred reactivity towards G over the other RNA nucleosides, A, C and U. Therefore, HPLC analysis was used to quantify the coordination rates for G compared to dG. The rates for dG or G reactions with mono-activated **5** were compared to those with cisplatin. The kinetic reactions were carried out under pseudo-first-order conditions, in which the Pt(II) concentration was 50 times higher than the nucleoside concentration (**Chapter 2, Section 2.4.4**).[47] The reactions were quenched at 0.5, 1, 2, 3, 4, and 6 h time points with NaCl (final concentration 188 μM).[47] The HPLC traces are shown in **Figure 3.4a**. The products had longer retention times than the unreacted nucleosides.

The disappearance of nucleosides was quantified rather than appearance of products since multiple products are observed. The fraction of unreacted nucleoside (y= unreacted nucleoside/total nucleoside) was obtained by integrating the peak areas of the products and reactant nucleosides. The fraction of unreacted nucleoside was plotted with quenching times and fit to Equation 2.3 (y= A $e^{-k_{obs}t}$) (**Figure 3.4b**) to obtain the pseudo-first-order rate constants (**Table 3.1**).

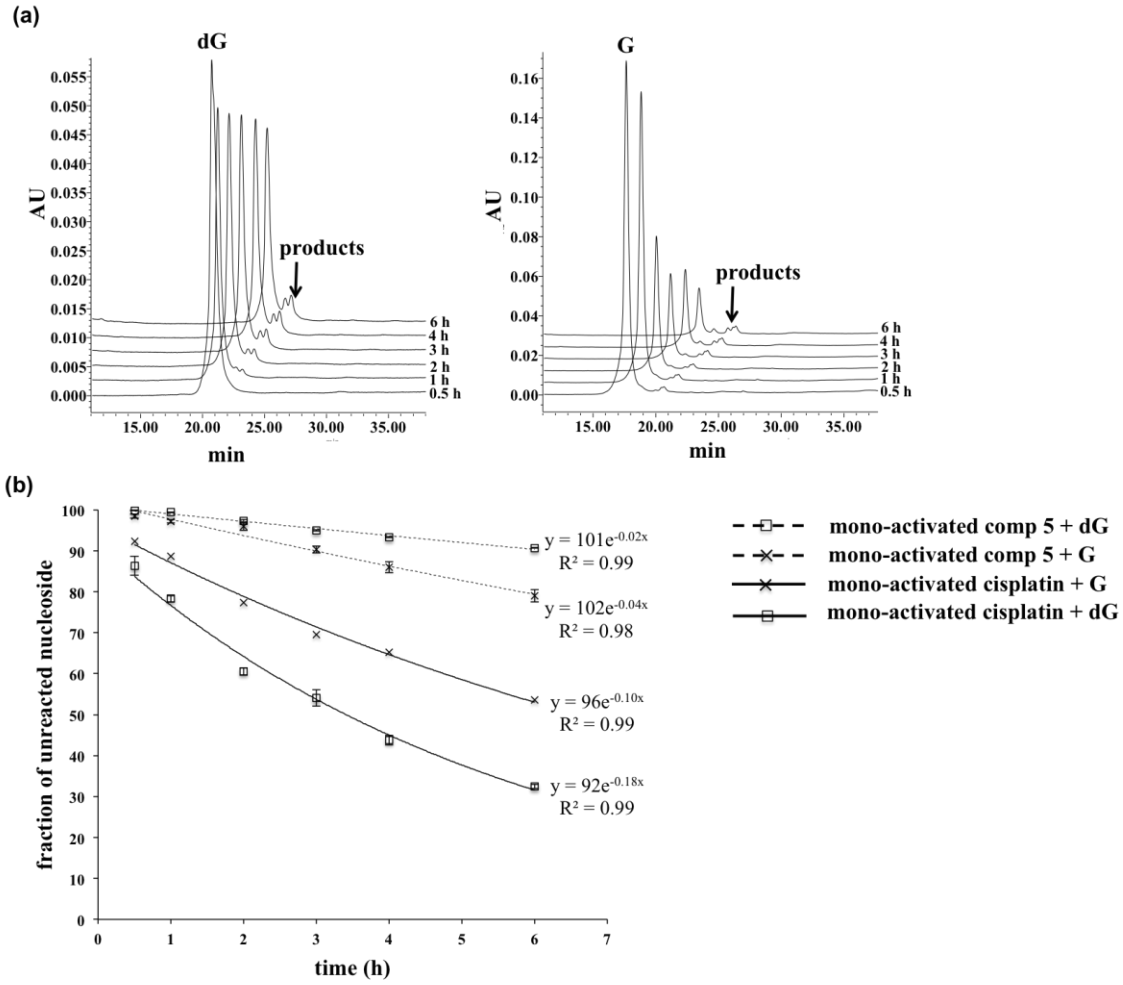

Figure 3.4. Results for the kinetic experiments with mono-activated Pt(II) and dG and G. (a) HPLC traces for the kinetic experiments with mono-activated **5** are shown. The reactions ([nucleoside]= 0.1 mM, [Pt(II)]= 5 mM, 25 mM Na_2HPO_4/NaH_2PO_4, pH 7, 37 °C) were quenched at 0.5, 1, 2, 3, 4, and 6 h and injected onto the HPLC (C18 column, linear gradient of B from 5 to 35% over 30 min, flow rate 1 mL/min). (b) Plots of the fraction of unreacted nucleoside (y) over time with fits to y= A $e^{-k_{obs}t}$ equation are given. The errors were calculated from three (two for cisplatin) independent experiments.

Table 3.1. Pseudo-first-order rates for the reactions of mono-activated Pt(II) complexes with nucleosides

	mono-activated cisplatin k_{obs} (s^{-1}) × 10^{-6}	mono-activated **5** k_{obs} (s^{-1}) × 10^{-6}
dG	49 ± 1	5 ± 0.2
G	28 ± 2	11 ± 0.8

The errors were calculated from three independent experiments.

Overall, mono-activated compound **5** show lower reaction kinetics compared to cisplatin; for dG, the rate is 9.8-fold lower, and for G it is 2.5-fold lower (**Table 3.1**). Slower kinetics have been observed previously for platinum(II) compounds with larger ligands, likely due to crowding at the platinum center.[51,168] Activated square planar Pt(II) complex coordination at dG residues has been explained by an associative substitution mechanism (**Scheme 3.1**).[168] The incoming ligand coordinates as a fifth ligand to form a trigonal-bipyramidal intermediate, after which the aqua ligand dissociates. The bulkier sugar moiety could slow down the rate-determining first step of associative substitution of activated compound, in which the dG residue coordinates to the Pt center.[168] Activated compound **5** could have different steric and ligand-exchange characteristics compared to activated cisplatin, as supported by the slower reactions with both dG and G. Slower reaction kinetics is a desirable property in anticancer drugs because it minimizes off-target binding.[168] In fact, bidentate or tridentate *N*-donor ligands in platinum-based drugs add stability to the platinum complexes and decrease the possibility of undesired substitution reactions.[90,169]

Scheme 3.1. Steps of the associative substitution mechanism of a nucleophile binding to mono-activated cisplatin. Platinum interactions with the incoming nucleophile and the aqua leaving group in the trigonal bipyramidal transition state are shown.

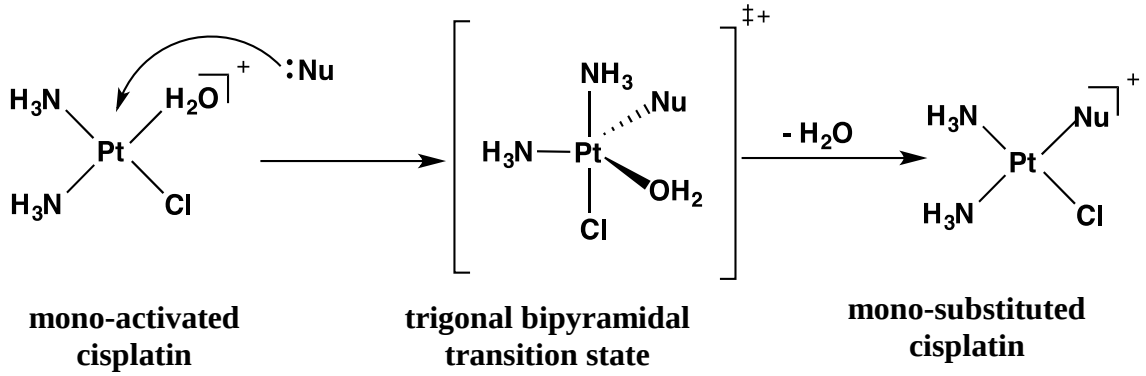

mono-activated cisplatin | **trigonal bipyramidal transition state** | **mono-substituted cisplatin**

Between dG and G, mono-activated compound **5** is more reactive towards G. Compound **5** show 2.2-fold greater reactivity towards G over dG, whereas cisplatin display a 2-fold higher rate for dG (**Table 3.1**). The G nucleoside has an additional hydroxyl group at the 2′ position of the ribose-sugar compared to dG, which could be involved in forming an additional hydrogen bond with the carbohydrate moiety of the Pt(II) compound, although this type of interaction was not verified in this thesis work. In an associative mechanism with a trigonal-bipyramidal transition state, the ligand *cis* to the leaving group becomes axial to the trigonal plane (**Figure 3.5**).[167,168] When the carbohydrate group becomes axial, it has the ability to interact with the entering and leaving groups at an angle of 90°. Therefore, I propose that the transition state is stabilized by an additional hydrogen bond with the incoming G and carbohydrate moiety of **5**, thus favoring the reaction with G as opposed to dG.

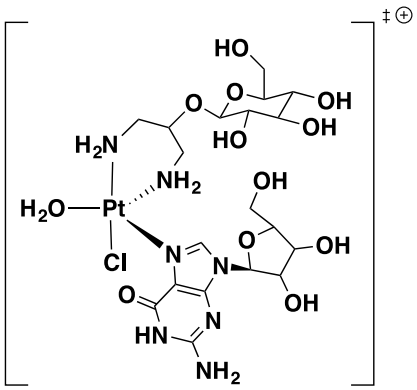

Figure 3.5. Possible trigonal-bipyramidal transition state for the mono-activated 5 reaction with G nucleoside. The aqua ligand, adenine base, and one $–NH_2$ of the carbohydrate ligand are in the trigonal plane. The other $–NH_2$ group of the carbohydrate ligand and the chlorido group become axial to the trigonal plane as shown. In this structure, the carbohydrate group of **5** and the ribose sugar group exist above the plane, which brings the sugar moiety of **5** closer to the ribose for additional hydrogen-bonding.[161,167]

3.4.3 Mass analysis of products (LC-MS)

The mixtures of products that are generated from the reactions between G or dG and mono-activated **5** were analyzed by using mass spectrometry, with either LC-MS or a direct injection method, to identify the adducts (**Chapter 2, Section 2.4.5**). The m/z of all the possible adducts were calculated and a specific mass range (calculated m/z ± 8 Da) was selected in the MS for adduct identification. Both mono- and bis-substituted adducts were detected in the reaction mixtures after 16 h.

Analysis of the guanosine-**5** reaction mixture by LC-MS (**Figure 3.6** and **3.7**) supports the product identities as $[Pt(C_9H_{20}O_6N_2)G(Cl)]^+$, $[Pt(C_9H_{20}O_6N_2)G(H_2O)]^{2+}$, and bis-substituted adduct $[Pt(C_9H_{20}O_6N_2)G_2]^{2+}$. The calculated exact masses for the mono-substituted $[Pt(C_9H_{20}O_6N_2)G(Cl)]^+$ and $[Pt(C_9H_{20}O_6N_2)G(H_2O)]^{2+}$ are 765 Da and 748 Da, respectively. The isotopic distribution due to Pt and Cl was observed in the LC-MS spectra and matched the predicted spectra as shown in **Figure 3.6** and **3.7**. The bis-substituted product, $[Pt(C_9H_{20}O_6N_2)G_2]^{2+}$, has a calculated mass of 1,013 Da; the major

peak in the spectrum appeared at 1,010 Da $[M\text{-}3H^+]^-$ in the negative mode. The retention times for the $[Pt(C_9H_{20}O_6N_2)G(H_2O)]^{2+}$, $[Pt(C_9H_{20}O_6N_2)G(Cl)]^+$, and $[Pt(C_9H_{20}O_6N_2)G_2]^{2+}$ adducts in the LC-MS are 1.5, 4.2, and 4.3 min, respectively.

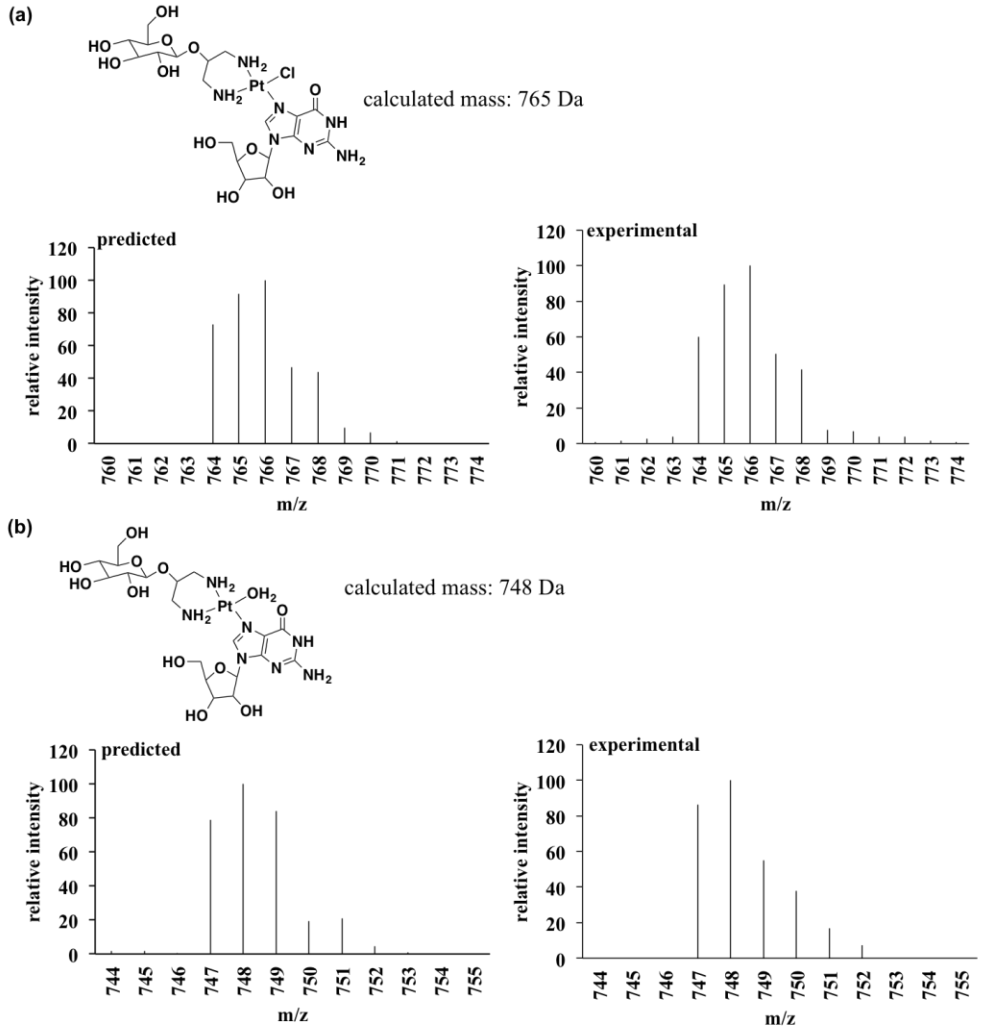

Figure 3.6. The predicted and experimental mass spectra for compound 5–G mono-substituted adducts with possible structures. (a) The calculated and observed (positive mode) m/z for $[Pt(C_9H_{20}O_6N_2)G(Cl)]^+$ were 765 Da. (b) The calculated mass for $[Pt(C_9H_{20}O_6N_2)G(H_2O)]^{2+}$ was 748 Da and the observed (positive mode) m/z for $[Pt(C_9H_{20}O_6N_2)G(H_2O)\text{-}H^+]^+$ was 747 Da.

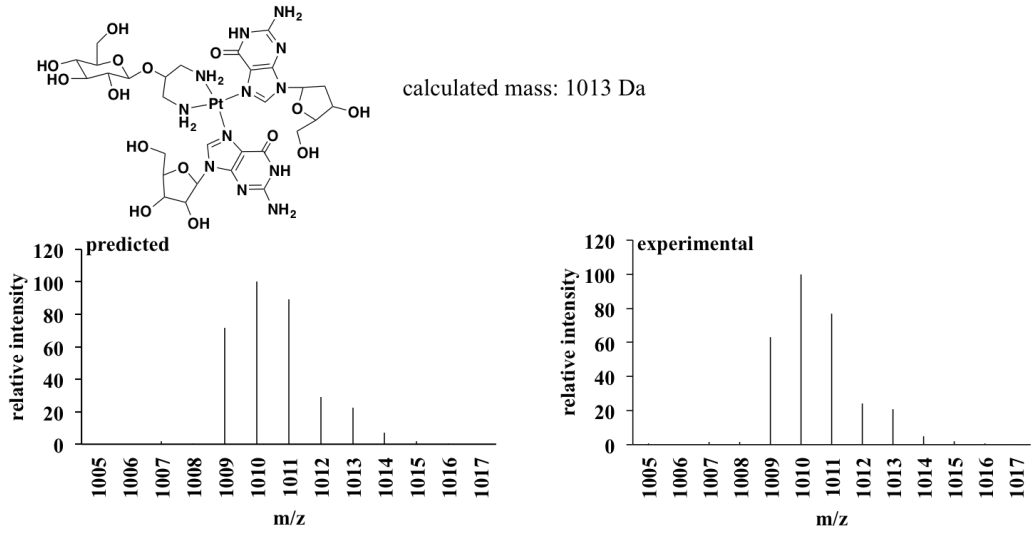

Figure 3.7. The predicted and experimental mass spectra for compound 5–G bis-substituted adduct with possible structure. The calculated mass for $[Pt(C_9H_{20}O_6N_2)2G]^{2+}$ was 1013 Da and the observed (negative mode) m/z for $[Pt(C_9H_{20}O_6N_2)2G\text{-}3H^+]^-$ was 1010 Da.

The dG reaction mixtures were analyzed by using mass spectrometry with direct injection of the sample. **Figure 3.8** depicts the mass spectra obtained for mono- and bis-substituted adducts with the isotropic distribution. The calculated exact masses for $[Pt(C_9H_{20}O_6N_2)dG(Cl)]^+$, $[Pt(C_9H_{20}O_6N_2)dG(H_2O)]^{2+}$, and $[Pt(C_9H_{20}O_6N_2)(dG)_2]^{2+}$ were 749 Da , 732 Da, and 981 Da, respectively. The observed peaks are similar to the predicted spectra in the positive mode with the masses 749 Da for $[Pt(C_9H_{20}O_6N_2)dG(Cl)]^+$, 731 Da for $[Pt(C_9H_{20}O_6N_2)dG(H_2O)\text{-}H^+]^+$, and 980 Da for $[Pt(C_9H_{20}O_6N_2)(dG)_2\text{-}H^+]^+$.

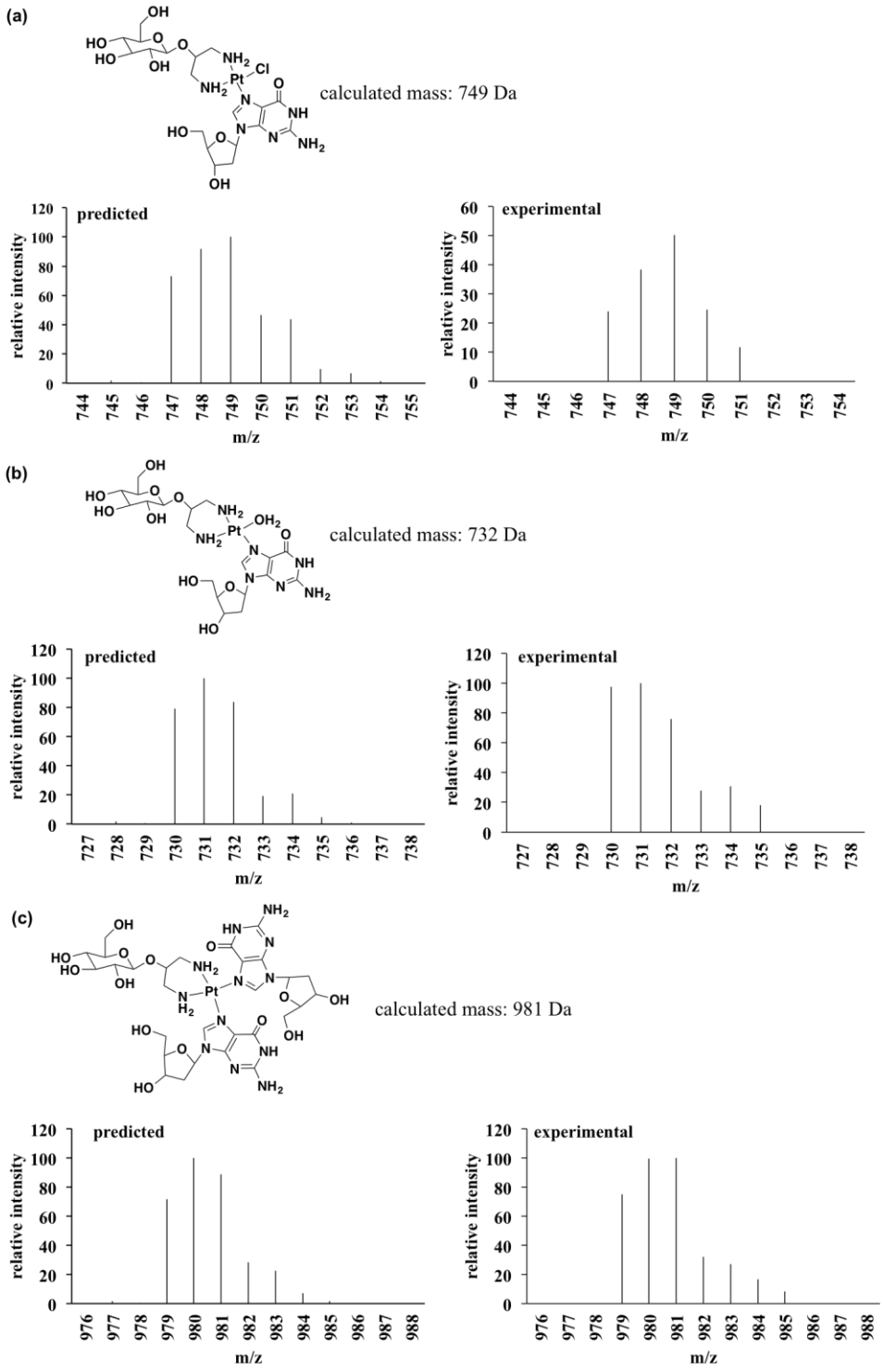

Figure 3.8. The predicted and experimental mass spectra for compound 5–dG adducts with possible structures. (a) The calculated and observed (positive mode) m/z for $[Pt(C_9H_{20}O_6N_2)dG(Cl)]^+$ was 749 Da. (b) The calculated mass for $[Pt(C_9H_{20}O_6N_2)G(H_2O)]^{2+}$ was 732 Da and $[Pt(C_9H_{20}O_6N_2)dG(H_2O)\text{-}H^+]^+$ was observed (positive mode) at 731 Da. (c) The alculated mass for $[Pt(C_9H_{20}O_6N_2)(dG)_2]^{2+}$ was 981 Da and $[Pt(C_9H_{20}O_6N_2)(dG)_2\text{-}H^+]^+$ was observed (positive mode) at 980 Da.

In this chapter, experimental results were presented for nucleoside-mono-activated compound **5** reactions and adduct identification. By using the nucleosides, the reactivity was evaluated with minimum complexity as opposed to the reactions with nucleic acids. The reactivity rates of mono-activated **5** were compared to that of cisplatin, and showed preferred binding to G over dG. However, the overall reaction kinetics were low for **5** compared to cisplatin, with a 2.5-fold lower rate for the reaction with G. The reactivity differences between mono-activated **5** and cisplatin may arise from the presence of different non-leaving group ligands. The lower reaction rates of mono-activated **5** could be due to the bulkiness of the sugar moiety, which sterically hinders the reactivity with nucleosides. Reactivity differences of **5** compared to cisplatin could afford unique biological consequences such as limited off-target binding, avoiding recognition by repair enzymes, or altering downstream biological pathways. Further experiments could be carried out to explore the reactivity differences and gain new perspectives for a rational design of new platinum antitumor drugs.

CHAPTER 4

REACTIVITY OF A CARBOHYDRATE-LINKED PLATINUM COMPOUND WITH NUCLEIC ACIDS

4.1 Abstract

This chapter describes the reaction kinetics and structural impacts caused by compound **5** (*cis*-dichlorido[(2-β-D-glucopyranosidyl)propane-1,3-diammine]platinum (II)) at the oligonucleotide level in order to obtain some mechanistic insight into how it works. With the guanosine ribonucleoside binding preference of **5** as described in **Chapter 3**, it was of interest to explore the reaction kinetics at the nucleic acid level to mimic the cellular targets. A series of gel-based kinetic experiments was carried out, comparing **5** and cisplatin reactions with DNA and RNA, using both mono- and bis-activated complexes. A salt-dependent kinetic study was also carried out to understand the contribution of RNA electrostatics on the reactivity of **5**. The DNA structural changes that occur upon mono-activated compound **5** binding were evaluated by using plasmid and small oligomer DNAs. A reverse transcription-based primer extension technique was used to analyze compound **5** binding sites on ribosomal RNA (rRNA). All of these experiments were done in parallel with cisplatin. Compound **5** and cisplatin both formed platinum adducts that lead to DNA bending. Slow reaction rates were observed for **5** for oligonucleotides compared to cisplatin (≥3.7-fold), which was similar to the reactions with nucleosides. These findings reveal the impact of the carbohydrate ligand on reaction kinetics and target selectivity. These results agree with the fact that by changing the size and nature of the non-leaving group ligands, a controlled activity can be achieved.

4.2 Introduction

Certain aspects of nucleic acid interactions have been studied at great lengths to understand the reaction mechanism of cisplatin.[17,170,171] DNA has long been the subject of intense investigation, but RNA has received more attention in recent years.[170] These studies include locating the platination sites, evaluating the stabilizing (or destablizing) and structural effects of cisplatin on nucleic acids, kinetic measurements, understanding sequence dependence of the compounds, and examining their impact on cellular function.[17,47,51,170,171]

4.2.1 Kinetic studies of cisplatin-nucleic acid reactions

Cisplatin binding to nucleic acids is a kinetically controlled reaction.[15] The chlorido ligand of cisplatin is not directly displaced by the purine base, rather it happens through a solvent-assisted mechanism.[172] Therefore, the rate-limiting step in the reaction is the initial cisplatin hydrolysis, which is a first-order reaction.[172] However, activated complexes have been used for studying the subsequent steps of platination *in vitro* without the interference from the initial rate-determining step. Kinetic studies have been done to get insight into the mechanism, primary reactive species, and sequence-dependent reactivity of cisplatin with DNA.[172] By directly using the activated complex, the role of the non-leaving group ligands can be elucidated as well. Sequence-dependent studies have identified that dGs in the context of -d(GG)- or -d(AG)- are more reactive towards cisplatin than other dGs, and the adduct formation is dependent on whether the sequence is in a single- or double-stranded region.[12,166,173] Furthermore, flanking bases have been shown to play a role in platination.[174,175] Importance of the location of the target site has also been shown with kinetic experiments, in which the target sites located

at the ends of an oligomer are platinated more slowly compared to those in the middle.[176,177] Moreover, the intial platination step was faster at the 5'dG than at 3'dG for 5'-d(GG)-3' target sites.[175] Platination rates are also affected by the ions present in the microenvironment of the nucleic acid, as well as the pH. Higher concentrations of cations and increasing pH reduce the platination rates for DNA.[47,177] Several kinetic studies for Pt(II)-RNA interactions have been reported.[44,48,51] One such study showed a kinetic preference of cisplatin for G-C-rich and wobble base-pair regions on full-length tRNA.[44] A comparison between Pt(II) compound coordination to DNA and RNA revealed a more pronounced salt-dependent reactivity with RNA.[51] Moreover, the effect of pH, salt, and RNA sequence on platination was studied in our lab by Dr. Dedduwa-Mudalige for her thesis work.[50]

4.2.2 Structural impacts of Pt(II)-nucleic acid interactions

DNA adducts of cisplatin and some other Pt(II) complexes have been extensively characterized by X-ray crystallography and NMR spectroscopy.[171] The physical effects of Pt(II) binding to DNA have been discussed in detail, as this has been identified as the main event to initiate cell apoptosis.[171] Mainly, the effects are categorized as unwinding, shortening, and bending of the double-helical DNA structure.[171] Intercalating Pt reagents such as $[Pt(terpy)(HET)]^{+}$ are known to lengthen and stiffen the DNA double helix, whereas cisplatin and transplatin binding shorten the DNA.[178] Cisplatin binding to DNA in a bidentate fashion has a large structural impact because the complex is able to kink the double helix at the binding site. [171] With mono-functional adducts, this effect is not as pronounced.[179] The DNA-bending angle for cisplatin has been quantified in several studies, but the values varied.[24,145,180,181] A molecular mechanics study revealed that

cisplatin binding to form a *cis*-d(GG) intrastrand cross-link on duplex oligomer bent the DNA about 60°.[182] By using a gel electrophoresis mobility shift assay, the *cis*-d(GG) bend angle was estimated to be about 40°.[180] Using a similar method in another study, the bend angles for *cis*-d(GG) and *cis*-d(AG) adducts were 32° and 34°, respectively.[24] In the case of the *cis*-d(GTG) 1,3 adduct, an angle of 35° was reported.[24] A crystal structure of cisplatin bound to duplex DNA showed a bend angle of 26°, which is smaller than what was obtained from the gel and solution studies.[183] The effect of flanking bases on DNA bending was evaluated in a recent study, in which the bend angles were found to be about 32-34° regardless of what the flanking bases are at the platinated d(GG) site.[25]

Bending causes the neighboring region to be destabilized and the Watson-Crick base pairing to be weakened.[171] The neighboring bases unstack and the sugar puckering changes from C2'-endo to C3'-endo; thus, the standard B-DNA conformation is changed to A-form DNA.[171] Changes in UV and circular dichroism spectra supported the idea of base unstacking within the helix.[179] Furthermore, a decrease in melting temperature upon cisplatin binding revealed destabilization of the DNA structure.[179] Alkylation at the N7 position of purines is known to destabilize the glycosidic bond and facilitate depurination.[184] However, with cisplatin binding, the glycosidic (N9-C1') linkage is stabilized, probably due to the better distribution of the positive charge over the Pt atom.[184] Lowering the pK_a of the N1 position of the purine ring from ≈ 10 to ≈ 8 upon platination supports this idea as well.[185] Therefore, the anticancer activity of platinum compounds is often correlated with distortion of the DNA structure, which affects regular biological functions in the cell.[171]

4.3 Objectives

In order to develop next-generation platinum anticancer drugs with less off-target effects, low resistance, and higher potency, it is important to understand their reactivity at the biomolecular level. Although clinically available platinum(II) drugs have been studied extensively, the biochemistry of other cisplatin derivatives is poorly understood. The purpose of this chapter is to evaluate the reaction kinetics of **5** with oligonucleotides, as well as its structural impacts on DNA and nucleotide preferences for rRNA binding to understand the effects of the carbohydrate ligand.

From **Chapter 3,** it was clear that the kinetics are different for **5** compared to cisplatin at the nucleoside level, in which the overall reactivity was low for **5** and the guanosine ribonucleotide binding was preferred. It was of interest to evaluate the reactivity on DNA and RNA oligonucleotides as well as the mononucleotides. Therefore, the first objective of this section was to evaluate the reaction kinetics of **5** with oligonucleotides to compare their binding preferences, and to gain insights into the basis of these differences. Kinetic studies with mono- and bis-activated compound **5** were done to compare the reaction rates with DNA and RNA oligonucleotides. Salt-dependent kinetic rates were also obtained for the reaction between mono-activated **5** with DNA and RNA to understand the electrostatic contributions on the reactivity. Similar experiments were carried out with cisplatin for comparison.

After establishing the reactivity with oligonucleotides, the next question to ask was what is the impact of binding on the nucleic acid structure? If a potentially active molecule does not distort the nucleic acid structure or inhibit a nucleic acid-related functions, its activity may not be the result of targeting nucleic acids.[171] Therefore, the

second objective of this study was to determine the structural changes caused by mono-activated **5** on DNA in comparison to cisplatin.

Previous studies showed that cisplatin's anticancer activity correlates with DNA binding. However, with more mechanistic studies available, this idea has been challenged and cisplatin has been shown to bind to other cellular targets such as RNA and proteins.[39,186,187] In particular, cellular RNA has received some attention in recent years.[187] Considering the abundance, accessibility, and functional importance, rRNA can be considered as one of the potential targets of Pt(II) compounds.[187] Furthermore, the biologically active compound **5** showed higher reactivity towards the guanosine ribonucleoside compared to the corresponding deoxy nucleoside. Therefore, the third objective was to evaluate the nucleotide preferences of **5** binding to rRNA. The effects of the carbohydrate ligand on structural and kinetic properties are clues in understanding the biological activities of glycoconjugated molecules. Overall, this chapter aims to provide information about steric, electronic, and hydrogen-bonding properties of compound **5** that influence nucleic acid binding and kinetics of the molecule.

4.4 Results and discussion

4.4.1 Kinetic studies for mono-activated 5 and nucleic acid reactions

Kinetics are crucial to the antitumor properties of a drug. **Chapter 3** evaluates the binding kinetics with the building blocks of nucleic acids in a simplified environment. However, it is important to compare these data to kinetic parameters of nucleic acids to get a better view of the activity of platinum compounds. More complex secondary and tertiary structures of nucleic acids, cations and solvents in the microenvironment, and electrostatic and hydrogen-bonding ability of the ligands are some of the factors that

determine the drug-nucleic acid interactions.[188] Kinetic, thermodynamic, and structural preferences of the drug are governed by these parameters.[188]

The DNA and RNA strands used for my kinetic experiments are similar in length (22-mer), sequence (except for T in DNA and U in RNA), and have only one -GG- site for platination (DNA1 and RNA1). The single-stranded nucleic acids were radiolabeled at the 5′ end for visualization during gel electrophoresis. The first hydrolysis of cisplatin is the rate-limiting step. Therefore, by using mono-activated platinum complexes, factors influencing the direct coordination step could be rapidly evaluated without interference from the first hydrolysis. Under excess Pt(II) concentration, this reaction was expected to obey pseudo-first-order conditions. The pseudo-first-order rate constant, k_{obs}, for the reaction between different concentrations of mono-activated **5** and DNA were obtained as described in **Chapter 2**, **Section 2.4.9**. The Pt(II) compound was maintained at a 134-fold higher concentration than that of the oligonucleotide. This condition maintained the pseudo-first-order rate. Specifically, the final concentration of the added mono-activated Pt(II) complex was 94 μM. This procedure was repeated with RNA for direct comparison. The experiment was also carried out with mono-activated cisplatin to compare the rates to those of the carbohydrate complex.

Results obtained with DNA are shown in **Figure 4.1** and the results obtained with RNA are shown in **Figure 4.2**. As shown in **Figure 4.1a** and **b**, addition of mono-activated **5** and cisplatin to nucleic acids results in a decrease of unplatinated nucleic acid in a time-dependent manner as observed on denaturing polyacrylamide gel images. Slower migrating product bands are observed on the gels. The fraction of unreacted nucleic acid over time is fitted to a single exponential decay (**Equation 2.3** and **Equation**

2.4) to obtain the k_{obs}. Standard errors were calculated from three independent experiments.

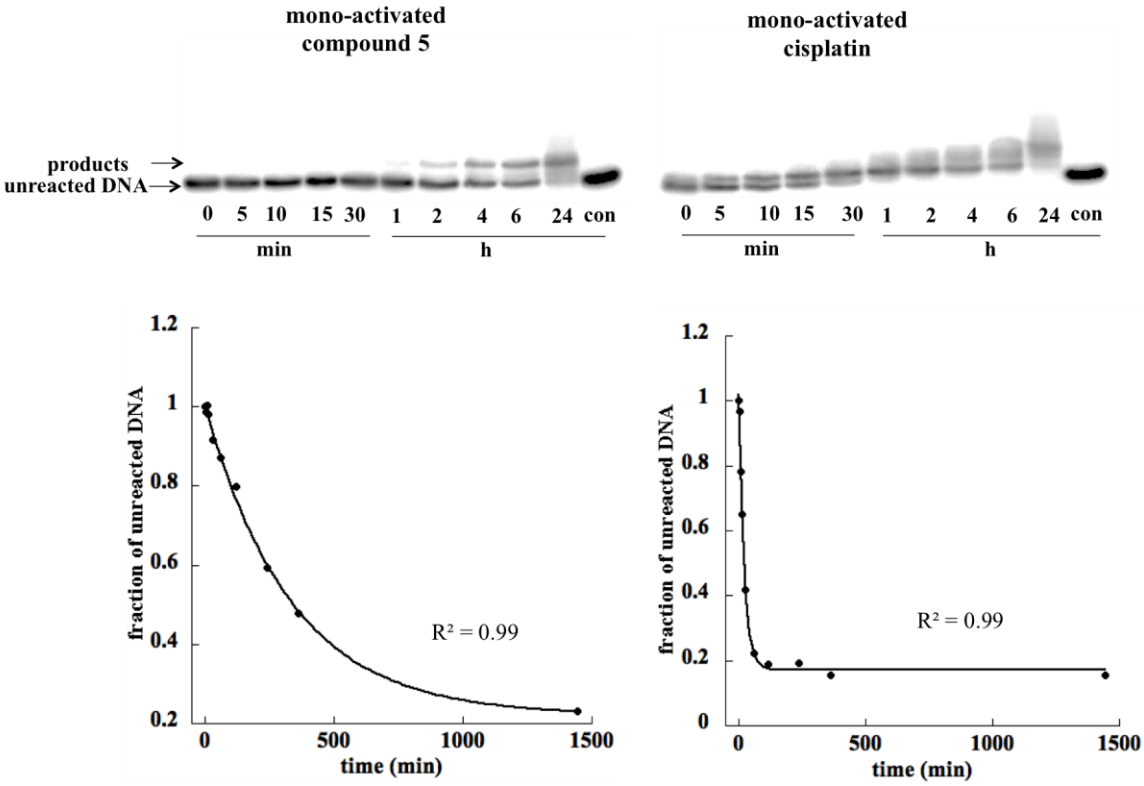

Figure 4.1. Representative results for the kinetic experiment between DNA and mono-activated Pt(II) complexes. The gel images for the reactions between DNA with mono-activated (a) compound **5** and (b) cisplatin showed the time-dependent decay of unreacted DNA and formation of the products ([DNA] = 0.7 μM, [Pt(II)] = 94 μM; 10 mM K_2HPO_4/KH_2PO_4, pH 6.2, with 20 mM $NaClO_4$, 37 °C). The fraction of unreacted DNA over time for the mono-activated (C) compound **5** and (d) cisplatin showed exponential decay.

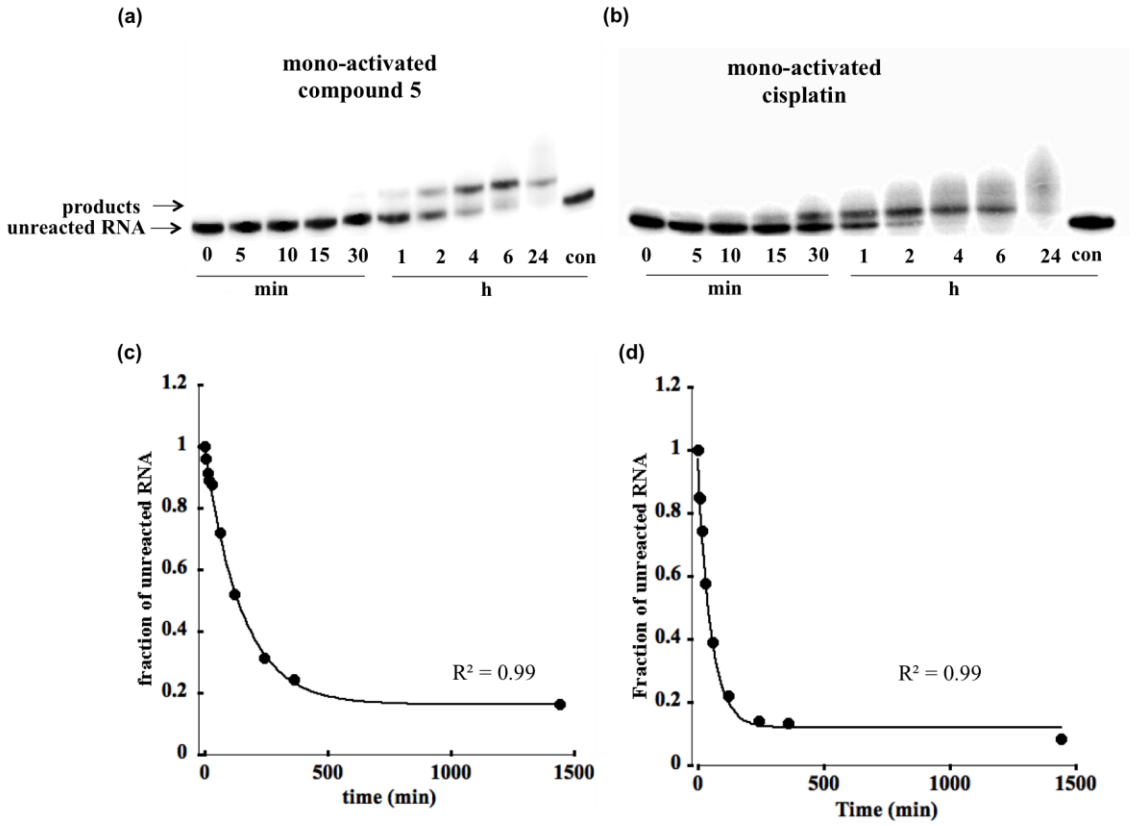

Figure 4.2. Representative results for the kinetic experiment between RNA and mono-activated Pt(II) complexes. The gel images for the reactions between RNA with mono-activated (a) compound **5** and (b) cisplatin showed the time-dependent decay of unreacted RNA and formation of the products ([RNA] = 0.7 μM, [Pt(II)] = 94 μM; 10 mM K_2HPO_4/KH_2PO_4, pH 6.2, with 20 mM $NaClO_4$, 37 °C). The fraction of unreacted RNA over time for the mono-activated (c) compound **5** and (d) cisplatin showed exponential decay.

For the reaction of mono-activated compound **5** with DNA, the rate is 14-fold lower than that of cisplatin (**Table 4.1**). For RNA, the rate is 3.7-fold lower. Therefore, mono-activated **5** shows slower reactivity with oligonucleotides compared to cisplatin, similar to the reactions with nucleosides in **Chapter 3**. This difference could be due to the steric hindrance caused by the larger carbohydrate group of **5** when approaching the target site because the carbohydrate group is in the axial position of the six-membered chelate ring.[161] Furthermore, the six-membered ring between the Pt and the carbohydrate ligand has the ability to accommodate different conformations (*i.e.*, boat and twist-boat)

during the coordination reaction. That difference could cause slower reactivity of mono-activated **5**. This effect is also observed for carboplatin, in which the bidentate leaving group ligand accommodates a boat configuration, which blocks reactions with the incoming nucleophiles.[189] Moreover, the Pt(II)-based anticancer compound picoline has also shown reduced reactivity due to steric effects caused by the non-leaving group ligand compared to cisplatin.[190] This characteristic has been considered beneficial in anticancer drugs in terms of minimizing the off-target reactions with glutathione or other cellular thiols.[191]

Table 4.1. Pseudo-first-order rate constants, k_{obs} for the reactions of mono-activated Pt(II) complexes with DNA, RNA

	mono-activated cisplatin k_{obs} (s^{-1}) × 10^{-4}	**mono-activated 5 k_{obs} (s^{-1}) × 10^{-4}**
DNA	7.4 ± 0.8	0.54 ± 0.05
RNA	3.3 ± 0.7	0.9 ± 0.1

As shown in **Table 4.1**, mono-activated cisplatin shows a 2.2-fold preference for DNA over RNA, whereas **5** shows a 1.7-fold preference for RNA. Therefore, the RNA preference of mono-activated compound **5** is also present at the oligonucleotide level, similar to the nucleosides. The geometric environment of the DNA and RNA might influence electrostatics of the nucleic acids, and subsequently the kinetics of Pt(II) interactions. The RNA structure creates multiple electrostatic pockets for metal binding.[192] In biology, Mg^{2+} is associated with the RNA regions to modulate electrostatic potentials.[127] In contrast to DNA, RNA adopts an A-form structure and the major groove is shown to be more electronegative than the minor groove.[192,193] This property may explain the preference of cationic drugs such as compound **5** for RNA over DNA. Sugar-

derived small molecules such as aminoglycosides preferably target RNA based on hydrogen-bonding capabilities of the drug.[122] Therefore, specific hydrogen-bonding interactions between the multiple sugar –OH groups of the carbohydrate ligand and RNA could be one of the reasons that the mono-activated **5** has preferred reactivity towards RNA compared to cisplatin.

4.4.2 Kinetic studies for bis-activated 5 and nucleic acid reactions

There could be various reasons for the observed low coordination rates of mono-activated compound **5** with DNA and RNA compared to cisplatin. The experiments were carried out with mono-activated Pt(II) compounds; therefore, the effect of the rate-limiting first hydrolysis step (10.2×10^{-5} s^{-1}) is not the reason for slow coordination.[16] The mono-activated compound can react with nucleosides or undergo second hydrolysis to produce the bis-activated complex. These competing reactions may impact the observed slow rates for the mono-activated compound **5**. Therefore, by using bis-activated compounds, we could analyze the effect of the structure or role of the overall charge of the complex (+1 vs. +2) on the reaction rate. As shown in **Table 4.2** and **Appendix B-Figure A1**, the experiment was carried out with both DNA and RNA.

Table 4.2. Pseudo-first-order rate constants, k_{obs} for the reactions of bis-activated Pt(II) complexes with DNA, RNA

	bis-activated cisplatin k_{obs} (s^{-1}) × 10^{-4}	**bis-activated 5 k_{obs} (s^{-1}) × 10^{-4}**
DNA	17 ± 2.7	0.2 ± 0.09
RNA	5.2 ± 1.6	0.3 ± 0.05

The same reactivity patterns are observed, similar to the mono-activated cisplatin, in which DNA is the preferred target with (3.2-fold) faster reactivity compared to RNA for

the bis-activated cisplatin. For bis-activated **5**, a significant difference between the rates for DNA and RNA is not observed.

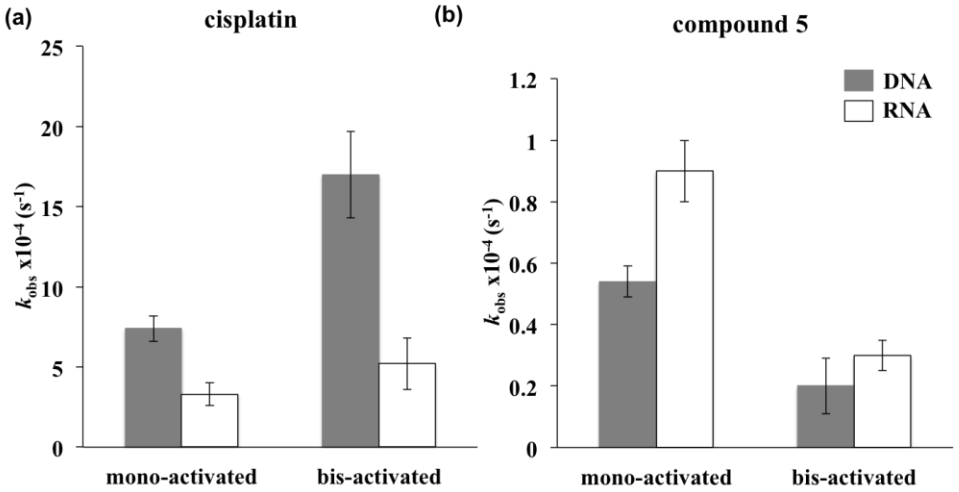

Figure 4.3. Comparison of reaction rates obtained from DNA and RNA with mono- and bis-activated Pt(II) complexes. The rate comparisons for (a) cisplatin and (b) compound **5** are shown. The errors were calculated from three independent experiments.

The obtained rates for mono- and bis-activated form of each compound are compared and summarized in **Figure 4.3**. Higher reaction rates for the bis-activated cisplatin (compared to mono-activated) are observed for both DNA and RNA.[167,194] This result also agrees with previously reported data, in which bis-activated cisplatin had a higher reaction rate than the mono-activated complex with DNA.[174,194] There are a few explanations to the observed higher rates for the bis-activated cisplatin. Compared to the monocation, the dication would facilitate the compound to be attracted more towards polyanionic nucleic acids and therefore increase the reaction rate. Moreover, the oxygen on the aqua ligand is less electronegative compared to the chlorido ligand, which would strengthen a hydrogen bond between the $-NH_3$ ligand and O6 of the guanine base. This interaction would increase the reaction rate of bis-activated cisplatin by stabilizing the transition state and decreasing the activation energy. In contrast, bis-activated **5** show a 3-fold decreased rate with both DNA and RNA compared to the mono-activated form. This

effect may be due to the larger carbohydrate non-leaving group near the Pt(II) reactive center as explained in the **Section 4.4.1** (so charge effect is reduced due to steric bulk).

4.4.3. Salt-dependent kinetic studies of 5 with nucleic acids

Coordination reactions between activated Pt(II) complexes with nucleic acids occur in two steps.[195] In the first step, the Pt(II) compound associates with DNA or RNA by displacing a fraction of surface-bound cations. The second step is direct coordination to the target. Activated-Pt(II) complexes are positively charged; therefore, the first association step is affected by cations in the media. Therefore, a salt-dependent kinetic study was carried out with mono-activated **5** in comparison to cisplatin with DNA and RNA to evaluate the contribution of electrostatics on the reaction. The platination rates were obtained from reactions in two buffer conditions, in which both had 12 mM K^+. Additionally, one condition was 5 mM Na^+, whereas the other was 20 mM Na^+. The comparative results are shown in **Table 4.3**, **Figure 4.4**, and **Appendix A-Figure A3**.

Table 4.3. Pseudo-first-order rate constants, k_{obs} for the reactions of mono-activated Pt(II) complexes with DNA, RNA in different buffer conditions

buffer condition 12 mM K^+	nucleic acid	mono-activated cisplatin k_{obs} (s^{-1}) × 10^{-4}	mono-activated 5 k_{obs} (s^{-1}) × 10^{-4}	fold change (cisplatin/comp 5)
5 mM Na^+	**DNA**	24 ± 5	2 ± 0.4	12
	RNA	33 ± 10	1.4 ± 0.3	23.6
20 mM Na^+	**DNA**	7.4 ± 0.8	0.54 ± 0.05	13.7
	RNA	3.3 ± 0.7	0.9 ± 0.1	3.7

At the low salt concentration (5 mM Na^+), the reaction rate differences between DNA and RNA are less prominent for both monoactivated-cisplatin and **5**. However, at

the high salt concentration (20 mM Na^+), mono-activated cisplatin shows a 2.2-fold preference for DNA over RNA, whereas **5** shows a 1.7-fold preference for RNA. This shows that the target preference can vary depending on the cations in the environment.[51] With increasing salt, the reaction rates decrease for both mono-activated cisplatin and **5**, likely due to increased competition for binding to the target. This result agrees with previous reports.[50] With DNA, both mono-activated compounds show a decline in the reactivity with increasing salt concentration (3.2-fold for cisplatin and 3.7-fold for **5**, respectively). A more pronounced salt effect was observed for the RNA and mono-activated cisplatin reaction (10-fold) in the two buffer conditions. However, only a 1.5-fold rate difference was observed for the reaction with mono-activated **5** and RNA at the two buffer conditions, suggesting that electrostatics play a less significant role in RNA-**5** interactions.

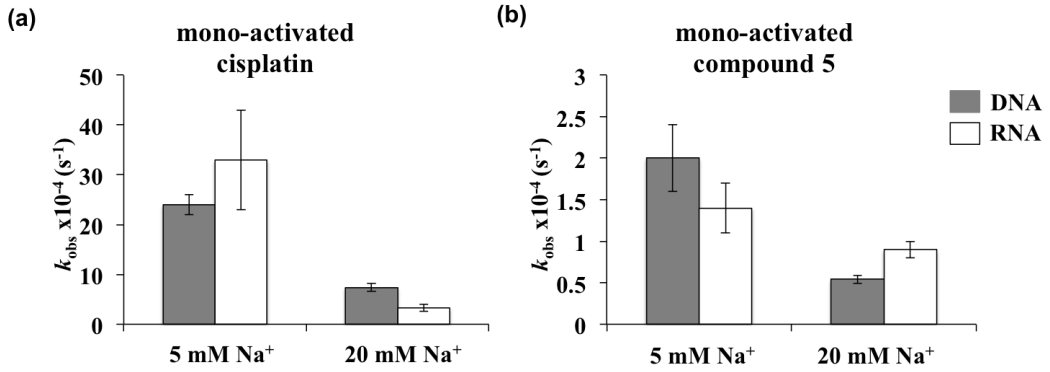

Figure 4.4. Comparison of salt-dependent reaction rates obtained for mono-activated (a) cisplatin and (b) compound 5 with DNA and RNA. The errors were calculated from three independent experiments.

Taken together, these kinetic data suggest that compound **5** has a slight preference for RNA over DNA. The size of the molecule may also play a role in governing the reaction. These results agree with previous studies, in which it was shown that large differences in rates occur when ligands occupying the Pt(II) coordination sphere are

changed.[189] These observations may influence the design of new carbohydrate-Pt(II) drugs that have reduced off-target binding. Additionally, compound **5** may favor RNA binding and therefore, future studies can be done to evaluate the reactivity of **5** with RNA.

4.4.4 Structural impacts of mono-activated 5 on plasmid DNA

Early studies with cisplatin and transplatin were done with plasmid DNA.[178] Plasmid DNA is topologically constrained, so that if there are any alterations causing changes in the number of helical turns, that effect is reflected on the DNA superhelicity.[178] Unwinding can be deduced by the changes in the superhelicity, which can be monitored by gel electrophoresis. Initial experiments to evaluate the structural effects of mono-activated **5** were carried out with pUC19 plasmid and compared to results with mono-activated cisplatin. Mono-activated **5** or cisplatin (160 μM each) were incubated with plasmid (0.5 μg) for different time periods as described in **Chapter 2**, **Section 2.4.11**. The reactions were quenched and analyzed on agarose gels (**Figure 4.5)**.

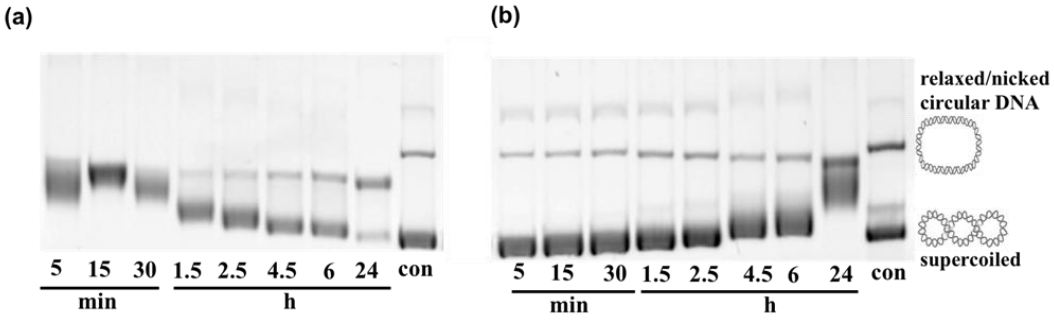

Figure 4.5. The gel images of the plasmid DNAs platinated by mono-activated (a) cisplatin and b) compound 5. ([DNA] = 0.5 μg, [Pt(II)] = 160 μM; 10 mM Na_2HPO_4/NaH_2PO_4, pH 7.4, 37 °C). The reactions were quenched at the time points indicated at the bottom of the images. The cartoon figures on the right show the topological forms of the closed circular DNA.

The bands corresponding to the supercoiled plasmid DNA exhibit different gel migration distances over various time points as adducts form with either mono-activated

cisplatin or compound **5**. The differing gel migration distances are caused by bending and unwinding of the plasmid DNA induced by the platinum adduct. The supercoiled plasmid platinated by mono-activated Pt(II) complexes becomes more relaxed, decreasing the electrophoretic mobility of the DNA. Upon further incubation with mono-activated cisplatin, relaxed plasmid DNA appears to rewind in the opposite direction to be supercoiled (30 min- 24 h time period). In contrast, the supercoiled region of plasmid platinated by mono-activated compound **5** is only seem to become more relaxed during the same incubation period. This suggests that compound **5** has a kinetically slower effect on the DNA plasmid structure than cisplatin.

4.4.5 Structural impacts of 5 on short duplex DNA oligomer

While the reactions with plasmid DNA allowed us to investigate more of the global structural changes, a DNA bending study was carried out with a short DNA duplex with a single -d(GG)- site as described in **Chapter 2**, **Section 2.4.12** to understand the structural impact at the local binding site. Depending on the binding mode the effect on the secondary structure can vary. A gel electrophoresis mobility shift assay that was reported in the literature for quantifying the DNA-bending angle was utilized in this study to evaluate the effect of **5**.[24] This method was developed based on a previous method that was used to study DNA bending at naturally occurring $d(A_5T_5)_2$ sequences known as A-tracts.[196] Presence of this sequence in the center of a DNA leads to bending of the DNA structure, thereby causing reduced mobility in a gel. Moreover, it has been shown that if there are multiple A-tracts in a DNA, the bends will be phased constructively if they are located ~10.5 helical turns apart.[145,196] Other spacings caused the bending to cancel out with no change in the mobility. The DNA duplex used for my

Pt bending studies was designed keeping the above facts in mind, in particular the spacing of the d(GG) site.

My experiments were carried out with a 22-base pair DNA duplex molecule (**Scheme 4.1**) that was used previously with cisplatin (top and bottom strands are referred to as DNA1 and DNA2).[24,144] The sequences were designed to have a two-nucleotide overhang on each end to facilitate ligation in only one orientation. DNA1 has a 5' phosphate and a single -d(GG)- site for platinum coordination. DNA2 is complementary to DNA1 and has hydroxyl groups at both the 3' and 5' ends, in which the 5' ends were radiolabeled using [γ^{32}-P]-ATP.

Scheme 4.1. Sequences of DNA used in the bending experiments.

DNA1: 5' p-TCT CCT TCT T**GG** TTC TCT TC TC–OH 3'
DNA2: 3' HO–AG AGA GGA AGA ACC AAG AGA AG-OH 5'

To facilitate the efficient platination of DNA1, it was reacted with a 1:2 ratio (DNA:Pt) of bis-aquated Pt(II) complexes (**Figure 4.6a**). The MALDI-MS spectra confirmed single platination of DNA1 in the gel-purified product (**Figure 4.6b and c**). The mass of DNA1 was calculated to be 6,640 Da and after coordination to cisplatin, the mass of the DNA1-Pt product was 6,868 Da, which corresponds to single platination most likely at the –d(GG)- site. For **5** coordinated to DNA1**,** the mass was 7086 Da with a shift of 447 Da that corresponds to bidentate coordination for a single adduct.

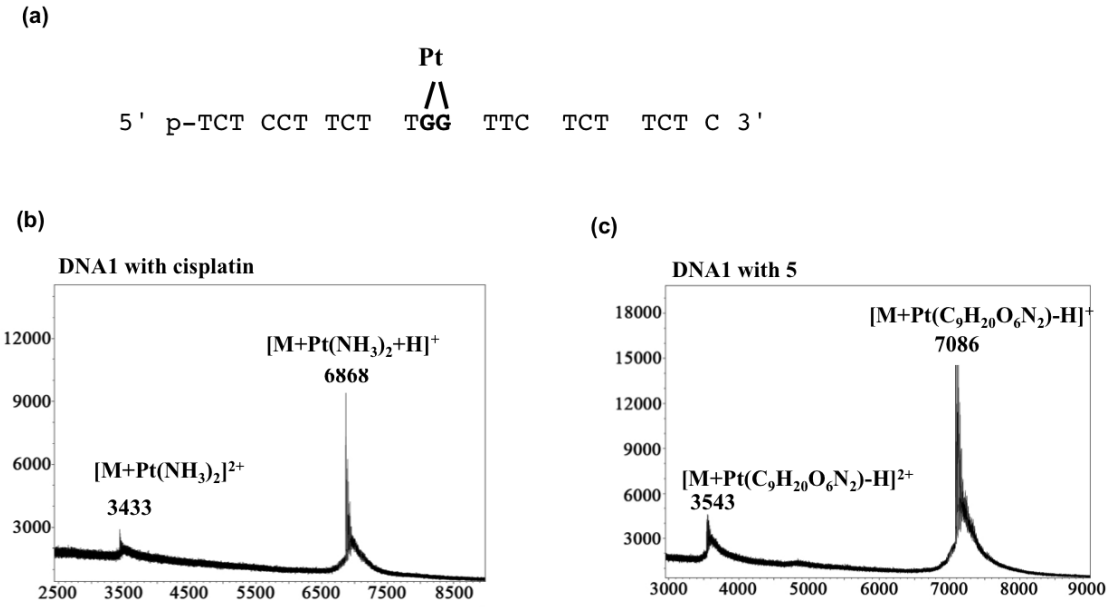

Figure 4.6. The platination of DNA1. (a) The DNA1 sequence with a single platination site and MALDI-MS spectra for the reaction of DNA with (b) cisplatin and (b) compound **5** are shown. The spectra were obtained in positive-ion reflector mode (3-HPA matrix). The calculated mass of the single-stranded DNA (M) is 6640 Da. The masses of the DNA1-Pt products correspond to bidentate coordination for a single adduct ([DNA1-$Pt(NH_3)_2]^{+/2+}$ for cisplatin and [DNA1-$Pt(C_9H_{20}O_6N_2)^{+/2+}$ for compound **5**).

Initial experiments were carried out with cisplatin to verify the DNA bending method and compare to published data.[24] The platinated and unplatinated DNA1 strands were annealed and ligated with bottom strand (DNA2) in separate reactions. The effects of platination on the DNA structure were determined by analyzing the reaction mixtures on 8% native polyacrylamide gels. The ligation of duplex monomers leads to the formation of DNA oligomers. Initially, different ligation times were tested. **Figure 4.7a** shows the results for one and 16 h ligations. Both conditions show the same results of ligation; therefore, future ligations were done for 1 h at room temperature.

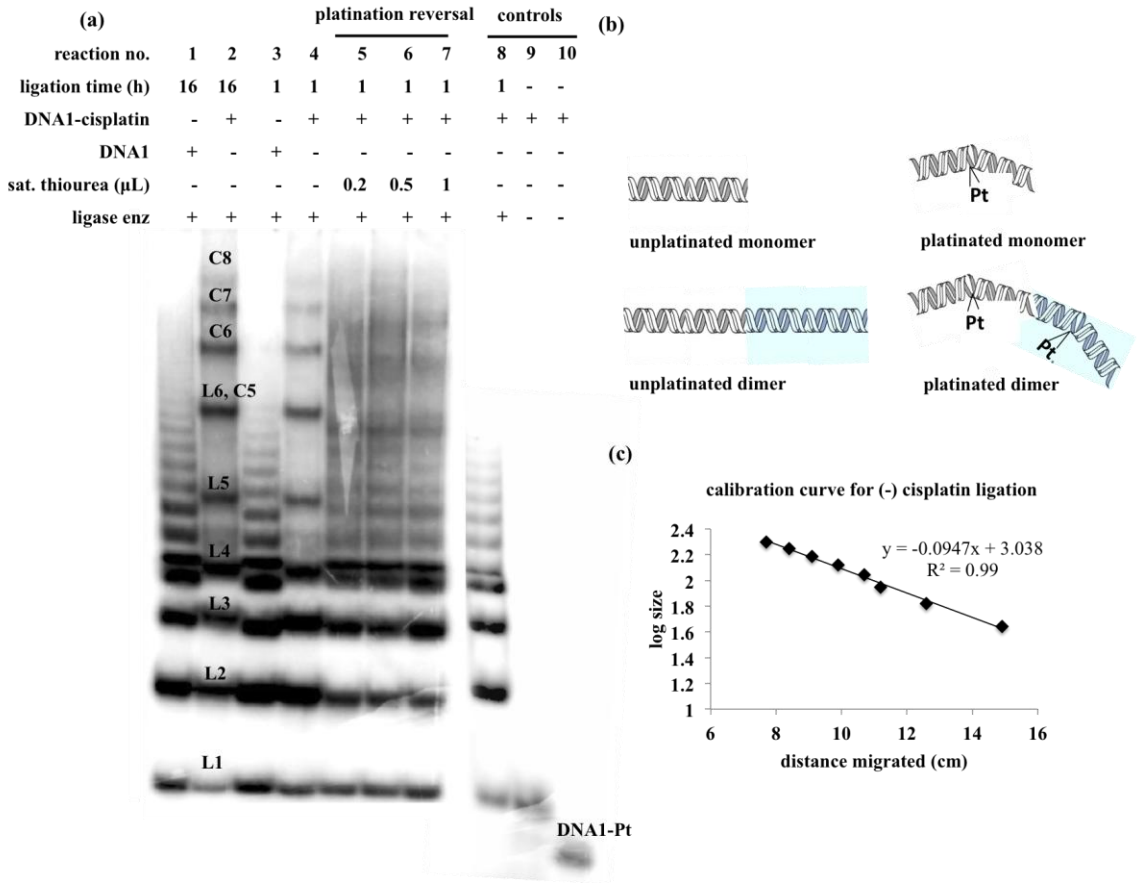

Figure 4.7. Results for DNA bending caused by cisplatin. (a) The 8% native polyacrylamide gel image for DNA bending experiments with and without cisplatin is shown. (L= linear ligated DNA oligomers, C= circular ligated DNA oligomers; the numbers 2, 3, 4, *etc.* correspond to the number of duplex monomers that are ligated together. Lanes 5-7 contain reaction mixtures treated with thiourea to remove the Pt adduct. Reactions 8-10 are controls (separate gel). (b) A schematic diagram of the DNA ligation with and without cisplatin, and (c) the calibration curve constructed for the (-) cisplatin DNA are shown.

In the reaction with unplatinated DNA1, the duplex monomers were expected to ligate to give linear oligomers, which is indeed observed in **Figure 4.7a** (for example, L4 represents a linear oligomer with four monomers ligated together). In contrast, the platinated DNA has a reduced mobility on the gel as seen in **Figure 4.7a**. We believe this effect is due to the bending effect of the cisplatin adduct on the DNA structure (**Figure 4.7b**). For the platinated DNA, migration retardation is observed particularly for the larger multimers. A decrease in gel mobility may result from a decrease in the end-to-end

distance of the ligated DNAs due to curvature introduced by the platinum adducts.[24] The chosen DNA sequence predicts the bends to be spaced evenly, such that constructive addition of bends leads to circular DNA. With an increasing number of bends that are added together, the gel mobility of the DNA products decrease. Similar to previous studies done with cisplatin,[24,25,144] the circularization occurs when five double-stranded monomers are ligated together (C5-110 bp) and the resulting circle comigrates with L6.

As reported by Bellon and Lippard, the difference in the migration of the platinated DNA relative to the unplatinated DNA can be used to quantify the bend angle caused by cisplatin.[145,197]The migration distances of the bands on the gel corresponding to unplatinated DNA (lanes 1 and 3) were measured manually and a calibration curve was constructed between the log size of the DNA and migrated distance (**Figure 4.7c**). From the plot, the calculated length for a particular linear platinated DNA can be obtained. The calculated length is based on an oligomer's mobility. Using the equation obtained from the calibration curve (y = -0.0947x + 3.038), the calculated lengths (y) were determined, in which x is the migration distance for the linear platinated DNA (**Table 4.4**).

Table 4.4. Calculated lengths and relative mobilities for the cisplatin-modified DNA

nucleic acid	DNA distance migrated (cm)	y = -0.0947x + 3.0378	calculated length (bp)	measured length (bp)	relative mobility (R_L)
L2	14.9	1.63	42	44	0.95
L3	12.5	1.85	71	66	1.1
L4	11.0	1.99	99	88	1.1
L5	8.6	2.22	167	110	1.5

The relative mobility (R_L) of the platinated DNA is the ratio between the calculated length of the oligomer and actual length. Since unplatinated DNA has the same

calculated length and actual length, the R_L is 1 for all points. With higher curvature in the DNA structure, mobility retardation is higher and results in higher R_L values. As shown in **Table 4.4**, the platinated DNA has R_L>1 for longer oligomers (≥L3). Determination of the DNA bend angle caused by cisplatin is performed using **Equation 4.1**, in which L represents the length of a particular oligomer with relative mobility R_L and RC is the curvature relative to DNA bending of an A tract (A DNA with a known bend angle).[24,144,145] Application of **Equation 4.1** to the 110-bp multimer composed of the 22-bp platinated monomers gives a curvature of 0.85. To determine the average bend angle in degrees, the RC value is multiplied by the absolute value of two A_6 tract (40°).[197,198] The result predicts the bend induced by the cisplatin 1,2-d(GG) intrastrand crosslink to be 34°, which corresponds well with previous studies.[24] The experiment was repeated three times and the bending angle was calculated using the 110-mer to be 34 ± 1°.

$$\mathbf{R_L - 1 = (9.6 \times 10^{-5} L^2 - 0.47) (RC)^2} \qquad \textbf{Equation 4.1}$$

After establishing the protocol with cisplatin, the same experiment was carried out with DNA platinated by bis-activated compound **5** (**Figure 4.8**). Similar bands are observed with reduced mobility, together with bands corresponding to circular products. The band corresponding to linear 5-mer, which is used for quantification, is more prominent in cisplatin than for compound **5**, which suggests the rate of cyclization could be different for the two compounds. Therefore, the 6-mer (132 bp) band was used to quantify the bend angle for compound **5**. The band migration distances were measured and the DNA-bending angle was computed to be 36 ± 1° (two trials), which is similar to that of cisplatin modified DNA.

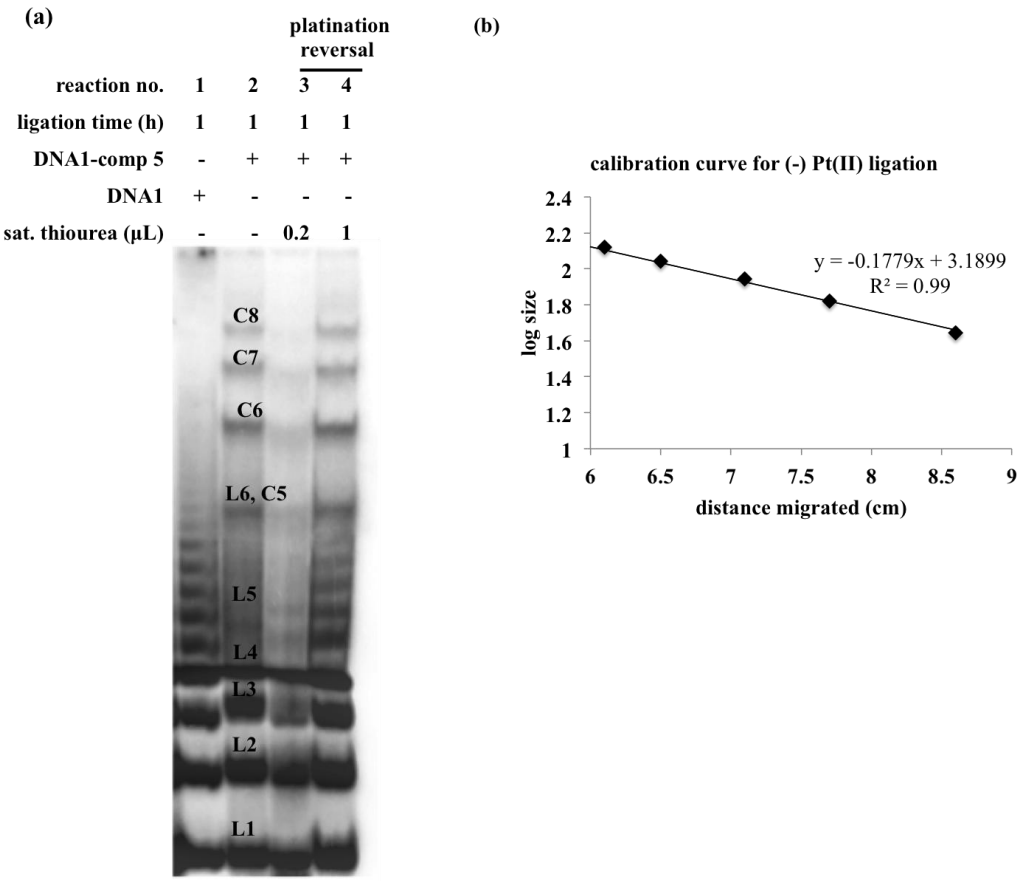

Figure 4.8. Results for DNA bending caused by 5. (a) The 8% native polyacrylamide gel image for DNA bending experiments with and without compound **5** is shown. (L= linear ligated DNA oligomers, C= circular ligated DNA oligomers; the numbers 2, 3, 4, *etc.* correspond to the number of duplex monomers that are ligated together. Lanes 3 and 4 are reactions treated with thiourea to remove the Pt adduct. (b) The calibration curve constructed for the (-) Pt DNA is shown.

To show that the mobility change is due to platinum adduct formation, saturated thiourea was used to reverse the platination.[199] When the ligation products modified with cisplatin and **5** were incubated with saturated thiourea (0.2, 0.5, or 1 μL) for 72 h at 37 °C (lanes 5-7 in **Figure 4.7** and lanes 3-4 in **Figure 4.8**), the linear platinated DNA bands show similar migration patterns as the unplatinated DNA (lane 1). Even after removing the Pt, the upper bands (corresponding to C5-C8)) in the gel have slower mobility, supporting a model in which the Pt binding has caused circularization. Presence of

circular products is evidence for the ability of **5** to significantly bend the DNA structure so that the ends will come closer together for ligation.

Figure 4.9 shows crystal structures of cisplatin and oxaliplatin bound DNA, in which the adducts are located in the major groove of DNA.[181,200] The crystal structures consist of a DNA dodecamer duplex with a sequence of 5′-CCTCTGGTCTCC.[181,200] There is only one platination site in the middle of the sequence. Irrespective of the length, this DNA duplex is very similar to the one used in my study. Thus, it is a good representation of the platinum adducts bound to duplex DNA. Compound **5** adduct was modeled onto the crystal structure of oxaliplatin to represent the binding. Although the positioning of the sugar pendent may slightly vary in an actual structure, this model structure gives an indication of how compound **5** sits in the major groove of a DNA duplex. The adduct of **5** is bulkier than cisplatin and oxaliplatin, and it likely sits in the DNA pocket with the sugar group protruded outside, similar to oxaliplatin.

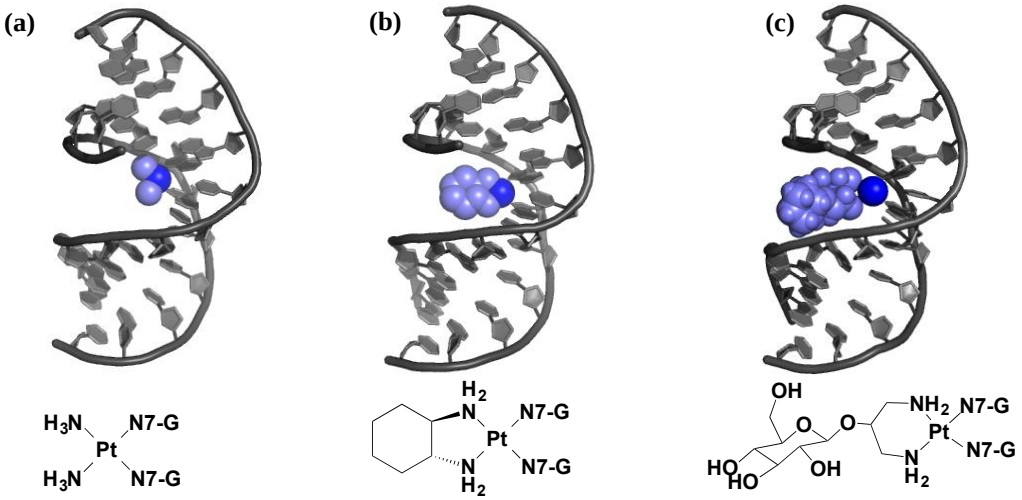

Figure 4.9. Crystal structures of Pt(II) complex-bound DNA duplex. The DNA dodecamer duplex has a single GG-site for platination with (a) cisplatin (PDB: 1AIO), (b) oxaliplatin (PDB: 1IHH) and (c) compound **5**.[181,200] The other nucleotides in the duplex are C and T. Platinum atom is shown is dark blue color and the chemical structure of the Pt(II) complex is shown below each crystal structure. The crystal structure for **5** was modeled based on the oxaliplatin-DNA structure.

Depending on the Pt(II) adduct, the effect on DNA structure varies. For example, monofunctional or intercalating adducts unwind DNA, whereas *cis* intra- and interstrand bifunctional adducts unwind and bend the DNA.[201] Moreover, *trans*-1,3-intrastrand adducts cause the middle nucleotide to bulge out.[171] Furthermore, *trans* adducts cause a hinge joint at the locus, which does not lead to cooperative bending. Previous studies showed that the formation of 1,2-d(GG) instrastrand cross-links by cisplatin leads to DNA bending towards the major groove and unwinding of the DNA.[183] Taken together, my results support the hypothesis that compound **5** makes a 1,2-d(GG) intrastrand cross-link with DNA that leads to DNA bending as well. Appearance of similar circular bands for cisplatin and compound **5** further suggests similar DNA bending caused by platination on duplex DNA. The calculated bend angles are in the same range as previously reported bend angles from similar gel-based assays (32-40°). In fact, additional hydrogen-bonding interactions of **5** could further restrain the DNA duplex and orient it for faster ligation than cisplatin. Such interactions has been shown with oxaliplatin where additional hydrogen-bonding interactions are present between the NH of the (*R*, *R*)-DACH ligand and the O6 atom of the 3′-dG of the d(GG) lesion.[200] The search for a better anticancer drug might include molecules that can form hydrogen bonds directly to DNA in the vicinity of the lesion, similar to oxaliplatin. Therefore, it may be promising to use compounds related to **5** that have similar hydrogen-bonding properties. The toxicity of cisplatin comes from these lesions on DNA; therefore, it was of interest to compare the biological effects of cisplatin and **5** as well. This will be further discussed in **Chapter 5**.

4.4.6 Evaluation of structural and sequence specificity of mono-activated 5 by probing ribosomal RNA

The size and charge of the non-leaving group ligands can affect the binding selectivity to oligonucleotides. With previous experiments, compound **5** binding to d(GG) sites of DNA has been shown. With the observed kinetic preference of mono-activated compound **5** for RNA over DNA, it was of interest to further explore the RNA binding aspects of compound **5**. Amino-sugar derived drugs are largely known to interact with RNA,[120] specifically rRNA, due to their capability of hydrogen bonding with the target. Furthermore, the ribosome has specific binding pockets to accommodate different ligands as a part of its normal biological role.[97] The ribosome is a ribonucleoprotein complex that plays a significant role in the protein translation process.[97] The ribosome is a highly abundant, complex structure that is a common drug target.[97] With the similarity between DNA and RNA purine nucleotides, the ribosome and other functionally important RNAs can be secondary targets for platinum drugs. There have been previous efforts to study cisplatin binding to RNA. These studies have included probing of rRNA to identify platination sites,[43] localization studies to show where cisplatin is accumulating in the cell,[46] and kinetic studies to determine the rates of RNA platination.[51] A crystal structure of the *T. Thermophilus* 70S ribosome modified with cisplatin is also available.[40] In this study, structural and sequence specificity of mono-activated compound **5** binding to rRNA was evaluated in the context of the ribosome. The method is included in **Chapter 2**, **Section 2.4.13-2.4.15** (this work was done in collaboration with Dr. Nisansala Muthunayake). Considering the bulky sugar ligand of **5** compared to the simple ammines of cisplatin, it was of interest to evaluate the preferred binding sites for each compound.

Certain regions in the ribosome are critical for its biological function, namely translation. Based on a recently published cisplatin-bound ribosome crystal structure,[40] h24 (790 loop), h44, h43, and the peptidyltransferase center (PTC) were chosen to map the binding sites of mono-activated **5** on the rRNA. Additionally, H69 has been extensively studied as a cisplatin-binding site in our lab; therefore, it was of interest to probe H69 as well. Out of the probed functionally important rRNA regions, h24, h44, and h43 are located in the small subunit of the ribosome, whereas the PTC region and H69 are located in the large subunit. The DNA primers were designed to anneal to complementary regions of RNA, upstream of the site of interest. For example, the radiolabeled primer for the 790 region anneals at positions 831-814 of 16S rRNA (*E. coli* numbering) and extends towards the 790 region during reverse transcription. The platinum-modified nucleotide locations can be detected by reverse transcriptase stops on the 3' side of the adduct. There are some stop sites visible in the control lane due to RNA secondary structures that block reverse transcriptase. Dideoxy sequencing was done in parallel to compare with the reverse transcription reactions. Band intensities at the stop sites were quantified and normalized to standard bands to achieve the % reactivity. The bands with ≥50% were considered as major stop sites, whereas the ones below 50% were considered as minor sites.

Figure 4.10 shows the result for probing the 790 loop, which is part of helix 24 (h24) in the small subunit, with mono-activated cisplatin and **5**.[202] There is a prominent stop site at U801 for cisplatin, which is consistent with previously published data from our lab.[43] As shown in the secondary structure map, this site is in the internal loop region and adjacent to two consecutive G residues, G799 and G800. Several other stop sites are

observed at A792, A777, and C770, and a minor stop site at C795 for cisplatin, where all residues are located 3' to purine reactive sites. Minor stop sites are observed for **5** at all of the above-mentioned residues. Nucleotides A792, A777, and C770 are proposed to participate in adduct formation with neighboring G residues, similar to cisplatin. In contrast, the stop at C795 suggests adduct formation at the adjacent A residue.

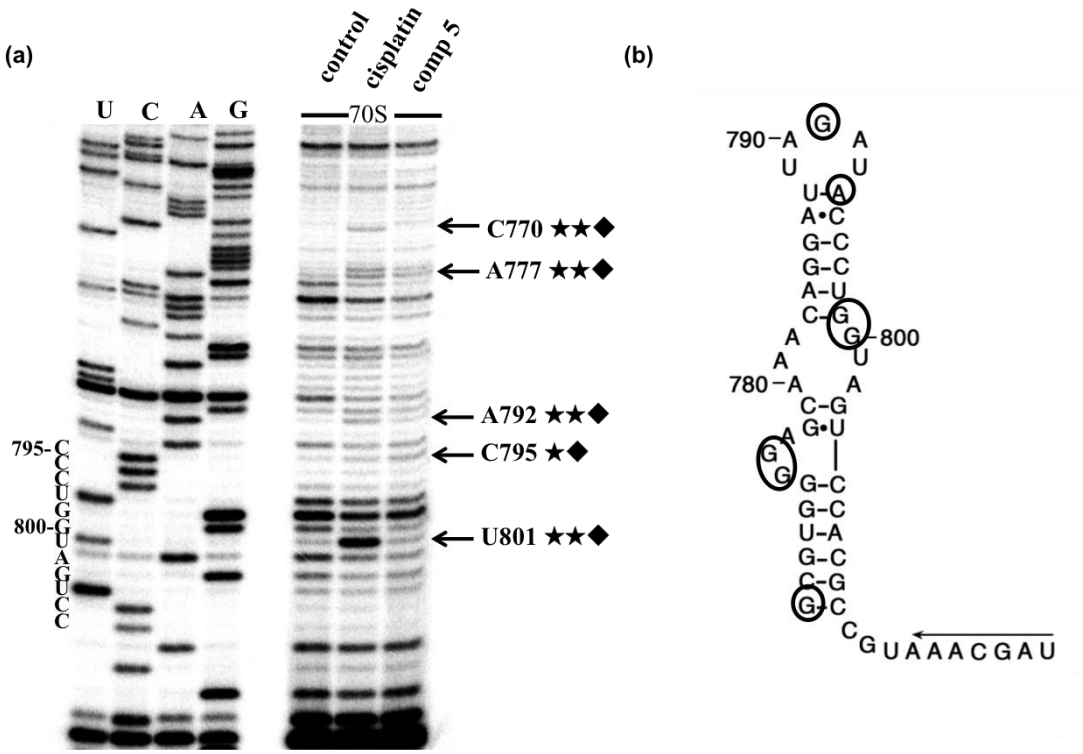

Figure 4.10. Probing result for ribosomal h24 (790 loop) region with mono-activated cisplatin and 5. (a)The autoradiogram shows reverse transcription mapping of *in vitro* reactive sites of mono-activated cisplatin and **5** on 70S ribosomes in a 1:200 molar ratio. The stop sites for cisplatin (□) and **5** (◆) are shown with symbols (□□,◆◆major, □,◆minor adduct). Dideoxy sequencing lanes are labeled as U, C, A, and G. (b) The rRNA secondary structure with the corresponding platinum-reactive sites is shown. The primer binding site is shown with an arrow.

The 790 loop is located near the ribosome decoding site. Chemical and enzymatic probing, as well as mutagenesis and structure studies, have revealed this region to be exposed on the surface of the 30S subunit, and directly involved in subunit association, as

well as playing a key role in translation initiation.[203] Notably, the Pt(II) modification site at A790 and G791 is at the mRNA channel, where the rRNA directly contacts the bound mRNA.[40] Cisplatin has been shown to coordinate to A790 and mRNA in a recent x-ray structure, and therefore may prevent mRNA translocation.[40] Furthermore, Pt(II) binding at A794 could affect P-site binding of tRNA, similar to the antibiotic edeine.[103] Therefore, platination at these positions could potentially prevent protein synthesis.

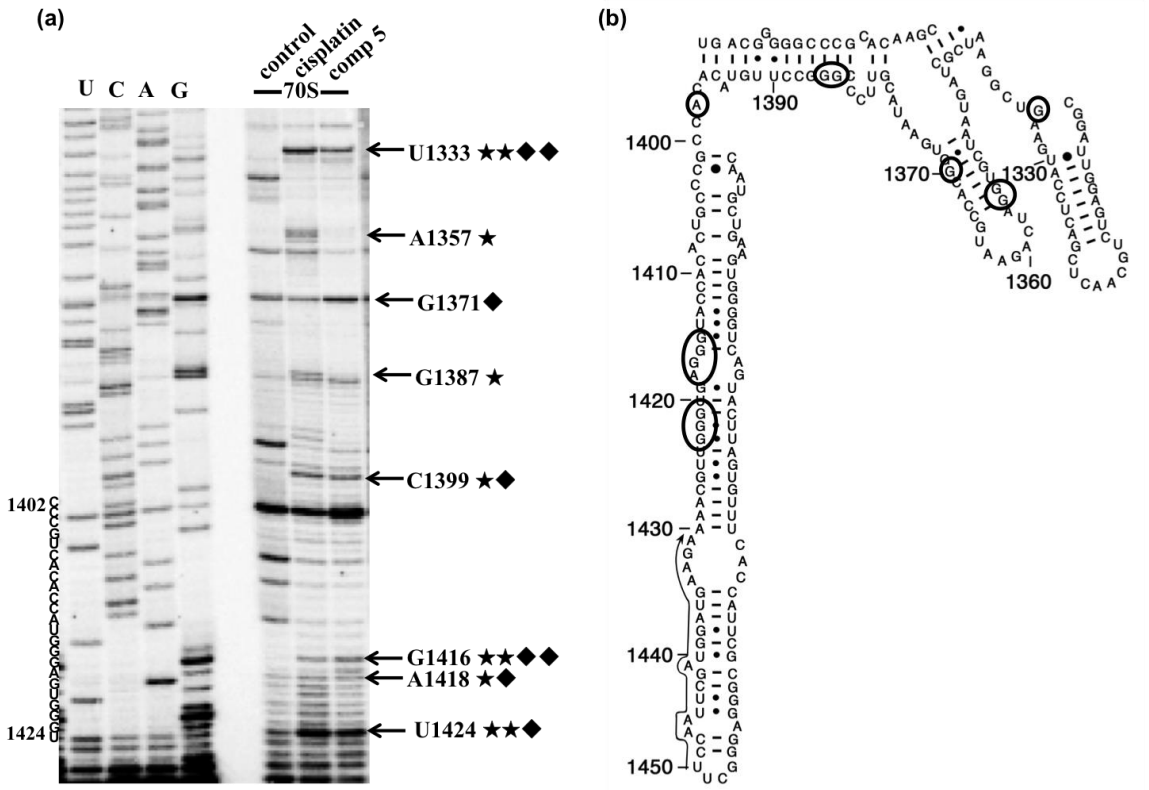

Figure 4.11. Probing result for ribosomal h44 (A site) and h43 regions with mono-activated cisplatin and 5. (a) The autoradiogram shows reverse transcription mapping of *in vitro* reactive sites of mono-activated cisplatin and **5** on 70S ribosomes in a 1:200 molar ratio. The stop sites for cisplatin (□) and **5** (◆) are shown with symbols (□,◆◆major, □,◆minor adduct). Dideoxy sequencing lanes are labeled as U, C, A, and G. (b) The rRNA secondary structure with the corresponding platinum-reactive sites is shown. The primer binding site is shown with an arrow.

The ribosomal decoding site (A site) is in h44 of 16S rRNA, and it is involved in maintaining translation fidelity.[103] Many antibiotics exert their activity by binding to the

A site (*e.g.*, neomycin and kanamycin) or regions near A site (hygromycin B) and thereby prevent the translocation of mRNA and tRNA on the ribosome.[204] Cisplatin and **5** show multiple coordination sites between the A1415 and G1423 region, which has many wobble pairs (**Figure 4.11**). A strong **5** binding site is located at G1334, next to a wobble pair and another minor binding is detected at G1370 of the h43 region.

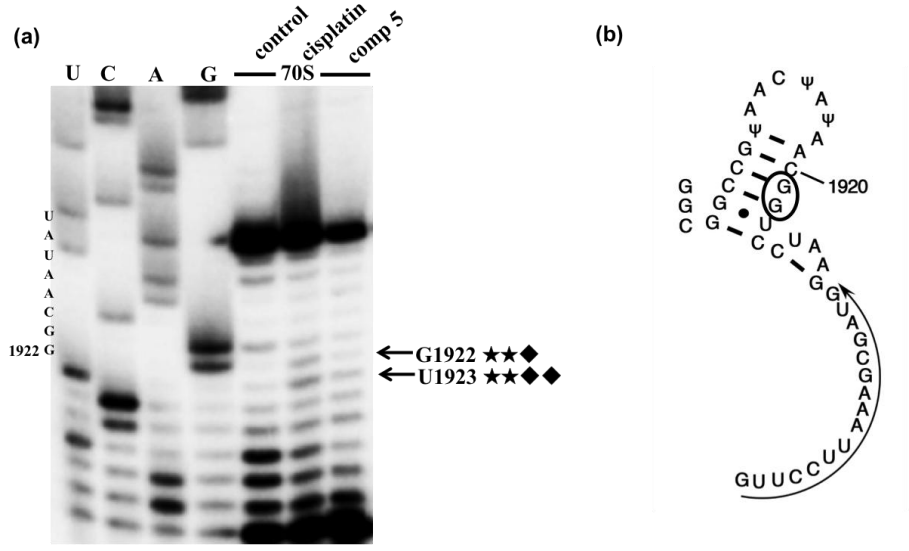

Figure 4.12. Probing result for the ribosomal H69 region with mono-activated cisplatin and 5. (a)The autoradiogram shows reverse transcription mapping of *in vitro* reactive sites of mono-activated cisplatin and **5** on 70S ribosomes in a 1:200 molar ratio. The stop sites for cisplatin (□) and **5** (◆) are shown with symbols (□□,◆◆major, □,◆minor adduct). Dideoxy sequencing lanes are labeled as U, C, A, and G. (b) The rRNA secondary structure with the corresponding platinum-reactive sites is shown. The primer binding site is shown with an arrow.

Mono-activated compound **5** binding to H69 region of the 23S rRNA is observed as shown in **Figure 4.12**. Platination is observed for both cisplatin and **5** at G1921-22 residues, which are next to a wobble pair. *In vitro* studies with model H69 hairpin loop have confirmed the cisplatin binding at G1921 and G1922 as well.[95] H69 region forms the intersubunit bridge B2a with h44 in the 70S ribosome.[205] This region undergoes conformational changes to facilitate translation initiation and ribosome recycling.[206]

Therefore, it is likely that Pt(II) drug binding to these dynamic motifs could inhibit protein translation.

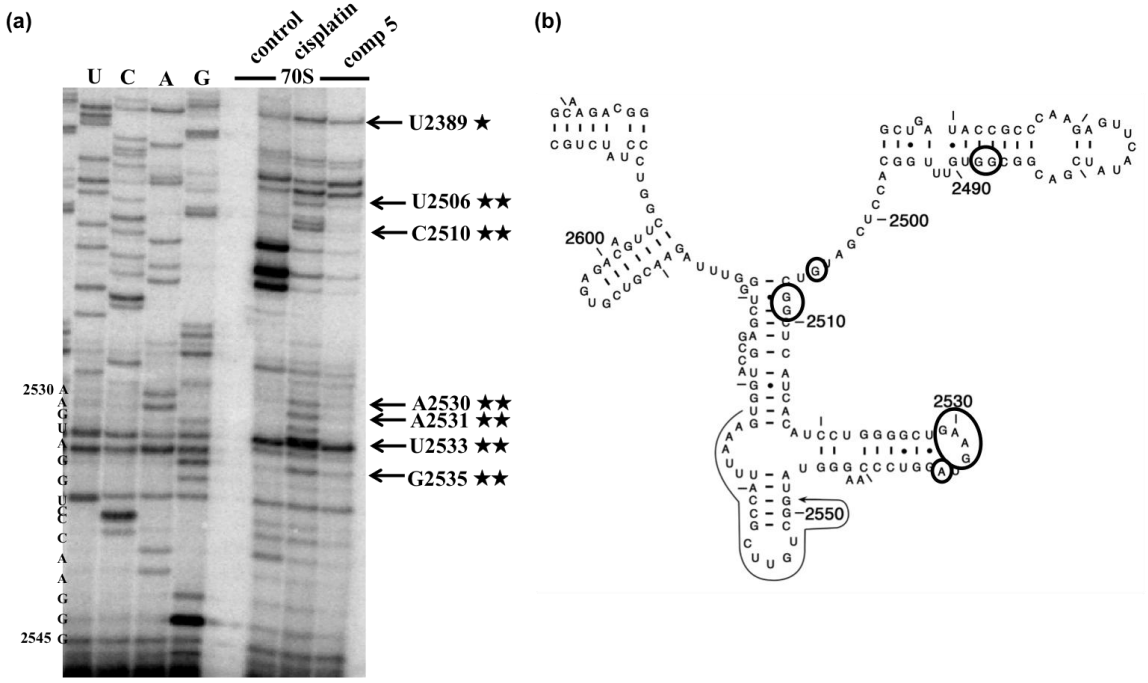

Figure 4.13. Probing result for ribosomal PTC region with mono-activated cisplatin and 5. (a)The autoradiogram shows reverse transcription mapping of *in vitro* reactive sites of mono-activated cisplatin and **5** on 70S ribosomes in a 1:200 molar ratio. The stop sites for cisplatin (□) and **5** (◆) are shown with symbols (□□,◆◆major, □,◆minor adduct). Dideoxy sequencing lanes are labeled as U, C, A, and G. (b) The rRNA secondary structure with the corresponding platinum-reactive sites is shown. The primer binding site is shown with an arrow.

The PTC region of the 23S large subunit of the ribosome is another targeted region for multiple drugs. My probing results reveal cisplatin binding sites at the PTC region, but none for **5 (Figure 4.13)**. Similar to the published crystal structure with the platinum-modified ribosome, strong stop sites at the A2530-G2535 region suggest cisplatin binding. This region interacts with the ribosomal protein L6, and therefore, the C-terminus of the protein is likely to interact with the Pt adduct.[40] These contacts at the GTPase activating center could affect possibly GTP hydrolysis or EF-G binding.[40] Larger

drugs such as macrolides and peptides are known to bind to the upper exit channel of the PTC region.[207] Preliminary probing data show interactions at A2058-2059, which are residues in the macrolide binding pocket (data not shown).[207]

The sequence preference for cisplatin binding to DNA is well characterized. Cisplatin prefers binding to G-C rich DNA sequences. The adducts mostly form at –d(GG)- or –d(AG)- sequences.[166] Furthermore, the flanking bases also play a role in platination.[174,175] The main factor governing the structural specificity of cisplatin is accessibility of the N7 of guanine base for reactions with aquated cisplatin. One study with a DNA hairpin, d(CGCGTTGTTCGCG) showed that guanine located in the loop is preferred for reactivity over guanines in the stem region due to the increased solvent accessibility.[47] Some of the types of adducts formed in RNA are similar to DNA.[43,208] Reactivity studies with RNA have also shown cisplatin binding at loop regions, A residues, G-C-rich, and wobble base-pair regions using full-length tRNA and ribosomal RNA.[44,208] The reactive sites observed in my probing studies showed similar trends as with the above-mentioned sequences and secondary structures. The adducts occur at purine residues in the context of –d(GG)- or –d(AG)- sequences. Furthermore, we observed that Pt(II) compounds seem to prefer binding to non-standard duplex regions, such as mismatches. Only a few adducts were located at the residues involved in canonical base pairing with a standard A-form helix. All other sites were involved with bulges, internal loops, hairpin loops, or G•U wobble pairs. Interestingly, many of the major binding sites of mono-activated **5** were at or next to wobble pairs. Wobble pairs have been implicated in RNA functioning in some studies.[127] The G•U wobble pair is the most common non-Watson-Crick pair in RNA.[209] Regions with tandem G•U pairs in the

major groove of RNA have more negative surface potentials, which may play a role in metal binding.[209,210] In the rRNA probing, some of the positively charged cisplatin and **5** binding sites were at G•U wobble pair sites, probably due to the high negative potential at those sites.

My results suggest that cisplatin and **5** have some similar reactive sites. But compared to cisplatin, **5** showed overall lower band intensities at the reactive sites. Irrespective of the bulky carbohydrate ligand of **5**, it is noteworthy to observe **5** reactivity at most of the cisplatin reactive sites. This agrees with the RNA preference of mono-activated **5** and implies that sugar conjugation has altered the target specificity of the platinum compound.

Overall, the data in this chapter shows the reactivity of compound **5** compared to cisplatin. The two compounds have different non-leaving group ligands, and by comparing similarly activated compounds side by side, we could evaluate the role of the ligands on the activity. My data show that carbohydrate conjugation reduces the reaction rates of compound **5** relative to the parent cisplatin, likely due to steric effects and restricted flexibility of the carbohydrate moiety. These key structural differences in the compound may help minimize off-target binding. The DNA structural changes caused by compound **5** binding were also analyzed by using plasmid and short oligomer DNAs. Compound **5** caused unwinding and bending of the DNA, similar to cisplatin, even though the binding event appeared to be slower than cisplatin. Kinetic studies of mono-activated compound **5** showed preference towards RNA over DNA. Furthermore, ribosome-binding studies showed that the compound **5** binding sites overlap with cisplatin and other common drug-binding sites, suggesting that the binding could

potentially disrupt the protein translation process. Therefore, further efforts towards the design of carbohydrate-linked platinum analogs for the treatment of specific cancers might include RNA as a potential target.

CHAPTER 5

POTENCY AND ACCUMULATION OF A CARBOHYDRATE-LINKED PLATINUM COMPOUND IN HUMAN CELL LINES

5.1 Abstract

Different platinum anticancer drugs have different levels of potency in different cancer types. To explore the cytotoxicity of the carbohydrate-platinum compound (**5**) towards various cancer cell lines, a series of MTT assays were carried out. Comparable cytotoxicities of compound **5** and cisplatin in ovarian and melanoma cancer cell lines was reported previously. In this work, we expanded the study to include several other cancer cell lines and to show low micromolar potency (4 μM) in a prostate cancer cell line, DU145. Despite previous success, a common problem associated with platinum compounds is their side effects originating from a lack of tumor selectivity. Selective targeting can be achieved by utilizing characteristic features of the cancer cells, such as enhanced glucose uptake. Therefore, it was of interest to examine compound **5** uptake and compare cytotoxicities (IC_{50} values) for DU145 prostate cancer and the corresponding normal cells. Compound **5** showed an 18-fold higher potency towards DU145 compared to normal cells, suggesting selectivity towards the cancer cells. A quantitative analysis of Pt levels in the cells was carried out using inductively coupled plasma mass spectrometry (ICP-MS), to determine whether the biological differences were due to higher accumulation of compound **5** in the cells or some other factor. There is a 24-fold higher accumulation of **5** in cancer cells over normal cells, whereas for cisplatin it is 18-fold. Therefore, these findings suggest the potential of using glycoconjugated platinum complexes as lead compounds for selective tumor targeting.

5.2 Introduction

The drawbacks associated with the antitumor drugs have stimulated the search for new compounds with improved pharmacological properties. In the search for new compounds, one of the first steps is testing their antitumor activity against a panel of cancer cells.[7,201,211] This approach will facilitate identification of tumor cells that are targeted as well as determine the level of selectivity of the chosen compounds. The cell studies together with biochemical assays will give insight into the mechanism and facilitate the development of compounds with an improved spectrum of activity. Although most of the existing anticancer drugs are believed to have a similar mechanism of action for cancer cell apoptosis by binding to DNA, their potency towards different cancer types varies.[7] This difference could be due to the inherent properties of the cancer cells, such as membrane components, in combination with the different properties of the drugs.[7]

5.2.1 The MTT assay

There are several ways to quantify viable cells following drug treatment. Traditional methods include counting cells using a hemocytometer and colony counting.[212] However, these methods can be tedious and time consuming. Another widely used method is the radionuclide incorporation assay, which can be expensive and time-consuming.[212] Compared to these methods, the MTT assay is a quantitative, sensitive, and reliable assay for cell viability measurements.[129,213] It is a colorimetric assay to indicate the cellular metabolic activity. MTT is a yellow-colored, water-soluble dye that can readily undergo reduction, primarily by mitochondrial dehydrogenases, to produce purple colored formazan crystals.[213] This conversion takes place in the presence of live

cells, in which MTT is taken up through endocytosis, and the formazan product is transported and crystallized on the cell surface.[214] The intensity of the color is therefore correlated with the number of live cells present. The absorbance is read (usually between 500 and 600 nm) after dissolving the formazan crystals in DMSO.[130] The absorbance is compared to the controls and normalized to calculate the percent survival of cells. The cytotoxicity of the drugs is given as the IC_{50} value after exposing the cells to different concentrations of the drug. The IC_{50} value is the drug concentration at which half of the cell activity is inhibited.[215] This value is obtained from a graph plotted against the percent survival and the relevant drug concentrations. Although used for cell viability, this assay can also be used to analyze cell proliferation.[213] The MTT assay has been widely adopted due to its simplicity and sensitivity. However, certain parameters have to be taken into consideration when optimizing the assay to obtain the best signal intensity. These include the number of cells and their metabolic activity, the concentration of MTT, and the length of incubation.[213] There are other tetrazolium reduction assays that are similar to MTT.[130] The most commonly used tetrazolium compounds include MTS (3-(4,5-dimethylthiazol-2-yl)-5-(3-carboxymethoxyphenyl)-2-(4-sulfophenyl)-2H-tetrazolium), XTT (2,3-bis-(2-methoxy-4-nitro-5-sulfophenyl)-2H-tetrazolium-5-carboxanilide), and WST (2-(2-methoxy-4-nitrophenyl)-3-(4-nitrophenyl)-5-(2,4-disulfophenyl)-2H-tetrazolium).[215] Resazurin reduction assay and trypan blue assays are also commonly used for cell viability.[130,215]

5.2.2 Potency of major platinum-based drugs in human cancer cell lines

Cisplatin, oxaliplatin, and carboplatin are FDA-approved, platinum-based anticancer drugs that are used around the globe.[17] These compounds exhibit a broad

spectrum of activity.[59] Their potency has been widely documented with different cancer cell lines using the above-mentioned methods.[216,217] The IC_{50} value for a drug in the same cell line can vary depending on many parameters, including the assay type and treatment period.[215] **Table 5.1** summarizes the IC_{50} values that have been reported for the major platinum-based anticancer drugs in several human cancer cell lines.

Table 5.1. IC_{50} values of cisplatin, oxaliplatin, and carboplatin in human cancer cell lines

	IC_{50} (μM)		
cell line	**cisplatin**	**oxaliplatin**	**carboplatin**
MDA-MB-231	1.4 ± 0.2 (120 h*)[216]	23 ± 0.1 (72 h*)[217]	8.3 ± 0.3 (120 h*)[216]
MDA-MB-435	5.8 ± 4 (24 h*)[191]	12.7 ± 5.6 (24 h*)[191]	-
H1299	21.4 ± 4 (72 h*)[218]	-	19.3 ± 3 (5 days*)[219]
DU145	3 (72 h*)[220]	-	10 ± 0.7 (5 days*)[219]
LNCaP	15.9 ± 4.7 (72 h◆)[221]	>50 (24 h*)[222]	>100 (72 h◆)[221]
IGROV1	5.6 ± 1.3 (24 h*)[191]	8.08 ± 2.9 (24 h*)[191]	49 ± 15 (96 h•)[223]
A549	2.7 ± 0.5 (120 h*)[216]	0.86 ± 0.09 (72 h*)[165]	20 ± 0.9 (120 h*)[216]
HOP-92	3.6 ± 3.2 (24 h*)[191]	2.70 ± 0.6 (24 h*)[191]	-
COLO205	16.7 ±7.2 (24 h*)[191]	2.8 ± 0.64 (24 h*)[191]	69 (72 h)
MCF7	15.6 ± 6.4 (24 h*)[191]	1.7 ± 0.54 (24 h*)[191]	62.2 (72 h)
HeLa	30. 4 ± 11 (24 h*)[224]	11.8 ± 1.4 (72 h*)[225]	5.4 ± 1.5 (96 h*)[151]

The drug treatment times are given in parenthesis. The IC_{50} values were determined by *the MTT or MTS assay, ◆□□□□□□□□□□□□□□□□□□□□, or • cell survival assay.
MDA-MB, IGROV1: ovarian cancer; H1299: lung cancer; DU145, LNCaP: prostate cancer; A549: lung cancer; HOP: non small cell lung cancer; COLO205: colorectal cancer; MCF7: breast cancer; HeLa: cervical cancer

5.2.3 Potency of carbohydrate-derived platinum(II) analogs

Several challenges such as low water solubility and high toxicity for normal cells in the traditional platinum-based drugs can be overcome by tuning the ligands.[151]

Carbohydrates are a class of bioavailable ligands that are non-toxic, inexpensive, and easy to modulate in order to introduce desirable properties for drug applications.[151] Multiple attempts have been made to synthesize platinum(II) and (IV) complexes with carbohydrates ligands, as described in the previous chapters of this thesis.[121,151,158,211] In this chapter, only the activities of platinum(II)-carbohydrate complexes will be discussed. Carbohydrate conjugation has been shown to help overcome some of the above-mentioned drawbacks associated with traditional drugs. For example, a series of glycoconjugated oxaliplatin derivatives were shown to have 50- to 120-fold increases in water solubility at 25 °C compared to the parent compound oxaliplatin.[211] Another feature that has been explored with glycoconjugated Pt(II) complexes is their selectivity towards tumors.[81,165,211] According to the Warburg effect, tumor cells have a higher metabolism, which is necessary to promote tumor growth, proliferation, and survival.[226,227] An outcome of this increased metabolism is increased glucose uptake and higher glucose transporter (GLUT) expression on the cell membrane to facilitate the uptake.[156,165] Therefore, this is a feature of malignant cells that can be exploited when designing glycoconjugated platinum complexes for selective targeting. There are 12 members of the glucose transporter gene family, in which GLUT1 is ubiquitously expressed in all tissue types.[154] Other than for achieving selectivity, glycoconjugation can also be used as a strategy to overcome cross-resistance due to decreased drug uptake.[165]

Tables 5.2 and **5.3** show potencies of a few glycoconjugated platinum(II) analogs with promising activity in comparison to clinically available platinum(II) drugs. **Figure 5.1a** shows glucose, mannose, and galactose-conjugated oxaliplatin derivatives, in which the sugar group is attached as the leaving group ligand. These compounds show improved

water solubility and comparable cytotoxicity to oxaliplatin (**Table 5.2**) in the tested human cancer cell lines.[165,211] Additionally, GLUT1-dependent uptake of these derivatives was observed in HT29 cells that overexpress glucose transporters.[165,211] The structure of a simple diaminosugar-platinum(II) complex with a 2,3-diamino-2,3-dideoxy-D-glucose non-leaving group ligand and different leaving group ligands are shown in **Figure 5.1b**.[158] The cytotoxicity for these derivatives was determined in human cancer cell lines using the MTT assay and shown to have low micromolar range IC_{50} values (≤10 μM) as given in **Table 5.3**.

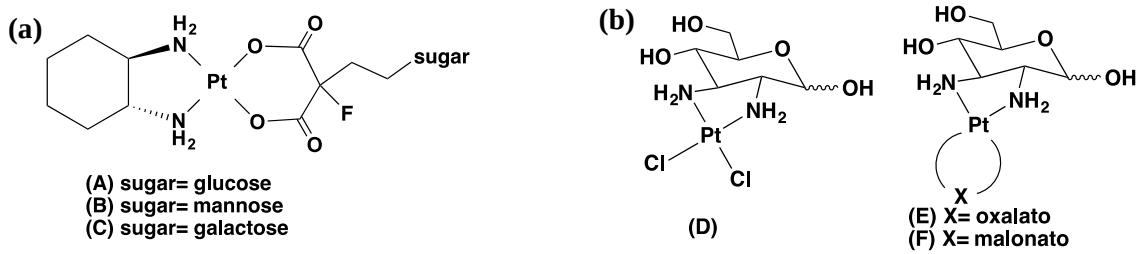

Figure 5.1. The chemical structures of sugar-conjugated platinum(II) complexes. (a) Sugar-conjugated (*trans-R,R*-cyclohexane-1,2-diammine)-2-flouromalonato platinum(II) and (b) a diaminosugar-platinum(II) complex with different leaving group ligands are shown.

Table 5.2. Cytotoxicity of sugar-conjugated oxaliplatin derivatives (Figure 5.1a) in human cancer cell lines compared to oxaliplatin[165]∗

	IC_{50} (μM)			
compound	**DU145**	**MCF7**	**HT29**	**H460**
A	5.9 ± 0.16	0.61 ± 0.13	0.53 ± 0.16	11 ± 0.11
B	2.6 ± 0.18	0.41 ± 0.09	2.2 ± 0.18	10 ± 0.15
C	5.1 ± 0.14	0.41 ± 0.09	1.1 ± 0.12	10 ± 0.15
oxaliplatin	2.1 ± 0.16	0.79 ± 0.11	5.1 ± 0.20	22 ± 0.17

∗The IC_{50} values were determined by the MTS assay for 72 h. DU145: prostate cancer; MCF7: breast cancer; HT29: colon cancer; H460: lung cancer

Table 5.3. Cytotoxicity of diaminosugar-platinum(II) complexes (Figure 5.1b) in human cancer cell lines compared to carboplatin and oxaliplatin[158]∗

	IC_{50} (μM)	
compound	**CH1**	**HeLa**
D	5.1 ± 0.3	7.3 ± 0.8
E	4.1 ± 0.1	10 ± 1
F	6.3 ± 0.4	23 ± 7
carboplatin	0.52 ± 0.01	5.4 ± 1.5
oxaliplatin	0.34 ± 0.09	0.3 ± 0.08

∗ The IC_{50} values were determined by the MTT assay for 96 h. CH1: ovarian cancer; HeLa: cervical cancer

5.3 Objectives

Platinum-based drugs are widely used in cancer therapy. Successful drug candidates are expected to show improved cytotoxicity, reduced side effects, and/or different mechanisms of action compared to the currently available drugs.[7] One purpose of this study was to evaluate the cytotoxicity of **5** in human cancer cell lines using the MTT assay (in collaboration with Dr. Fidelis Ndombera and Bett Kimutai). The percent survival of the cell lines was measured in response to compound **5** compared to the parent platinum drug, cisplatin. High cytotoxicity in tumor cell cultures doesn't necessarily mean a compound is only cytotoxic towards the cancer cells; it could be toxic for normal cells as well. Therefore, one of the goals of this thesis was to discriminate between toxic and antitumor effects of **5** by parallel testing on normal cells. I hypothesized that the sugar group in **5** would facilitate selective uptake of the complex in cancer cells due to the higher GLUT1 transporter expression compared to normal cells. Therefore, the second objective of this study was to determine the level of selectivity of the compound in cancer cells compared to normal cells. For that, the IC_{50} values were determined and

compared by using the MTT assay. Thirdly, the platinum levels were quantified in cancer and normal prostate cells to compare the cellular uptake levels of **5**.

5.4 Results and discussion

5.4.1 Cytotoxicity of 5 in human cancer cell lines

The *in vitro* antitumor activity of compound **5** was previously reported for two human carcinoma cell lines, A2780S and MeWo, in comparison to cisplatin (**Table 5.4**).[82]

Table 5.4. *In vitro* antitumor activity of compound 5∗[82]

	median effect dose (μM)	
cell line	**compound 5**	**cisplatin**
A2780S	2.5	3.3
MeWo	11.2	8

A2780S: ovarian cancer; MeWo: human melanoma
∗ Cytotoxicity was measured by clonogenic survival assay.[228]

Previously, compound **5** showed comparable cytotoxicity as cisplatin with A2780S and MeWo cell lines.[82] The reported low micromolar potency of **5** encouraged me to evaluate its cytotoxicity in several other cancer cell lines with different origins in order to relate the molecular structure of **5** with cytotoxicity, as compared to cisplatin. The IC_{50} values were determined by the dose dependence of cell viability after exposure to **5** and cisplatin (**Figures 5.2** and **5.3**) for 48 to 72 h (**Chapter 2, Section 2.4.18**). The treatment time was increased from 48 h to 72 h in the prostate cell lines to compare the values with literature. The data are given in **Table 5.5**. The IC_{50} values are the averages of at least two trials (except for **5** with MDA-MB-453 and LNCaP cell lines, in which IC_{50} values were calculated from one trial).

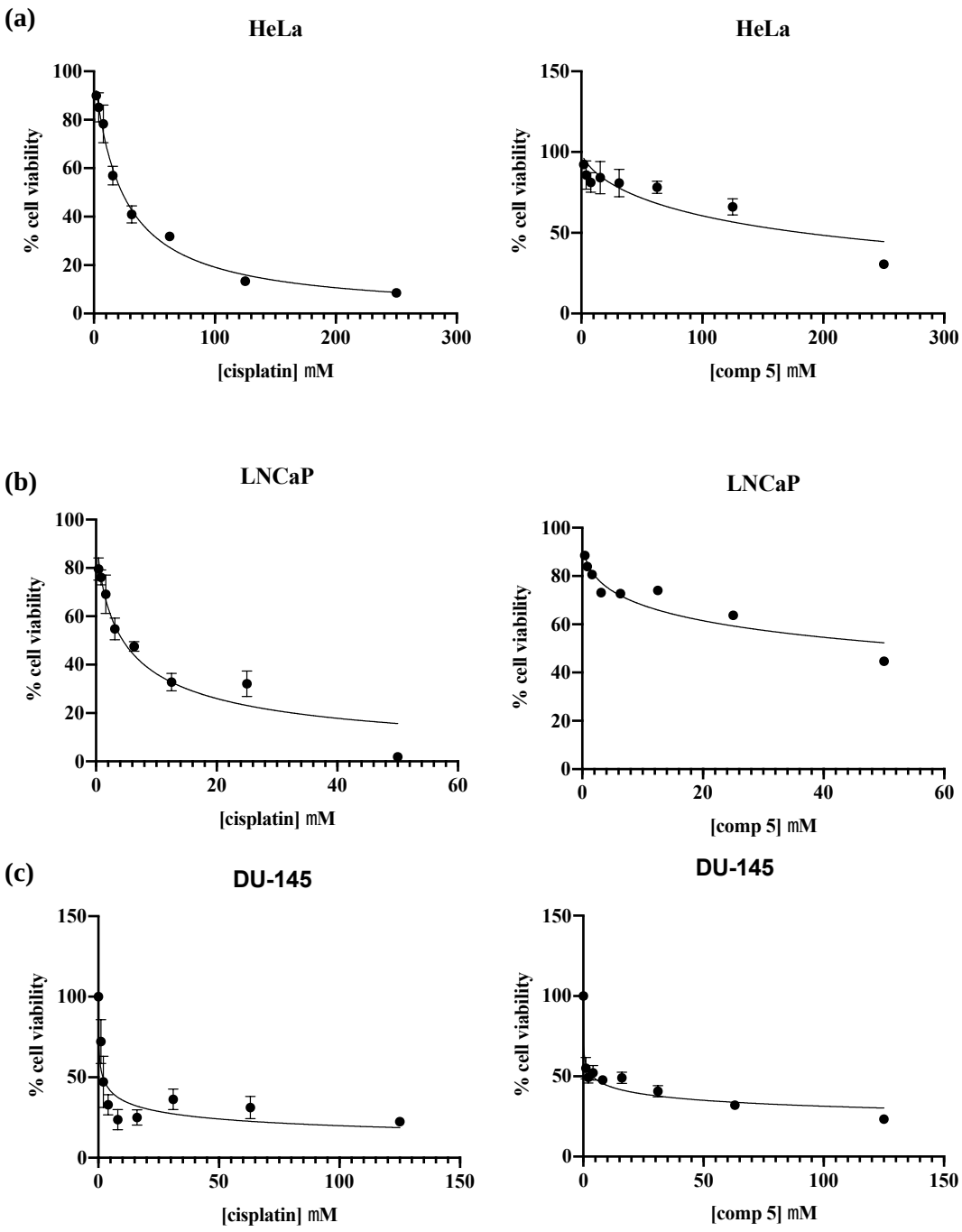

Figure 5.2. Dose-response curves for cisplatin and compound 5 by using the MTT assay for human cancer cell lines. The drug concentration that gives the 50% cell viability (IC_{50} values) and the errors were obtained by a nonlinear regression curve fitting by using the GraphPad software.

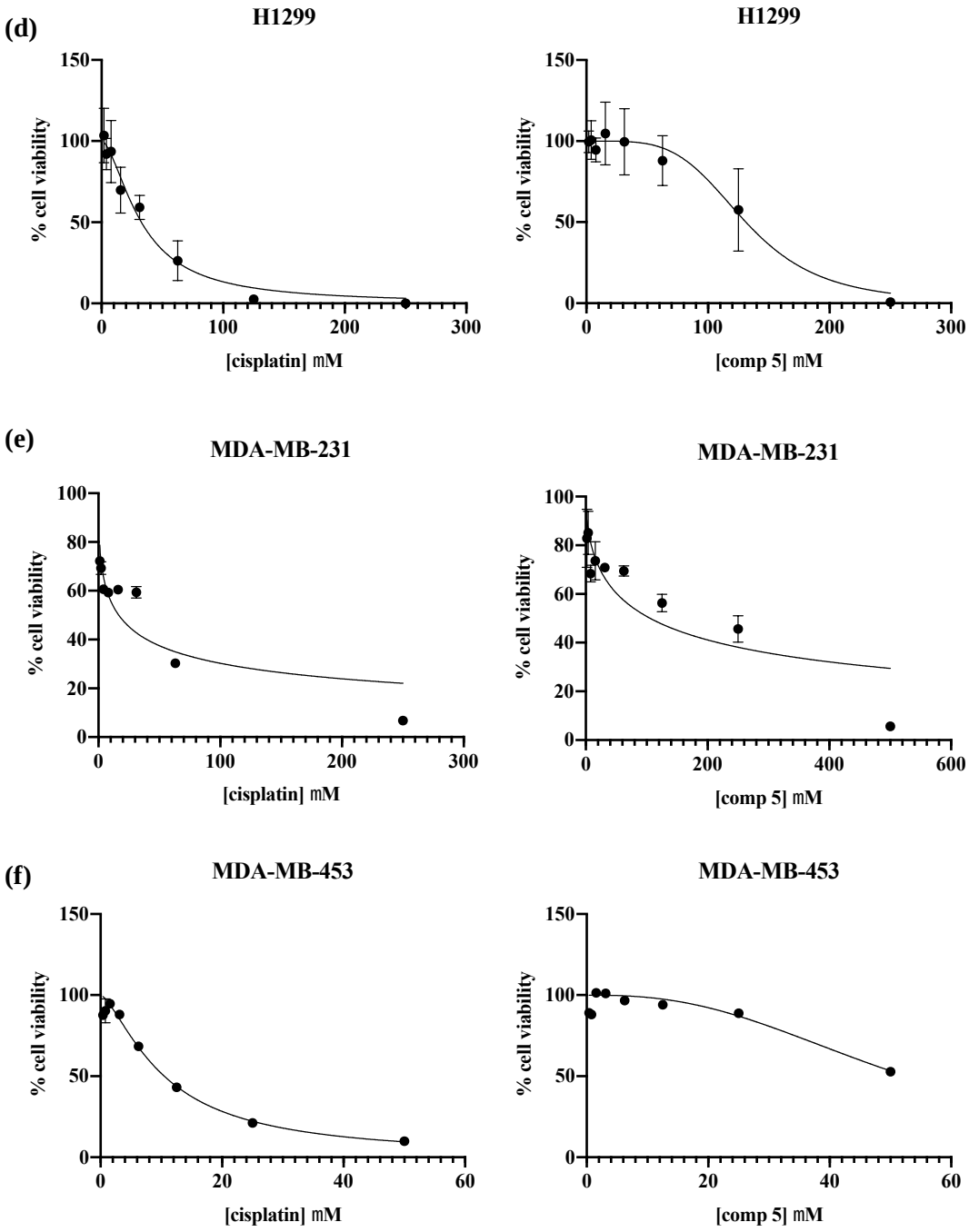

Figure 5.3. Dose-response curves for cisplatin and compound 5 by using the MTT assay for human cancer cell lines. The drug concentrations that give the 50% cell viability (IC_{50} values) and the errors were obtained by a nonlinear regression curve fitting by using the GraphPad software.

Table 5.5. The IC_{50} values for compound 5 and cisplatin in human cancer cell lines as evaluated by the MTT assay

cell line	cancer type	treatment time	IC_{50} (μM)	
			compound 5	cisplatin
HeLa	cervical	48 h	184 ± 41	23 ± 1.4
LNCaP	prostate	64 h	63	4 ± 0.6
DU145	prostate	72 h	4 ± 0.7	2 ± 0.7
H1299	non small cell lung	48 h	131 ± 8	33 ± 3
MDA-MB-231	breast	48 h	106 ± 30	17 ± 4
MDA-MB-453	breast	64 h	53	10 ± 0.7

Notably, in the prostate cancer cell line DU145, compound **5** has comparable cytotoxicity to cisplatin with an IC_{50} value of 4 ± 0.7 μM. It is interesting to see a higher potency of **5** in DU145 cells irrespective of the previously observed slower reaction kinetics. This result suggests that DU145 cells are more sensitive to **5** compared to other tested cell lines. Multiple cancers have shown characteristic overexpression of genes that are related to glycolysis.[156] Prostate cancer is one of them, and the cells are particularly prone to overexpression of GLUT1, which is responsible for sugar uptake.[156] The DU145 cell line has been previously used for cell uptake studies with glycoconjugated platinum(II) complexes due to this reason.[83,165] Thus, higher sensitivity of DU145 towards glycoconjugated **5** compared to other cancer cells may be partly due to the higher accumulation of the compound in the cells, which will be discussed later.

The IC_{50} values of **5**, however, are higher than that of cisplatin in all the other cell lines tested (**Table 5.5**). Cervical, breast, and lung cancer cell lines do not overexpress the GLUT1 gene,[156] which is also reflective in the cell toxicity assay data with higher IC_{50} values (**Table 5.5**). There can be various other reasons for low potency of a drug.

The activity of cancer drugs depends on many factors, including cell entry, drug activation, binding to targets, and inhibition of function.[211] These factors vary depending on the characteristics of the tumor, drug-resistance mechanisms, and features of the drug itself, and therefore, mediate the potency of the drug in a certain cell line. Additionally, the assay type and the treatment times also affect the IC_{50} values. Considering the slower kinetics of **5**, increased treatment times would result in better cytotoxicity. In a previous study, a similar trend was seen for carboplatin in which a higher cytotoxicity was observed after a 24 h exposure period compared to a 1 h exposure period in six human ovarian cell lines.[212] Overall, compound **5** could be considered as a lead compound for treating cancers with higher GLUT expression. Future studies can be carried out to test the potency of compound **5** on other cancer cells lines that overexpress GLUT.

5.4.2 Cytotoxicity of 5 in normal human prostate cell line

MTT assays were carried out to investigate the selectivity of compound **5** towards the cancer cells over normal cells. Since **5** exhibited more cytotoxicity towards DU145 prostate cancer cells, the corresponding normal prostate epithelial cell line, RPWE1, was used to test for selectivity. Furthermore, DU145 cells have been shown to overexpress GLUT, which is not the case for RPWE1. The hypothesis is that **5** would show higher cytotoxicity against DU145 than RWPE1 due to GLUT-dependent uptake of the compound. In fact, the IC_{50} values obtained from the MTT assays for **5** show an 18-fold higher cytotoxicity towards DU145, whereas cisplatin did not show such a difference (**Table 5.6**). The higher toxicity and selectivity of **5** towards the DU145 cancer cell line compared to the normal cell line could be due to its higher accumulation in the cell, which will be discussed later.

Table 5.6. *In vitro* cytotoxicity of 5 and cisplatin on prostate cell lines as evaluated by the MTT assay

cell line	cell type	treatment time	IC_{50} (μM)	
			compound 5	cisplatin
DU145	prostate cancer	72 h	4 ± 0.7	2 ± 0.7
RWPE1	normal prostate	72 h	72 ± 2.6	4 ± 0.1

5.4.3 Quantification of 5 in cells using ICP-MS

In order to evaluate whether the cytotoxicity difference observed in **Section 5.4.2** is due to Pt accumulation differences in the cells, whole cell Pt levels were quantified after treatment. This was done by ICP-MS. First, the experimental protocol for sample preparation and ICP-MS analysis method were optimized to obtain reproducible data to evaluate the platinum content in the whole cell.[229] The experiment was started with the same cell number (4.6×10^5) in each plate (**Chapter 2, Section 2.4.19**). To minimize the effects from the media, both cell lines were incubated in the same keratinocyte media during the drug treatment. Cells were treated with 50 μM Pt(II) compounds for 2 h and the cells were washed several times with PBS to remove excess Pt. Cells were trypsinized, pelleted, and digested with nitric acid (16 h), and then the total cellular platinum content was determined by ICP-MS. As shown in **Figure 5.4**, compound **5** displays a level of 31.5 nmol Pt per 10^6 cells in cancer cells, which is 24-fold higher compared to the level in normal cells. Compared to cisplatin, **5** shows a 1.3-fold selective accumulation in cancer cells over normal cells after 2 h treatment. Although cisplatin accumulation levels in cancer over normal cells show an 18-fold difference, the cytotoxicity is similar in the two cell lines. This may be due to the increased activity of cisplatin in the cancer cells.

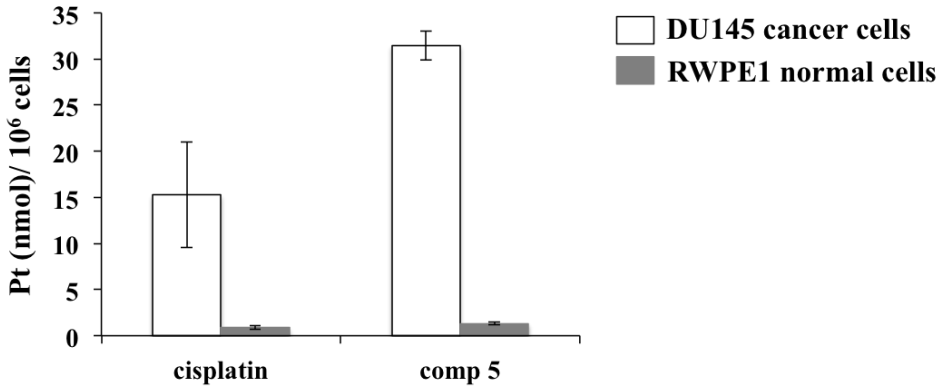

Figure 5.4. Accumulation of Pt(II) compounds in prostate cancer (DU145) and normal (RPWE1) cells. The cells were treated with 50 μM compound for 2 h and the Pt levels were quantified by ICP-MS. The errors were calculated from two independent trials.

The strategy of glycoconjugation for targeted delivery *via* glucose transporters has been explored previously with oxaliplatin derivatives;[83,121,165,211] however, this effect has not been examined with cisplatin derivatives such as **5**. A recent study from the Lippard group focused on glucose-platinum(II) conjugates for cancer cell targeting.[83] In that study, glucose-oxaliplatin derivative uptake levels were compared between DU145 and RWPE2 and showed a 4-fold preference for cancer cells, which was discussed by the authors as a significant difference.[83] Moreover, the same compound showed a 2-fold reduced cancer cell viability compared to the normal cells. In comparison, we were able to show that compound **5** has better selectivity towards DU145 cells with a significant difference in the Pt uptake (23-fold) and cytotoxicity (18-fold) compared to RPWE1. While the overall results from this study showed the potential of compound **5** in DU145 cell line, it is worth exploring ways to improve the activity and selectivity towards other cancer types as well. Glycoconjugated compounds can be synthesized with modifications to the sugar, varying linker sizes, and with different leaving group ligands to optimize the activity and selectivity towards cancer cells. This study not only identifies the potential of

glycoconjugated anticancer agents for selective targeting, but also sheds light on the design of more potent sterically hindered platinum(II) complexes.

CHAPTER 6

RNA-AMINOGLYCOSIDE INTERACTIONS PROBED THROUGH PLATINATION KINETICS

6.1 Abstract

Electrostatics play an important role in RNA-drug interactions; however, studying these interactions experimentally in solution can be challenging. Positively charged drug molecules such as aminoglycosides are attracted to the negatively charged RNA. Other ions present in the environment affect the electrostatic properties and influence these interactions. Based on a previous study from our lab that showed salt-dependent cisplatin coordination rates to RNA, we postulated that positively charged aminoglycosides could change the platination rates by competing with mono-activated cisplatin for the target (H69 RNA). Herein, we describe a kinetic method to monitor aminoglycoside interactions with RNA using cisplatin coordination rates. The platination rate was found to decrease significantly in the presence of aminoglycosides. This change in mono-activated cisplatin reaction rates indicated the involvement of electrostatics in aminoglycoside-RNA interactions. In addition, we postulated that the pseudouridine (Ψ) modifications present in a rRNA construct used in this report were perhaps important for the binding of the aminoglycosides. However, a significant difference between modified and unmodified H69 RNA constructs was not observed when probed with the platination kinetics. Overall, these findings are important for providing information on drug-RNA interaction mechanisms, improving cationic drugs for nucleic acids, identifying unique RNA drug targets, and developing tools to investigate RNA microenvironments.

6.2 Introduction

The phosphate backbone of nucleic acids makes them highly charged, anionic biopolymers.[230] Therefore, electrostatics play an important role in various ligand-nucleic acid interactions. Specifically, electrostatic microenvironments created by RNA folding are important for their biological function, stability, and ligand interactions.[192] For example, local electrostatic pockets created by the ribosome are important for its key interactions with mRNA and tRNA.[231] Furthermore, RNA-protein interactions are governed by electrostatic interactions,[232] which has been established in numerous examples, including transcription activating (Tat) protein binding to trans-active responsive element (TAR) RNA and Rev-peptide binding to Rev-response element (RRE) RNA.[232,233] Additionally, some drugs that target the ribosome rely on the electrostatic interactions to bind to their target sites.[120] For example, the aminoglycoside antibiotics, including compounds neomycin, kanamycin, and paromomycin (**Figure 6.1**), bind to the ribosome and interfere with various steps in protein synthesis in bacteria.[120] Neomycin and paromomycin, which are the focus of this chapter, interact with the h44 region of the 16S rRNA to induce codon misreading and decrease translation fidelity.[108,109] Crystal structures have also revealed a secondary binding site for neomycin and paromomycin at H69 of 23S rRNA.[106,110,111] Interactions in the H69 major groove are believed to inhibit the recycling and translocation steps of protein synthesis.[112] The positively charged amine groups of aminoglycosides form electrostatic interactions with RNA.[122,123] In addition, anticancer drugs such as cisplatin are also shown to bind to RNA.[234] Once cisplatin enters the cell, it undergoes aquation to produce cationic reactive

species. Electrostatic interactions between the positively charged cisplatin and the negatively charged RNA attract the two species for the coordination reaction to occur.

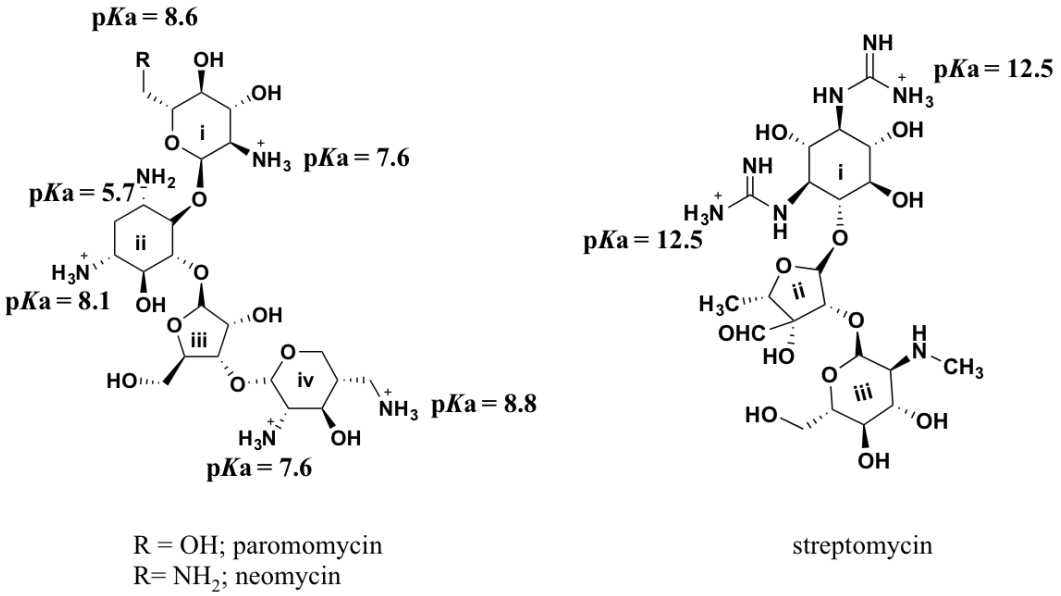

Figure 6.1. Chemical structures of aminoglycosides at pH 7. The structures of neomycin, paromomycin, and streptomycin at pH 7 with the pK_a values of amino and guanidinium groups are shown.

As mentioned before, RNA microenvironments and their interactions with other ligands are important for RNA biology. Inside living cells, biological molecules, including RNA are in constant contact with cations.[230,235] Cations such as Na^+ and Mg^{2+} neutralize the negative charge of RNA and facilitate folding and stabilizing.[235,236] They also play an important role in ligand interactions.[230,235] Numerous studies have shown salt-dependent binding and rate constants for RNA-ligand interactions.[122,237-243] Additionally, a broad kinetic study done by Dr. Dedduwa-Mudalige determined the salt-dependent coordination rates and electrostatics in cationic metal complexes-rRNA reactions using mono-activated cisplatin.[50] The salt-dependent nature of mono-activated cisplatin coordination to RNA suggested the possibility of using the cisplatin kinetics as a tool to investigate other cationic ligand-rRNA interactions. In a previous study, weakly

bound aminoglycosides with the Rev-responsive element (RRE) of HIV-1 mRNA were shown to readily dissociate from the mRNA at relatively high salt concentrations.[244] We hypothesized that, under pseudo-first-order conditions, positively charged cisplatin would compete and cause dissociation of aminoglycosides in a similar fashion, and then coordinate to RNA to block further interactions. Depending on the charge state and binding mode of the drug, the degree of competition could vary, potentially being reflected through the cisplatin coordination rate. This knowledge was employed in developing a tool to monitor positively charged aminoglycoside binding to H69.

Computational studies can predict the varying electrostatic potentials on RNA and potential locations of ligand interactions.[192,245,246] However, there is a lack of methods to evaluate the role of electrostatics in RNA-ligand interactions experimentally. This chapter describes a method to monitor the RNA-aminoglycoside interactions by using platination kinetics, and therefore elucidate the electrostatic involvement in drug binding to RNA.

6.3 Objectives

The ribosome is an important drug target due to its abundance, accessibility, lack of repair mechanisms, and vital biological function in the cell.[97] One of the common features of the drugs that target RNA is their positive charge, which facilitates the initial binding step through electrostatic contacts. A lack of experimental methods to support the role of electrostatic interactions between RNA and drugs delays the drug development process against resistant pathogens. The primary objective of this work was to use of cisplatin kinetics to probe and determine the electrostatic dependence of polycationic drugs such as aminoglycosides in binding to RNA.

Two model H69 rRNA hairpins (**Figure 6.2**) were chosen for this study. The H69 RNA hairpin possesses three pseudouridine nucleotides (**Figure 6.2**) that have been shown to be involved in regulating the H69 structure, stability, and function.[247-250] The contribution of pseudouridines to the electrostatics of nucleic acids have been reported previously.[251] Therefore, two H69 constructs containing either uridines (unmodified H69) or pseudouridines (modified H69) were studied in order to understand the influence of the modifications on electrostatics and aminoglycoside binding of rRNA.

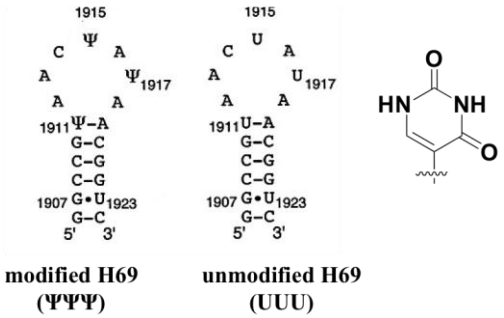

Figure 6.2. Structures of RNA constructs used in the kinetic study. Modified (ΨΨΨ) and unmodified (UUU) H69 rRNA constructs are shown, in which Ψ is pseudouridine (shown to the right).

6.4 Results and discussion

The mono-activated cisplatin coordination rates to H69 were obtained in the presence of 1, 3, and 6 μM neomycin, paromomycin, and streptomycin as described in **Chapter 2**, **Section 2.4.10**. A representative result for the kinetic experiment in the presence of 1 μM neomycin is shown in **Figure 6.3a**. The fraction of unreacted RNA was plotted over times to obtain the platination rates in the presence of aminoglycoside (**Figure 6.3c**). The control platination reaction contained no aminoglycosides (**Figure 6.3b** and **d**). Streptomycin does not bind with H69 RNA; therefore, streptomycin was

used as a negative control.[112] The disappearance of RNA was quantified rather than appearance of products since multiple products are observed.

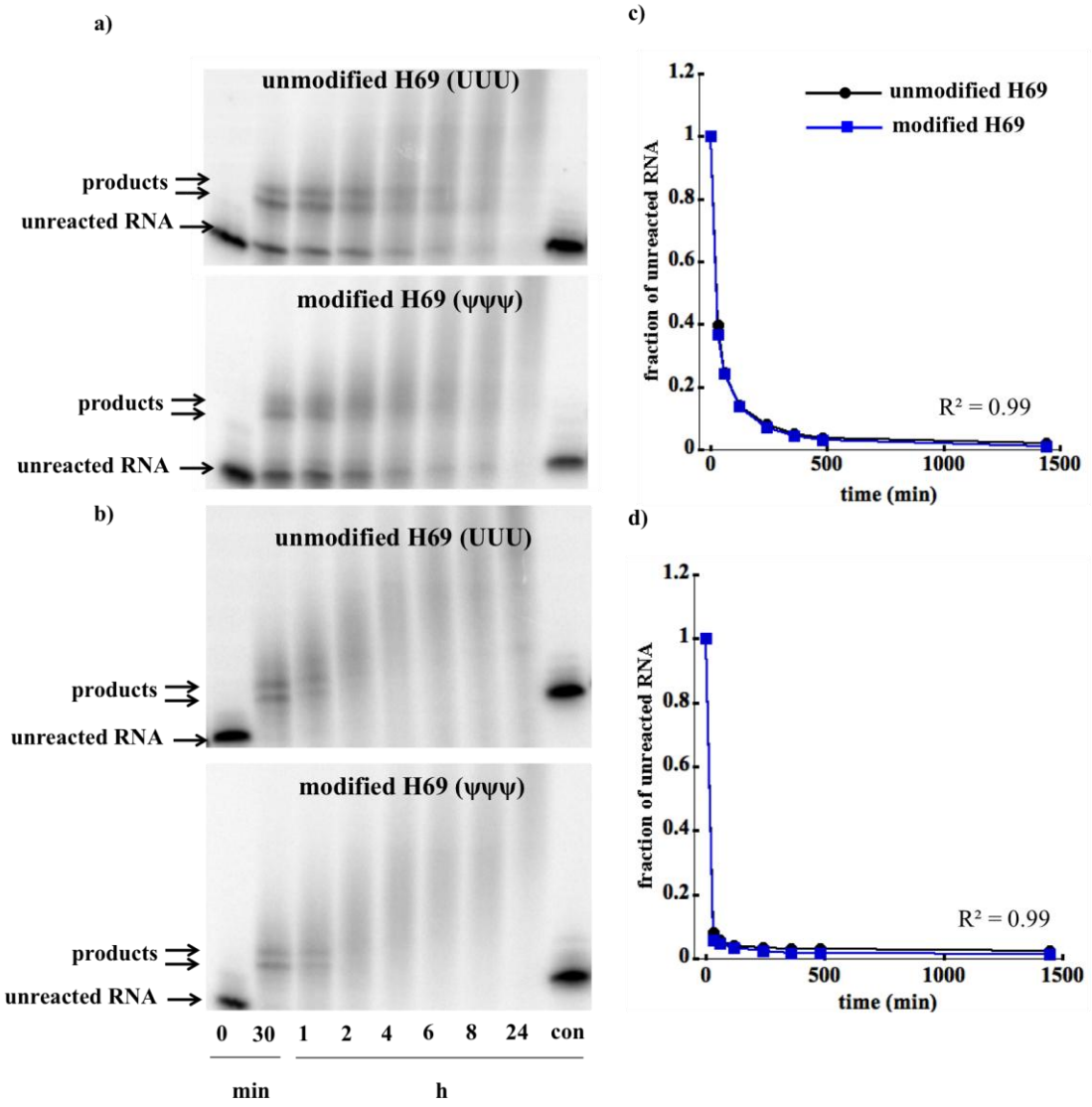

Figure 6.3. Reaction kinetics of mono-activated cisplatin and RNA constructs in the presence and absence of aminoglycoside. Autoradiograms for unmodified and modified H69 (a) in the presence of 1 μM neomycin and (b) absence of aminoglycoside are shown ([RNA] = 0.7 μM, [mono-activated cisplatin] = 188 μM; 10 mM K_2HPO_4/KH_2PO_4, pH 6.2, with 20 mM $NaClO_4$, 37 °C). Single-exponential-decay fits for the disappearance of unreacted RNA (c) in the presence of 1 μM neomycin and (d) absence of aminoglycoside as a function of time (min) are shown.

The k_{obs} and $k_{2,app}$ values for both modified and unmodified H69 in the presence of different aminoglycosides are summarized in **Table 6.1**. The platination rates decrease in

the presence of neomycin (>2-fold) and paromomycin (>1.3-fold) compared to the no aminoglycoside control, revealing that cisplatin-RNA interactions are competing with the aminoglycosides.

Table 6.1. Observed pseudo-first-order rate constants, k_{obs}, and the second-order rate constants, $k_{2,app}$ for the reactions of mono-activated cisplatin with H69 RNA in the presence of varying concentrations of aminoglycosides

oligonucleotide	aminoglycoside	[aminoglycoside] (μM)	k_{obs} (10^{-4} s^{-1})	$k_{2,app}$ ($M^{-1}s^{-1}$)
unmodified H69	no aminoglycoside	0	14.8 ± 2.9	7.9 ± 1.6
	neomycin	1	6.0 ± 1.1	3.2 ± 0.6
		3	2.3 ± 0.4	1.2 ± 0.2
		6	0.7 ± 0.1	0.4 ± 0.05
	paromomycin	1	10.8 ± 2.7	5.8 ± 1.4
		3	4.2 ± 1.0	2.2 ± 0.5
		6	3.0 ± 0.9	1.6 ± 0.5
	streptomycin	1	17.0 ± 3.7	9.0 ± 1.9
		3	15.3 ± 2.4	8.1 ± 1.3
		6	18.0 ± 1.9	9.6 ± 1.1
modified H69	no aminoglycoside	0	14.1 ± 3.1	7.5 ± 1.7
	neomycin	1	3.9 ± 0.9	2.1 ± 0.5
		3	1.8 ± 0.3	0.9 ± 0.2
		6	1.0 ± 0.2	0.5 ± 0.1
	paromomycin	1	8.8 ± 1.7	4.7 ± 0.9
		3	1.5 ± 0.7	1.1 ± 0.4
		6	1.6 ± 0.5	0.9 ± 0.3
	streptomycin	1	13.6 ± 2.1	7.2 ± 1.1
		3	12.1 ± 2.1	6.4 ± 1.1
		6	18.2 ± 2.4	9.7 ± 1.3

[RNA] = 0.7 μM, [cisplatin] = 188 μM; 10 mM K_2HPO_4/KH_2PO_4, pH 6.2, with 20 mM $NaClO_4$, 37 °C

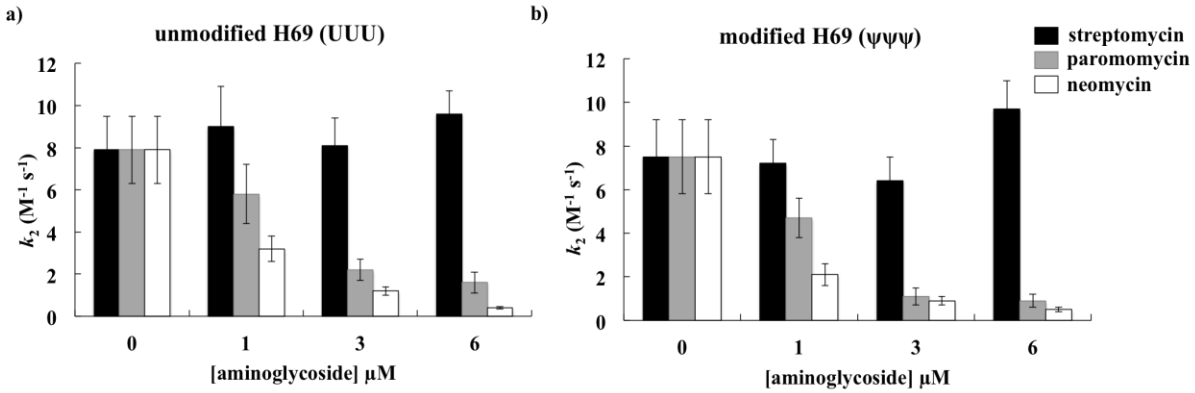

Figure 6.4. A comparison of platination rates in the presence and absence of aminoglycosides. The platination rates obtained with unmodified H69 (UUU) and modified H69 (ΨΨΨ) are shown. Reaction conditions: [RNA] = 0.7 μM, [mono-activated cisplatin] = 188 μM, [aminoglycoside] = 1, 3, or 6; 10 mM K_2HPO_4/KH_2PO_4, pH 6.2, with 20 mM $NaClO_4$, 37 °C.

The platination rate differences in the presence of varying aminoglycosides for unmodified H69 construct are summarized in **Figure 6.4**. Both RNA constructs show a decrease in cisplatin reactivity as the aminoglycoside concentration increases. Analogous to the impact of salts on cisplatin-RNA interactions as reported previously,[50] a similar influence can be expected for coordination of mono-activated cisplatin in the presence of positively charged aminoglycosides. Association of positively charged aminoglycosides with H69 screens the negative charges on RNA. Therefore, neutralizing effects by positively charged ligands decrease the cisplatin reactivity on RNA.[50] Specifically, between 1 and 6 μM neomycin concentrations, there is an 8-fold decrease in the platination rate compared to a 3.6-fold decrease for paromomycin with unmodified H69. Comparison between neomycin and paromomycin at every concentration level shows higher cisplatin reactivity for paromomycin (about a 2-fold difference) compared to the no aminoglycoside control. The changes in the platination rates in the presence of aminoglycosides could be explained by differing electrostatic interactions. Neomycin has six amino groups, of which five are positively charged at the chosen experimental

conditions (pH=6.2) (**Figure 6.1**).[252] Paromomycin has four out of five amino groups that are positively charged at pH 6.2. The observed cisplatin kinetics differences for neomycin and paromomycin can be rationalized by the different charges of the aminoglycosides, in which neomycin has one extra positive charge that can screen the RNA more effectively than paromomycin, thus decreasing the reactivity of cisplatin. The differences in platination rates correlate well with aminoglycoside binding preferences to H69. For instance, neomycin has tighter binding to unmodified H69 than paromomycin (*K*d values of 0.3 and 5.4 μM, respectively). Cisplatin binding rates are proportional to the *K*d values of tested aminoglycosides.

The streptomycin control has the highest platination rates. Streptomycin has two guanidinium groups with pK_a values of 12.5, which are positively charged at the given conditions, but this molecule has been reported previously to not bind to the H69 region.[112] Thus, in the presence of streptomycin, the cisplatin-binding rate does not change significantly from the rate in the absence of aminoglycoside. These results indicate that electrostatic contacts are likely to be important for aminoglycoside binding to RNA. Therefore, as the overall positive charge of the aminoglycoside is decreased, the competitive effect of mono-activated cisplatin increases.

Aminoglycoside dependent platination rates were determined in a buffer containing 32 mM (12 mM K^+ + 20 mM Na^+) total monovalent cations. In the previous salt-dependent studies,[50] as the total cation concentration increased from 32 to 112 mM, the platination rate (k_2) decreased 6-fold for unmodified H69.[102] This is analogous to the decrease in the platination rate with increasing aminoglycoside concentration from 0 to 6 μM (20-fold decrease for neomycin-unmodified H69). For modified H69, a 4-fold (salt-

dependent kinetic data) and 15-fold (neomycin-dependent kinetic data) decrease is observed. This result indicated that in the presence of aminoglycosides (as low as 6 μM), the decrease in platination rate is more prominent than in the presence of higher salt concentration (112 mM). Since the kinetic model for platination kinetics involves a preassociation step and a coordination step,[235] aminoglycosides would likely interfere with not only the preassociation step but also the direct coordination step due to overlapping binding locations. In fact, previous studies have shown cisplatin and aminoglycosides binding at the H69 stem.[95,111] Specifically, RNase T1 probing, MALDI MS, and dimethylsulfate (DMS) mapping revealed platination at G1921-G1922 and G1906-G1907.[95] Neomycin and paromomycin binding interactions at the H69 stem has been shown by Dr. Sakakibara by using DMS footprinting.[253] These results were also consistent with bacterial 70S ribosome X-ray crystal structures with neomycin bound to the H69 stem region near residues G1906, G1921, and G1922.[111] Therefore, the observed prominent aminoglycoside-dependent rate changes could be the result of increased competition that cisplatin faces when coordinating to RNA. Overall, the results demonstrated that platination rate variations can be used as an indication of aminoglycoside or other cationic compound interactions with RNA.

In aminoglycoside-dependent studies, platination rate differences between modified and unmodified H69 were not observed, implying that pseudouridine modification does not impact aminoglycoside interactions with H69. This result also correlates with the similar Kd values for the two RNA constructs as determined by ESI MS.[254] This could be due to minimal influence of Ψ modifications on the global electrostatics for H69 under the experimental conditions used to evaluate with Brønsted-

Debye-Hückel and polyelectrolyte theories in a previous study by Dr. Gayani Dedduwa-Mudalige.[50]

In conclusion, this study showed the utility of coordinating compounds, such as cisplatin, as probes to obtain information about cationic, non-metallic ligand interactions with RNA. As hypothesized, the effects of the bound aminoglycosides were to slow down the cisplatin coordination rates, thereby reflecting different affinities of aminoglycosides to H69. This method was sensitive enough to detect differences in RNA binding by neomycin and paromomycin, which differ by a single charge. Moreover, cisplatin kinetics could be used to evaluate the effects of varying pH on cationic drug-RNA interactions. This tool could also be expanded to probe aminoglycoside binding to other RNA or DNA targets. Overall, this study highlighted the importance of electrostatic interactions in drug binding, and therefore provides insight into drug binding modes that can be used to improve their affinity and efficacy.

CHAPTER 7

OVERALL CONCLUSIONS AND FUTURE DIRECTIONS

7.1 Overall conclusions

With the discovery of cisplatin anticancer activity, a large number of platinum-based compounds have been developed and tested for their activity. Only a few of those have entered the clinic. Even 40 years after the discovery of cisplatin, there are still wide gaps in our understanding of its mechanism of action.[3] Also, the clinical success of these drugs has been limited due to the intrinsic and acquired resistance and side effects.[255] However, a deeper understanding of how these drugs work has opened the door to explore new platinum-based anticancer drugs.[7,90] Many researchers are investigating the biochemical and biomolecular aspects of platinum-based drug mechanism in the hope of identifying properties that could enhance the efficacy or minimize the drawbacks of the currently available drugs.[3,90]

A characteristic feature of platinum-based complexes is the ability to replace the leaving- and/or non-leaving group ligands with a variety of functional groups. These ligands determine different aspects of the compound activity.[73] Careful selection of the ligands facilitates tuning of cytotoxic characteristics of the complexes. Since one of the drawbacks associated with the current platinum anticancer drugs is off-target reactions and resistance through increased cytosolic deactivation, researchers have aimed at decreasing reactivity through the introduction of bulky non-leaving group ligands.[255] Decreased reactivity was also expected to reduce the toxicity, as was the case with carboplatin.[74] Another approach is to introduce ligands with other biological roles in the cell to reduce the toxicity and improve selectivity.[255] The work discussed in the first part

of this thesis focused on studying a carbohydrate-linked cisplatin analog, *cis*-dichlorido[(2-*β*-D-glucopyranosidyl)propane-1,3-diammine] platinum(II) (compound **5**), which has a bulky, biologically active non-leaving group ligand. Although there were multiple cellular studies with such complexes, biochemical studies to understand the reactivity, structural effects, and impact of the non-leaving group ligand were lacking. Therefore, studies in this thesis work were carried out to investigate the reaction kinetics and selectivity of compound **5** with nucleosides and oligonucleotides in order to understand the impact of the carbohydrate non-leaving group ligand on its reactivity.

One of the main goals of this thesis was to identify the kinetics of carbohydrate-linked platinum(II) compound, **5**, in the context of nucleic acids and their building blocks (*e.g.*, nucleosides). Impact of the carbohydrate moiety of compound **5** on the reaction kinetics and nucleic acid binding preference were discussed in **Chapter 3** and **4**, in the context of steric and electrostatic properties. A comparison was made with the parent compound, cisplatin, which is sterically less crowded. Mono-activated compound **5** showed ≥2.5-fold slower reaction kinetics compared to mono-activated cisplatin with nucleosides, a DNA oligonucleotide (13.7-fold slower), and an RNA oligonucleotide (3.6-fold slower). The slower kinetic effect can be attributed to the bulkier carbohydrate moiety of the complex, in which the reactivity may be reduced due to the crowding at the Pt reactive center. This observation suggests that compound **5** might have reduced off-target binding.

Furthermore, mono-activated **5** showed preference towards RNA over DNA (1.7-fold) in contrast to cisplatin, which preferred DNA. Ribosome-targeting drugs such as aminoglycosides have sugar moieties with multiple hydrogen-bonding sites. With the

RNA-binding preference and multiple hydrogen-bond donating and accepting sites, compound **5** may have target sites within the ribosome. Therefore, ribosome-probing studies were carried out to locate the ribosome binding sites of the compound. Compound **5** showed binding at functionally important regions of ribosomal RNA such as the A site, the 790 loop, and H69. The binding sites overlapped with cisplatin and other common drug binding sites, suggesting that the binding could potentially disrupt the protein translation process. Therefore, further efforts towards the design of carbohydrate-linked platinum analogs for the treatment of cancers might include the RNA as a potential target. The structural effects caused by compound **5** binding were also analyzed using plasmid and short oligomer DNA as described in **Chapter 4**. Compound **5** showed unwinding and bending of DNA, similar to cisplatin, even though the kinetics appeared to be slower than cisplatin. To best of our knowledge, this is the first attempt to determine reaction kinetics and structural effects at the oligonucleotide level for a carbohydrate-linked Pt(II) compound. Our studies were carried out to understand the influence of the sugar moiety on the reactivity.

A large number of new Pt-based compounds have been synthesized and tested over the past few decades.[7,150,162] Unfortunately, very few have entered clinical trials, and some very promising drug candidates were abandoned due to their toxic effects.[255] One of the reasons for this is that testing in model cell lines poorly reflects the clinical situation. For example, high cytotoxicity in tumor cells doesn't necessarily mean it is only cytotoxic towards the cancer cells; the compound could be toxic to normal cells as well. Therefore, one of the goals of this thesis work was to discriminate between toxic and antitumor effects of **5** by parallel testing on normal cells. The high potency of **5** towards

DU145 prostate cancer cells against normal prostate cells provided evidence for the targeted effect of glycoconjugation as described in **Chapter 5**. This effect could be due to the utilization of highly expressed glucose transporters (GLUT) on DU145 cells for compound **5** uptake as opposed to normal cells, in which the GLUT expression is low.[165] Platinum levels upon compound treatment were quantified by using ICP-MS to further suggest the selective accumulation of **5** on cancer cells vs. normal cells. Compound **5** showed higher accumulation (24-fold) in DU145 cancer cells compared to normal cells, which makes **5** a promising candidate for targeted delivery compared to cisplatin.

Modifying existing drugs to use them as tools to obtain information about drug-target interactions is another approach. **Chapter 6** describes an attempt to establish cisplatin as a tool to predict the RNA-cationic drug interactions. Both cisplatin and aminoglycosides use electrostatic interactions to bind to their target. Therefore, cisplatin binding rates were sensitive to the cationic aminoglycoside binding to RNA, identifying drugs that interact with RNA. Furthermore, this tool can be expanded to monitor other charged-small molecule-RNA interactions.

In conclusion, to gain clinical success of drugs, it is important to understand the fundamental biochemistry behind their activity. These factors contribute to the improvement of existing drugs and also to the rational design of new drugs with few drawbacks. During the search for new anticancer drug candidates, biological ligands such as carbohydrates have received more attention. This thesis work provides evidence for carbohydrate-linked Pt(II) derivatives to act as promising anticancer drug candidates with tunable steric, electronic, and/or H-bonding properties for nucleic acid binding. Furthermore, carbohydrate-linked platinum compound studied in this thesis showed

comparable structural effects and potency (in DU145 cancer cells) as cisplatin, also with selectivity towards cancer cells. Overall, this study provided new perspectives for a future design of carbohydrate-linked platinum(II) antitumor compounds.

Techniques and tools to understand how existing drugs work are likely to influence drug development to a similar extent as the development process of new drugs. This thesis work also demonstrated cisplatin's ability to act as an electrostatic probe in giving information about other cationic drug binding to RNA. It was successfully shown to predict the aminoglycoside binding to RNA based on the changes in the cisplatin reaction rates that are sensitive to the cationic molecules in the environment. It could be used to evaluate environmental and other factors that influence the drug-target interactions and therefore likely to shape future drug development.

7.2 Future directions

7.2.1 Evaluate the reactivity of compound 5 with thiol-containing molecules

One of the mechanisms for cancers to develop resistance towards Pt-based drugs is through deactivating the compounds by binding with thiol-containing molecules in the cell (*e.g.,* glutathione, sulfur-containing peptides, and proteins).[59] The slower reaction kinetics of **5** suggested that it could have limited off-target binding, which could be advantageous for avoiding drug resistance. To evaluate the binding kinetics of **5** with a sulfur-containing ligand, an HPLC-based kinetic study could be carried out with glutathione. Furthermore, a competition assay with guanosine or deoxyguanosine nucleosides with glutathione by using the same method could be used to compare the binding rates of each target.

7.2.2 Characterize the adducts of compound 5

Multiple products were observed for compound **5** reaction with G and dG nucleosides. In rRNA probing experiments, compound **5** coordinating to G and A residues were observed. In this thesis work, only the adducts with G and dG nucleosides were identified by mass spectrometry. However, the coordination site of compound **5** on the nucleobases was not identified in this work. This can be done by using ^{1}H-NMR analysis of **5**-purine nucleobase adducts. Furthermore, computational modeling and energy calculations can be used to identify the reactivity preferences of **5** and understand the roles of the carbohydrate ligand.

7.2.3 Translation inhibition assay

Ribosome probing data showed compound **5** binding at functionally important regions of the ribosome. Furthermore, some binding sites were overlapping with well-known drug binding sites. Therefore, the next step would be to analyze the effects of binding on the protein translation process. There are commercial *in vitro* protein translation kits that could be easily used to obtain such information. For example, the translation level of a marker protein (*e.g.*, green fluorescence protein) could be measured to evaluate the ribosome function upon treatment with compound **5**. Cisplatin treated ribosomes could be used as a positive control in such an experiment.

7.2.4 Study cellular uptake mechanism of compound 5

Cellular assays in this study showed higher potency and compound **5** accumulations in GLUT-overexpressing cancer cells compared to normal cells. To confirm the GLUT-dependent compound **5** uptake, a competition study could be carried out in the presence of glucose. The optimized protocol used in this thesis work could be

used to quantify the Pt accumulation levels by using ICP-MS. The cells could be treated with compound **5** in the presence and absence of the competitor (glucose), and the *in vivo* Pt level then quantified. Furthermore, to confirm the transporter as GLUT1, the MTT assay could be carried out in the presence and absence of a GLUT inhibitor such as EDG (4,6-*O*-ethylidene-α-D-glucose).[83]

APPENDIX A

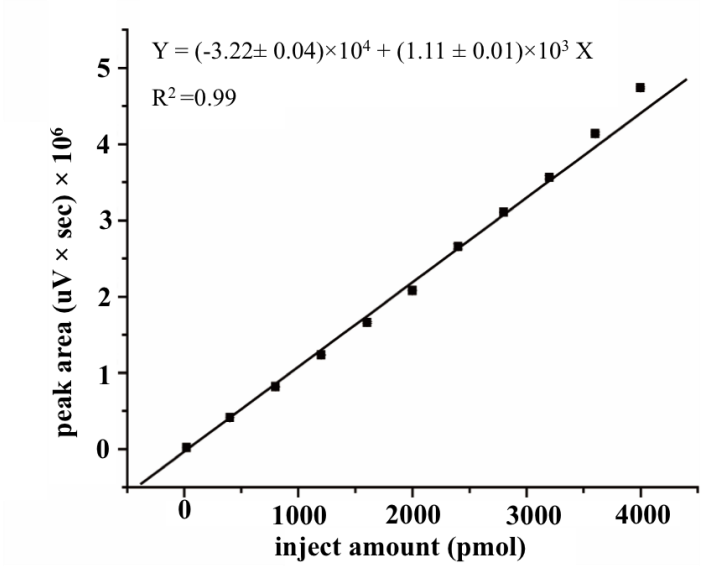

Figure A1. HPLC standard curve for G.

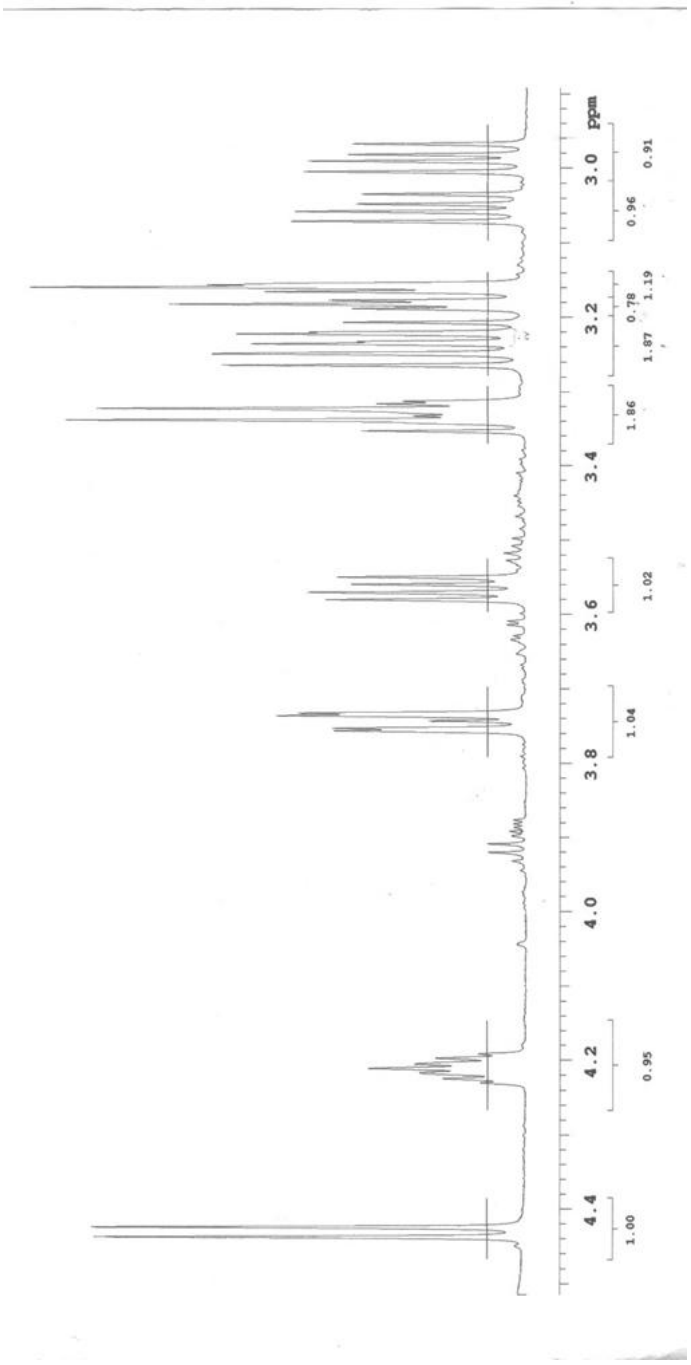

Figure A2. ^{1}H-NMR spectrum of compound 4.

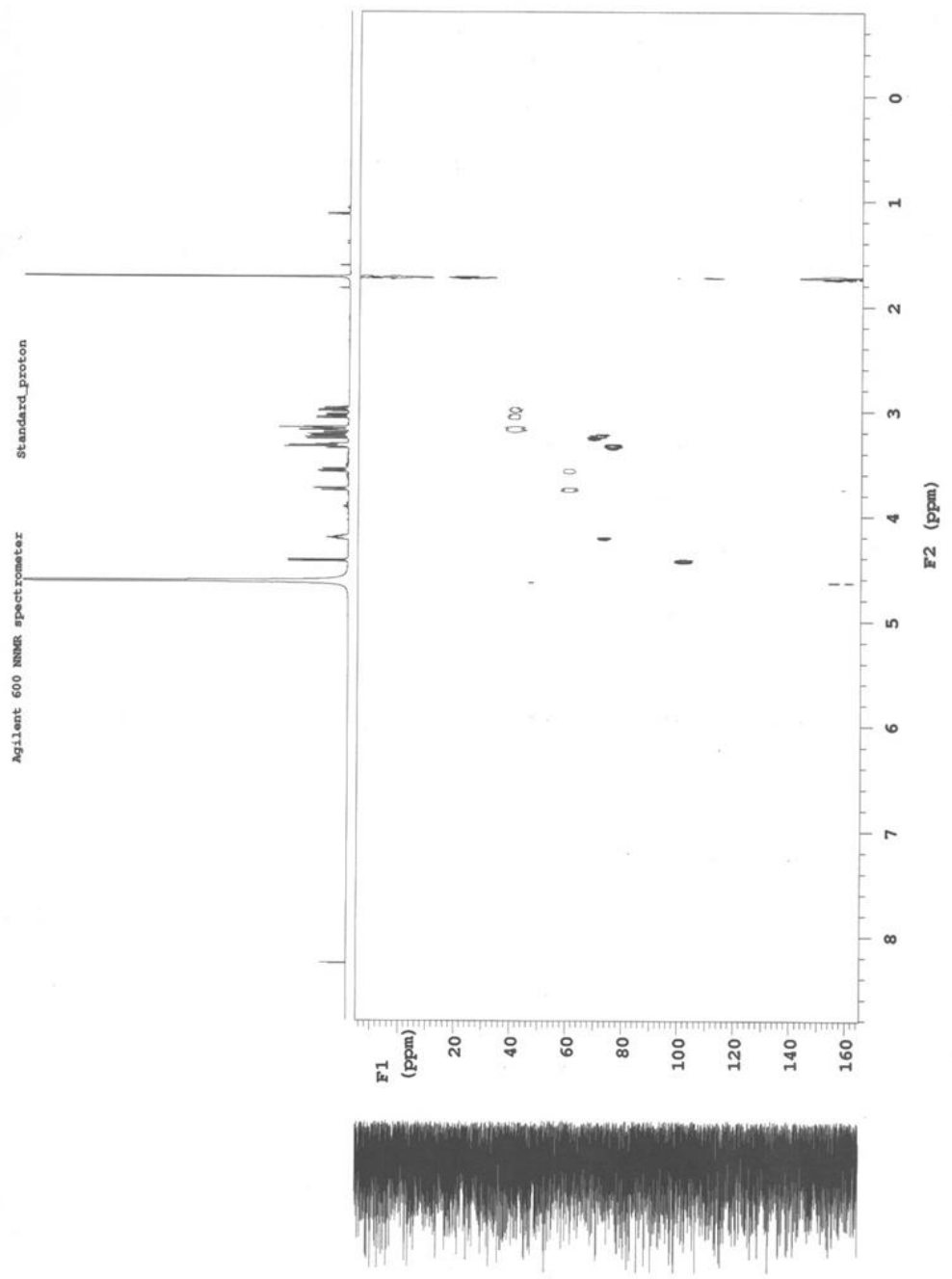

Figure A3. HSQC spectrum of compound 4.

Figure A4. ^{1}H-NMR spectrum of compound 5.

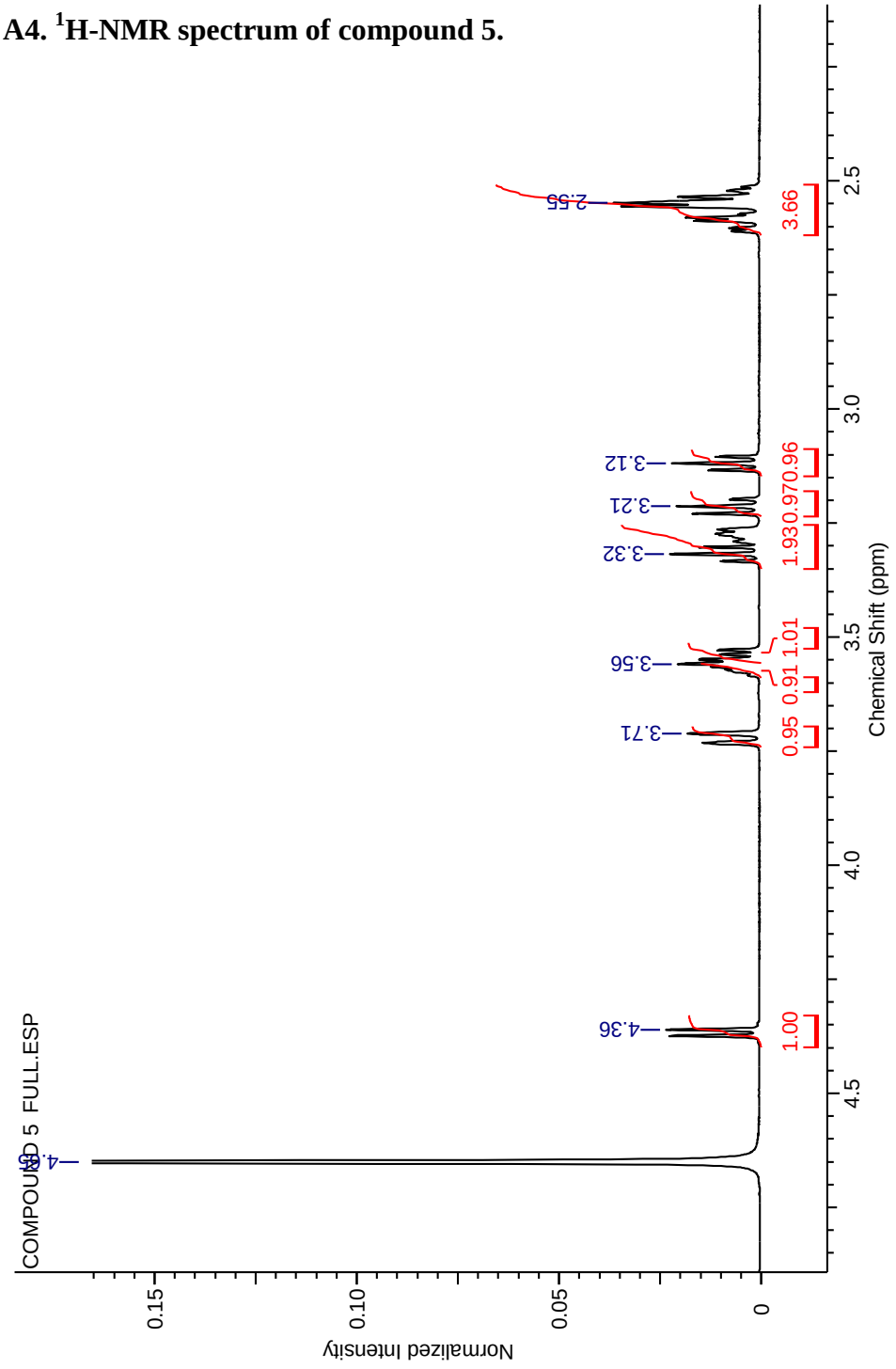

APPENDIX B

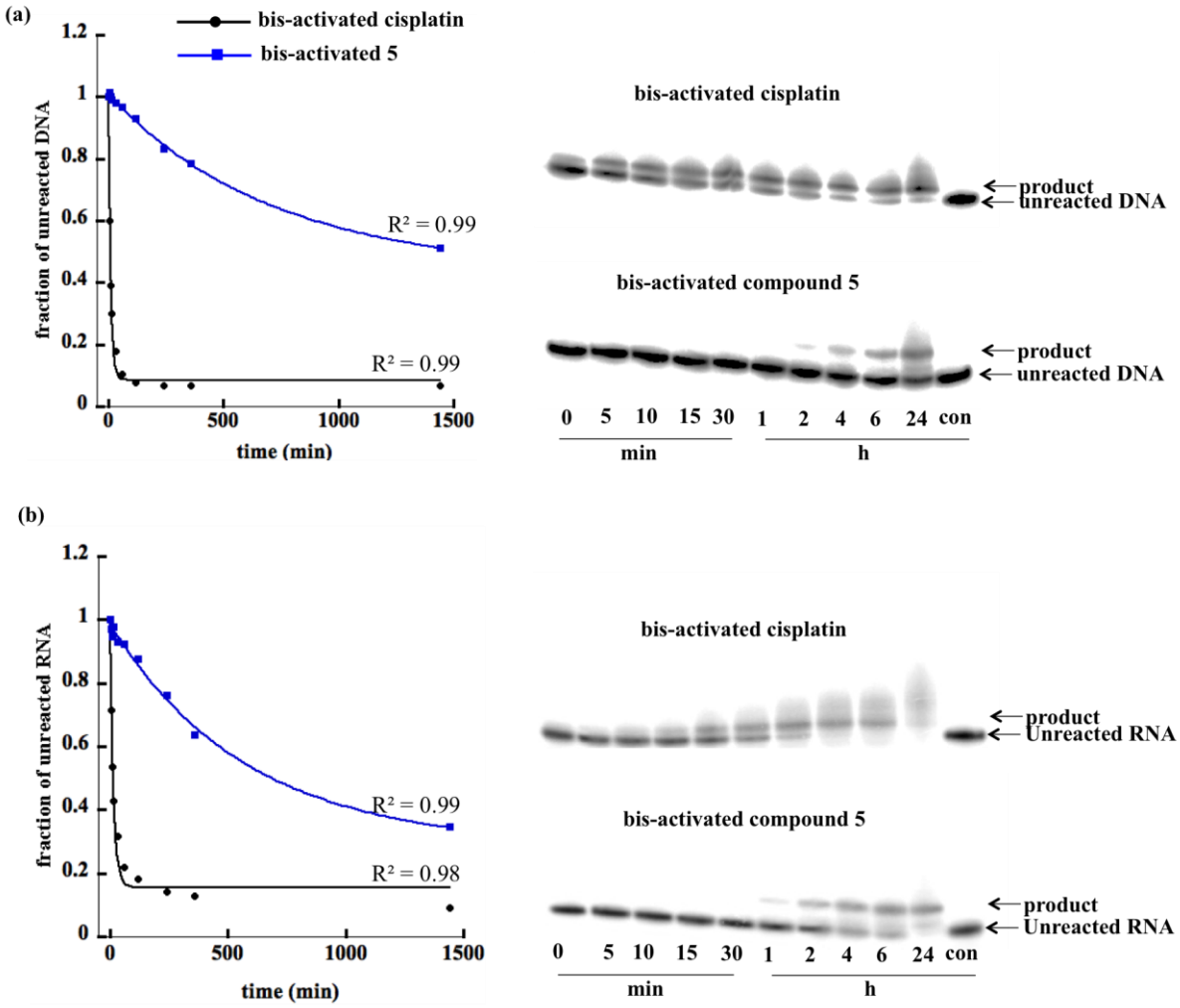

Figure B1. Representative results for the reactions of bis-activated Pt(II) complexes with DNA, RNA. Plots and gels for the reactions of bis-activated Pt(II) complexes with (a) DNA and (b) RNA are shown. The fraction of unreacted nucleic acid over time showed an exponential decay. ([DNA or RNA] = 0.7 μM, [Pt(II)] = 94 μM; 10 mM K_2HPO_4/KH_2PO_4, pH 6.2, with 20 mM $NaClO_4$, 37 °C).

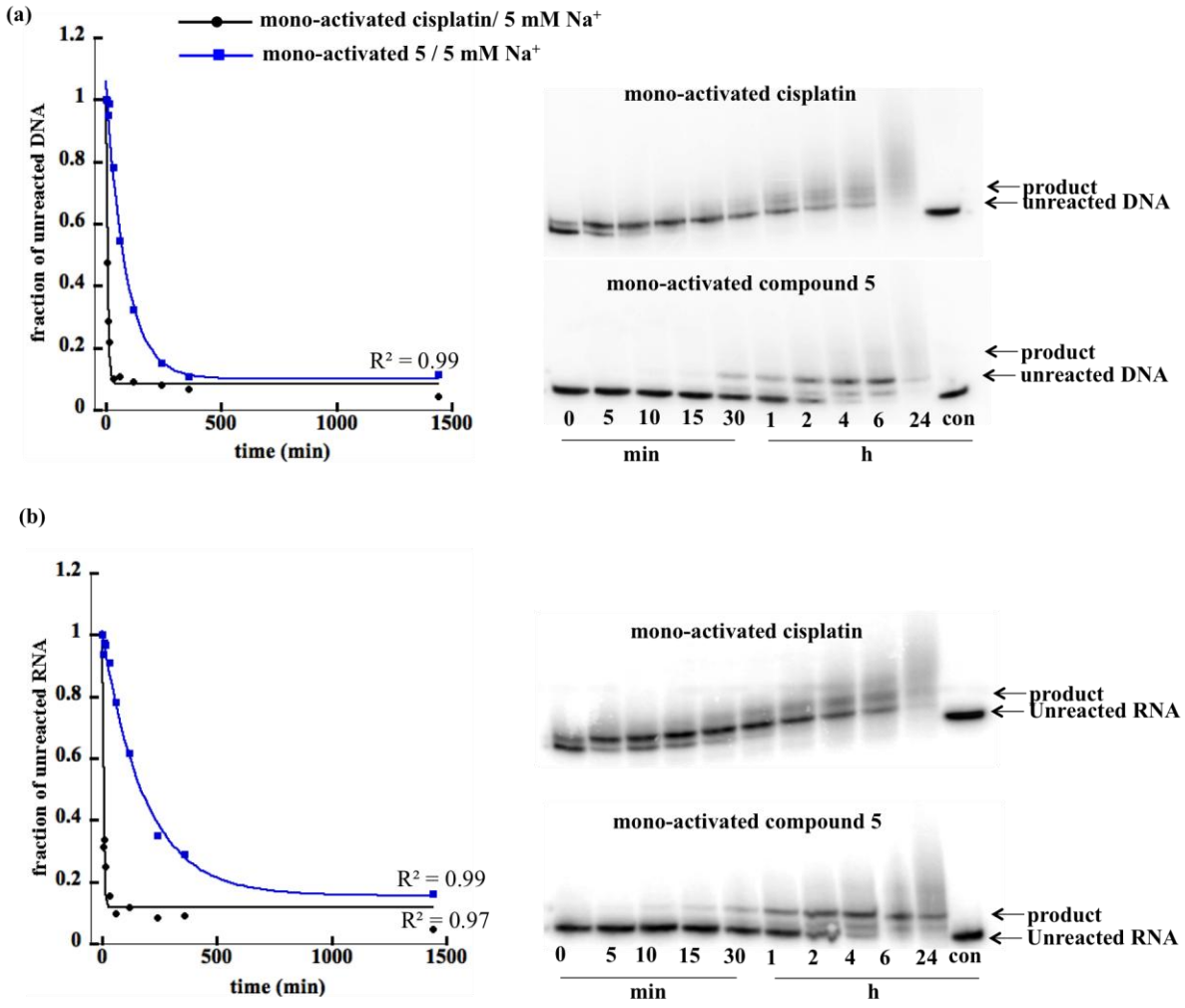

Figure B2. Representative results for the salt-dependent kinetic experiment of mono-activated Pt(II) complexes with DNA, RNA. Plots and gels for the reactions of bis-activated Pt(II) complexes with (a) DNA and (b) RNA are shown. The fraction of unreacted nucleic acid over time showed an exponential decay. The experiments were carried out with lower Na^+ concentration with [DNA or RNA] = 0.7 μM, [Pt(II)] = 94 μM; 10 mM K_2HPO_4/KH_2PO_4, pH 6.2, with 5 mM $NaClO_4$ at 37 °C.

REFERENCES

(1) Wang, D.; Lippard, S. J. *Nat Rev Drug Discov.* **2005**, *4*, 307.

(2) Prestayko, A. W.; D'Aoust, J. C.; Issell, B. F.; Crooke, S. T. *Cancer Treat Rev.* **1979**, *6*, 17.

(3) Jamieson, E. R.; Lippard, S. J. *Chem Rev.* **1999**, *99*, 2467.

(4) Gottlieb, J. A.; Drewinko, B. *Cancer Chemother Rep.* **1975**, *59*, 621.

(5) Galluzzi, L.; Senovilla, L.; Vitale, I.; Michels, J.; Martins, I.; Kepp, O.; Castedo, M.; Kroemer, G. *Oncogene* **2012**, *31*, 1869.

(6) Shen, D. W.; Pouliot, L. M.; Hall, M. D.; Gottesman, M. M. *Pharmacol Rev.* **2012**, *64*, 706.

(7) Johnstone, T. C.; Suntharalingam, K.; Lippard, S. J. *Chem Rev.* **2016**, *116*, 3436.

(8) Rosenberg, B.; VanCamp, L.; Krigas, T. *Nature.* **1965**, *205*, 698.

(9) Rosenberg, B.; Renshaw, E.; Vancamp, L.; Hartwick, J.; Drobnik, J. *J Bacteriol.* **1967**, *93*, 716.

(10) Rosenberg, B.; VanCamp, L. *Cancer Res.* **1970**, *30*, 1799.

(11) Kelland, L. *Nat Rev Cancer.* **2007**, *7*, 573.

(12) Eastman, A. *Cisplatin : Chemistry and Biochemistry of a Leading Anticancer Drug*; Verlag Helvetica Chimica Acta: Zürich, 1999.

(13) Gately, D. P.; Howell, S. B. *Br J Cancer.* **1993**, *67*, 1171.

(14) Ishida, S.; Lee, J.; Thiele, D. J.; Herskowitz, I. *Proc Natl Acad Sci U S A.* **2002**, *99*, 14298.

(15) Bancroft, D. P.; Lepre, C. A.; Lippard, S. J. *J Am Chem Soc.* **1990**, *112*, 6860.

(16) Hindmarsh, K.; House, D. A.; Turnbull, M. M. *Inorg Chim Acta.* **1997**, *257*, 11.

(17) Jung, Y.; Lippard, S. J. *Chem Rev.* **2007**, *107*, 1387.

(18) Sherman, S. E.; Gibson, D.; Wang, A. H.; Lippard, S. J. *Science.* **1985**, *230*, 412.

(19) Kartalou, M.; Essigmann, J. M. *Mutat Res.* **2001**, *478*, 1.

(20) Vaisman, A.; Lim, S. E.; Patrick, S. M.; Copeland, W. C.; Hinkle, D. C.; Turchi, J. J.; Chaney, S. G. *Biochemistry.* **1999**, *38*, 11026.

(21) Reslova, S. *Chem Biol Interact.* **1971**, *4*, 66.

(22) Brouwer, J.; van de Putte, P.; Fichtinger-Schepman, A. M.; Reedijk, J. *Proc Natl Acad Sci U S A.* **1981**, *78*, 7010.

(23) Fichtinger-Schepman, A. M. J.; van Oosterom, A. T.; Lohman, P. H. M.; Berends, F. *Cancer Res.* **1987**, *47*, 3000.

(24) Bellon, S. F.; Lippard, S. J. *Biophys Chem.* **1990**, *35*, 179.

(25) Stehlikova, K.; Kostrhunova, H.; Kasparkova, J.; Brabec, V. *Nucleic Acids Res.* **2002**, *30*, 2894.

(26) Coste, F.; Malinge, J.-M.; Serre, L.; Leng, M.; Zelwer, C. *Nucl Acids Res.* **1999**, *27*, 1837.

(27) Harder, H. C.; Smith, R. G.; Leroy, A. F. *Cancer Res.* **1976**, *36*, 3821.

(28) Comess, K. M.; N., B. J.; F., E. J.; Lippard, S. J. *Biochemistry.* **1992**, *32*, 3975.

(29) Lemaire, M. A.; Schwartz, A.; Rahmouni, A. R.; Leng, M. *Proc Natl Acad Sci U S A.* **1991**, *88*, 1982.

(30) Kimura, H.; Tao, Y.; Roeder, R. G.; Cook, P. R. *Mol Cell Biol.* **1999**, *19*, 5383.

(31) Svejstrup, J. Q. *Nat Rev Mol Cell Biol.* **2002**, *3*, 21.

(32) Kornberg, R. D. *Science.* **1974**, *184*, 868.

(33) Bubley, G. J.; Xu, J.; Kupiec, N.; Sanders, D.; Foss, F.; O'Brien, M.; Emi, Y.; Teicher, B. A.; Patierno, S. R. *Biochem Pharmacol.* **1996**, *51*, 717.

(34) Mymryk, J. S.; Zaniewski, E.; Archer, T. K. *Proc Natl Acad Sci U S A.* **1995**, *92*, 2076.

(35) Wang, D.; Lippard, S. J. *J Biol Chem.* **2004**, *279*, 20622.

(36) Danford, A. J.; Wang, D.; Wang, Q.; Tullius, T. D.; Lippard, S. J. *Proc Natl Acad Sci U S A.* **2005**, *102*, 12311.

(37) Charlet-Berguerand, N.; Feuerhahn, S.; Kong, S. E.; Ziserman, H.; Conaway, J. W.; Conaway, R.; Egly, J. M. *EMBO J.* **2006**, *25*, 5481.

(38) Furuta, T.; Ueda, T.; Aune, G.; Sarasin, A.; Kraemer, K. H.; Pommier, Y. *Cancer Res.* **2002**, *62*, 4899.

(39) Karasawa, T.; Sibrian-Vazquez, M.; Strongin, R. M.; Steyger, P. S. *PLoS One.* **2013**, *8*, e66220.

(40) Melnikov, S. V.; Söll, D.; Steitz, T. A.; Polikanov, Y. S. *Nucleic Acids Res.* **2016**, *44*, 4978.

(41) Speelmans, G.; Sips, W. H. H. M.; Grisel, R. J. H.; Staffhorst, R. W. H. M.; Fichtinger-Schepman, A. M. J.; Reedijk, J.; de Kruijff, B. *Biochim Biophys Acta.* **1996**, *1283*, 60.

(42) Dedduwa-Mudalige, G. N. P.; Chow, C. S. *Int J Mol Sci.* **2015**, *16*, 21392.

(43) Rijal, K.; Chow, C. S. *Chem Commun.* **2008**, 109.

(44) Papsai, P.; Aldag, J.; Persson, T.; Elmroth, S. K. C. *Dalton Trans.* **2006**, 3515.

(45) Papsai, P.; Snygg, Å. S.; Aldag, J.; Elmroth, S. K. C. *Dalton Trans.* **2008**, 5225.

(46) Hostetter, A. A.; Osborn, M. F.; DeRose, V. J. *ACS Chem Biol.* **2012**, *7*, 218.

(47) Meroueh, M.; Kjellström, J.; Mårtensson, K. S. M.; Elmroth, S. K. C.; Chow, C. S. *Inorg Chim Acta.* **2000**, *297*, 145.

(48) Alshiekh, A.; Clausen, M.; Elmroth, S. K. C. *Dalton Trans.* **2015**, *44*, 12623.

(49) Bernges, F.; Holler, E. *Nucleic Acids Res.* **1991**, *19*, 1483.

(50) Dedduwa-Mudalige, N. G. Ph.D. Dissertation, Wayne State University, 2015.

(51) Hägerlöf, M.; Papsai, P.; Chow, C. S.; Elmroth, S. K. C. *J Biol Inorg Chem.* **2006**, *11*, 974.

(52) M., S.; Jr, R.; Rao, S. T. *Prog Clin Biol Res.* **1985**, *172B*, 175.

(53) Rosenberg, J.; Sato, P. *Mol Pharmacol.* **1988**, *33*, 611.

(54) Hostetter, A. A.; Chapman, E. G.; DeRose, V. J. *J Am Chem Soc.* **2009**, *131*, 9250.

(55) Chapman, E. G.; DeRose, V. J. *J Am Chem Soc.* **2012**, *134*, 256.

(56) Burger, A. M.; Double, J. A.; Newell, D. R. *Eur J Cancer.* **1997**, *33*, 638.

(57) Dasari, S.; Tchounwou, P. B. *Eur J Pharmacol.* **2014**, *740*, 364.

(58) Siddik, Z. H. *Oncogene.* **2002**, *22*, 7265.

(59) Giaccone, G. *Drugs.* **2000**, *59*, 9.

(60) Stordal, B.; Davey, M. *IUBMB Life* **2007**, *59*, 696.

(61) Cui, Y.; König, J.; Buchholz, U.; Spring, H.; Leier, I.; Keppler, D. *Mol Pharmacol.* **1999**, *55*, 929.

(62) Nakayama, K.; Kanzaki, A.; Ogawa, K.; Miyazaki, K.; Neamati, N.; Takebayashi, Y. *Int J Cancer.* **2002**, *101*, 488.

(63) Ho, T. *Chem Rev.* **1975**, *75*, 1.

(64) Kelland, L. R. *Crit Rev Oncol Hematol.* **1993**, *15*, 191.

(65) Wolf, C. R.; Hayward, I. P.; Lawrie, S. S.; Buckton, K.; McIntyre, M. A.; Adams, D. J.; Lewis, A. D.; Scott, A. R. R.; Smyth, J. F. *Int J Cancer.* **1987**, *39*, 695.

(66) Kelley, S. L.; Basu, A.; Teicher, B. A.; Hacker, M. P.; Hamer, D. H.; Lazo, J. S. *Science.* **1988**, *241*, 1813.

(67) Hamaguchi, K.; Godwin, A. K.; Yakushiji, M.; Dwyer, P. J.; Ozols, R. F.; Hamilton, T. C. *Cancer Res.* **1993**, *53*, 5225.

(68) Slater, A. F.; Nobel, C. S.; Maellaro, E.; Bustamante, J.; Kimland, M.; Orrenius, S. *Biochem J.* **1995**, *306 (Pt 3)*, 771.

(69) Dabholkar, M.; Vionnet, J.; Bostick-Bruton, F.; Yu, J. J.; Reed, E. *J Clin Invest.* **1994**, *94*, 703.

(70) Sawant, A.; Kothandapani, A.; Zhitkovich, A.; Sobol, R. W.; Patrick, S. M. *DNA Repair (Amst).* **2015**, *35*, 126.

(71) Fink, D.; Aebi, S.; Howell, S. B. *Clin Cancer Res.* **1998**, *4*, 1.

(72) Kothandapani, A.; Sawant, A.; Dangeti, V. S. M. N.; Sobol, R. W.; Patrick, S. M. *Nucleic Acids Res.* **2013**, *41*, 7332.

(73) Wilson, J. J.; Lippard, S. J. *Chem Rev.* **2014**, *114*, 4470.

(74) Harrap, K. R. *Cancer Treat Rev.* **1985**, *12*, 21.

(75) Muggia, F. M.; Bonetti, A.; Hoeschele, J. D.; Rozencweig, M.; Howell, S. B. *J Clin Oncol.* **2015**, *33*, 4219.

(76) Ho, G. Y.; Woodward, N.; Coward, J. I. G. *Crit Rev Oncol Hematol.* **2016**, *102*, 37.

(77) Graham, J.; Muhsin, M.; Kirkpatrick, P. *Nat Rev Drug Discov.* **2004**, *3*, 11.

(78) Lebwohl, D.; Canetta, R. *Eur J Cancer.* **1998**, *34*, 1522.

(79) Shimada, M.; Itamochi, H.; Kigawa, J. *Cancer Manag Res.* **2013**, *5*, 67.

(80) Reddy, B.; Venkata, P.; Mukherjee, S.; Mitra, I.; Moi, S. *Chem Phys Lett.* **2017**, *690*, 105.

(81) Liu, P.; Lu, Y.; Gao, X.; Liu, R.; Zhang-Negrerie, D.; Shi, Y.; Wang, Y.; Wang, S.; Gao, Q. *Chem Comm.* **2013**, *49*, 2421.

(82) Chen, Y.; Heeg, M. J.; Braunschweiger, P. G.; Xie, W.; Wang, P. G. *Angew Chem Int Ed.* **1999**, *38*, 1768.

(83) Patra, M.; Johnstone, T. C.; Suntharalingam, K.; Lippard, S. J. *Angew Chem Int Ed Engl.* **2016**, *55*, 2550.

(84) Tsubomura, T.; Yano, S.; Kobayashi, K.; Sakurai, T.; Yoshikawa, S. *J Chem Soc.* **1986**, 459.

(85) Gabano, E.; Cassino, C.; Bonetti, S.; Prandi, C.; Colangelo, D.; Ghiglia, A.; Osella, D. *Org Biomol Chem.* **2005**, *3*, 3531.

(86) Knight, W. A.; Livingston, R. B.; Gregory, E. J.; McGuire, W. L. *Cancer Res.* **1977**, *37*, 4669.

(87) Lee, M.; Simpson, J. E.; Burns, A. J.; Kupchinsky, S.; Brooks, N.; Hartley, J. A.; Kelland, L. R. *Med Chem Res.* **1996**, *6*, 365.

(88) Rijal, K.; Bao, X.; Chow, C. S. *Chem Commun.* **2014**, 3918.

(89) Cubo, L.; Groessl, M.; Dyson, P. J.; Quiroga, A. G.; Navarro-Ranninger, C.; Casini, A. *ChemMedChem.* **2010**, *5*, 1335.

(90) Lovejoy, K. S.; Lippard, S. J. *Dalton Trans.* **2009**, 10651.

(91) Zou, Y.; Van Houten, B.; Farrell, N. P. *Biochemistry.* **1994**, *33*, 5404.

(92) Brabec, V.; Kašpárková, J.; Vrána, O.; Nováková, O.; Cox, J. W.; Qu, Y.; Farrell, N. *Biochemistry.* **1999**, *38*, 6781.

(93) Schilder, R. J.; LaCreta, F. P.; Perez, R. P.; Johnson, S. W.; Brennan, J. M.; Rogatko, A.; Nash, S.; McAleer, C.; Hamilton, T. C.; Roby, D.; Young, R. C.; Ozols, R. F.; Dwyer, P. J. *Cancer Res.* **1994**, *54*, 709.

(94) Wirth, R.; White, J. D.; Moghaddam, A. D.; Ginzburg, A. L.; Zakharov, L. N.; Haley, M. M.; DeRose, V. J. *J Am Chem Soc.* **2015**, *137*, 15169.

(95) Dedduwa-Mudalige, N. G.; Chow, C. S. *Int J Mol Sci.* **2015**, *16*.

(96) Montagner, D.; Yap, S. Q.; Ang, W. H. *Angew Chem Int Ed.* **2013**, *52*, 11785.

(97) Böttger, E. C. *Trends Biotechnol.* **2006**, *24*, 145.

(98) Ziehler, W. A.; Engelke, D. R. *Curr Protoc Nucleic Acid Chem.* **2001**, *0 6*, Unit.

(99) Ehresmann, C.; Baudin, F.; Mougel, M.; Romby, P.; Ebel, J. P.; Ehresmann, B. *Nucleic Acids Res.* **1987**, *15*, 9109.

(100) Brunel C, R. P. *Methods Enzymol.* **2000**, *318*, 3.

(101) Huntzinger, E.; Possedko, M.; Winter, F.; Moine, H.; Ehresmann, C.; Romby, P. *Handbook of RNA Biochemistry* **2008**.

(102) Krause, K. M.; Serio, A. W.; Kane, T. R.; Connolly, L. E. *Cold Spring Harb Perspect Med.* **2016**, *6*, a027029.

(103) Moazed, D.; Noller, H. F. *Nature.* **1987**, *327*, 389.

(104) Ogle, J. M.; Brodersen, D. E.; Clemons, W. M.; Tarry, M. J.; Carter, A. P.; Ramakrishnan, V. *Science.* **2001**, *292*, 897.

(105) Yoshizawa, S.; Fourmy, D.; Puglisi, J. D. *Science.* **1999**, *285*, 1722.

(106) Fourmy, D.; Recht, M. I.; Blanchard, S. C.; Puglisi, J. D. *Science.* **1996**, *274*, 1367.

(107) Wang, L.; Pulk, A.; Wasserman, M. R.; Feldman, M. B.; Altman, R. B.; Cate, J. H. D.; Blanchard, S. C. *Nat Struct Mol Biol.* **2012**, *19*, 957.

(108) Ogle, J. M.; Ramakrishnan, V. *Annu Rev Biochem.* **2005**, *74*, 129.

(109) Rodnina, M. V.; Wintermeyer, W. *Annu Rev Biochem.* **2001**, *70*, 415.

(110) Wasserman, M. R.; Pulk, A.; Zhou, Z.; Altman, R. B.; Zinder, J. C.; Green, K. D.; Garneau-Tsodikova, S.; Cate, J. H. D.; Blanchard, S. C. *Nat Commun.* **2015**, *6*, 7896.

(111) Borovinskaya, M. A.; Pai, R. D.; Zhang, W.; Schuwirth, B. S.; Holton, J. M.; Hirokawa, G.; Kaji, H.; Kaji, A.; Cate, J. H. D. *Nat Struct Mol Biol.* **2007**, *14*, 727.

(112) Scheunemann, A. E.; Graham, W. D.; Vendeix, F. A. P.; Agris, P. F. *Nucleic Acids Res.* **2010**, *38*, 3094.

(113) Cleare, M. J.; Hoeschele, J. D. *Bioinorg Chem.* **1973**, *2*, 187.

(114) Graham, J.; Muhsin, M.; Kirkpatrick, P. *Nat Rev Drug Discov.* **2004**, *3*, 11.

(115) Li, T.; Gao, X.; Yang, L.; Shi, Y.; Gao, Q. *Chem Med Chem.* **2016**, *11*, 1069.

(116) Barragán, F.; Moreno, V.; Marchán, V. *Chem Comm.* **2009**, 4705.

(117) Descôteaux, C.; Provencher-Mandeville, J.; Mathieu, I.; Perron, V.; Mandal, S.; Asselin, E.; Bérubé, G. *Bioorg Med Chem Lett.* **2003**, *13*, 3927.

(118) Vitols, K. S.; Montejano, Y.; Duffy, T.; Pope, L.; Grundler, G.; Huennekens, F. M. *Adv Enzyme Regul.* **1987**, *26*, 17.

(119) Hansen, M. R.; Hurley, L. H. *Acc Chem Res.* **1996**, *29*, 249.

(120) Chittapragada, M.; Roberts, S.; Ham, Y. W. *Perspect Medicin Chem.* **2009**, *3*, 21.

(121) Patra, M.; Awuah, S. G.; Lippard, S. J. *J Am Chem Soc.* **2016**, *138*, 12541.

(122) Cowan, J. A.; Ohyama, T.; Wang, D.; Natarajan, K. *Nucleic Acids Res.* **2000**, *28*, 2935.

(123) Stage, T. K.; Hertel, K. J.; Uhlenbeck, O. C. *RNA.* **1995**, *1*, 95.

(124) Rijal, K.; Chow, C. S. *Chem Commun.* **2009**, *1*, 107.

(125) Warburg, O.; Wind, F.; Negelein, E. *J Gen Physiol.* **1927**, *8*, 519.

(126) Effert, P.; Beniers, A. J.; Tamimi, Y.; Handt, S.; Jakse, G. *Anticancer Res.* **2004**, *24*, 3057.

(127) Correll, C. C.; Freeborn, B.; Moore, P. B.; Steitz, T. A. *Cell.* **1997**, *91*, 705.

(128) Helfer, A.-C.; Romilly, C.; Chevalier, C.; Lioliou, E.; Marzi, S.; Romby, P. *Handbook of RNA Biochemistry* **2014**.

(129) Mosmann, T. *J Immunol Methods.* **1983**, *65*, 55.

(130) Präbst, K.; Engelhardt, H.; Ringgeler, S.; Hübner, H. In *Cell Viability Assays: Methods and Protocols*; Gilbert, D. F., Friedrich, O., Eds.; Springer New York: New York, NY, 2017, p 1.

(131) Bao, X., Wayne State University, 2015.

(132) Lundblad, R. L.; Macdonald, F. *Handbook of Biochemistry and Molecular Biology*; CRC Press: Boca Raton, 2010.

(133) Kallansrud, G.; Ward, B. *Anal Biochem.* **1996**, *236*, 134.

(134) Lucey, B. P.; Nelson-Rees, W. A.; Hutchins, G. M. *Arch Pathol Lab Med.* **2009**, *133*, 1463.

(135) Cailleau, R.; Young, R.; Olivé, M.; Reeves, J. W. J. *J. Natl. Cancer Inst.* **1974**, *53*, 661.

(136) Cailleau, R.; Olive, M.; Cruciger, Q. V. *In Vitro.* **1978**, *14*, 911.

(137) Giaccone, G.; Battey, J.; Gazdar, A. F.; Oie, H.; Draoui, M.; Moody, T. W. *Cancer Res.* **1992**, *52*, 2732.

(138) Horoszewicz, J. S.; Leong, S. S.; Kawinski, E.; Karr, J. P.; Rosenthal, H.; Chu, T. M.; Mirand, E. A.; Murphy, G. P. *Cancer Res.* **1983**, *43*, 1809.

(139) Stone, K. R.; Mickey, D. D.; Wunderli, H.; Mickey, G. H.; Paulson, D. F. *Int J Cancer.* **1978**, *21*, 274.

(140) Bello, D.; Webber, M. M.; Kleinman, H. K.; Wartinger, D. D.; Rhim, J. S. *Carcinogenesis.* **1997**, *18*, 1215.

(141) Bruce, A. G.; Uhlenbeck, O. C. *Nucleic Acids Res.* **1978**, *5*, 3665.

(142) Sambrook, J.; Russell, D. W. *Cold Spring Harb Protoc.* **2006**, *2006*, pdb.prot2936.

(143) Richardson, C. C. In *The Enzymes*; Academic Press: 1981.

(144) Bellon, S. F.; Coleman, J. H.; Lippard, S. J. *Biochemistry.* **1991**, *30*, 8026.

(145) Koo, H. S.; Crothers, D. M. *Proc Natl Acad Sci U S A.* **1988**, *85*, 1763.

(146) Moazed, D.; Stern, S.; Noller, H. F. *J Mol Biol.* **1986**, *187*, 399.

(147) Riisom, M.; Gammelgaard, B.; Lambert, I. H.; Stürup, S. *J Pharm Biomed Anal.* **2018**, *158*, 144.

(148) Zhang, T.; Cai, S.; Forrest, W. C.; Mohr, E.; Yang, Q.; Forrest, M. L. *Appl Spectrosc.* **2016**, *70*, 1529.

(149) Tariman, J. D. *Nurs Clin North Am.* **2017**, *52*, 65.

(150) Christian, G. H.; Alexey, A. N.; Shaheen, M. A.; Paul, J. D.; Bernhard, K. K. *Curr Med Chem.* **2008**, *15*, 2574.

(151) Hartinger, C. G.; Nazarov, A. A.; Ashraf, S. M.; Dyson, P. J.; Keppler, B. K. *Curr Med Chem.* **2018**, *15*, 2574.

(152) Zhang, Y.; Wang, F. *Drug Discov Ther.* **2015**, *9*, 79.

(153) Klyosov, A. *Glycobiology and Drug Design*; American Chemical Society, 2013; Vol. 1102.

(154) Medina, R. A.; Owen, G. I. *Biol Res.* **2002**, *35*, 9.

(155) Cura, A. J.; Carruthers, A. *Compr Physiol.* **2012**, *2*, 863.

(156) Altenberg, B.; Greulich, K. O. *Genomics.* **2004**, *84*, 1014.

(157) Nangia-Makker, P.; Conklin, J.; Hogan, V.; Raz, A. *Trends Mol Med.* **2002**, *8*, 187.

(158) Berger, I.; Nazarov, A. A.; Hartinger, C. G.; Groessl, M.; Valiahdi, S.-M.; Jakupec, M. A.; Keppler, B. K. *Chem Med Chem.* **2007**, *2*, 505.

(159) Sachinvala, N. D.; Chen, H.; Niemczura, W. P.; Furusawa, E.; Cramer, R.; Rupp, J. J.; Ganjian, I. *J Med Chem.* **1993**, *36*, 1791.

(160) Zunino, F.; Savi, G.; Pasini, A. *Cancer Chemother Pharmacol.* **1986**, *18*, 180.

(161) Mikata, Y.; Shinohara, Y.; Yoneda, K.; Nakamura, Y.; Brudziñska, I.; Tanase, T.; Kitayama, T.; Takagi, R.; Okamoto, T.; Kinoshita, I.; Doe, M.; Orvig, C.; Yano, S. *Bioorg Med Chem Lett.* **2001**, *11*, 3045.

(162) Anas, N.; Naeema, R.; Rafik, K. *Curr Pharm Des.* **2017**, *23*, 2366.

(163) Ma, J.; Wang, Q.; Yang, X.; Hao, W.; Huang, Z.; Zhang, J.; Wang, X.; Wang, P. G. *Dalton Trans.* **2016**, *45*, 11830.

(164) Ma, J.; Wang, Q.; Huang, Z.; Yang, X.; Nie, Q.; Hao, W.; Wang, P. G.; Wang, X. *J. Med. Chem.* **2017**, *60*, 5736.

(165) Liu, R.; Fu, Z.; Zhao, M.; Gao, X.; Li, H.; Mi, Q.; Liu, P.; Yang, J.; Yao, Z.; Gao, Q. *Oncotarget.* **2017**, *8*, 39476.

(166) Davies, M. S.; Berners-Price, S. J.; Hambley, T. W. *J Am Chem Soc.* **1998**, *120*, 11380.

(167) Baik, M.-H.; Friesner, R. A.; Lippard, S. J. *J Am Chem Soc.* **2003**, *125*, 14082.

(168) Chen, Y.; Guo, Z.; Parsons, S.; Sadler, P. J. *Chem Eur J.* **1998**, *4*, 672.

(169) Saad, J. S.; Benedetti, M.; Natile, G.; Marzilli, L. G. *Inorg Chem.* **2010**, *49*, 5573.

(170) Sigel, A.; Sigel, H.; Sigel, R. K. *Met Ions Life Sci.* **2011**, *9*, 7.

(171) Sherman, S. E.; Lippard, S. J. *Chem Rev.* **1987**, *87*, 1153.

(172) Kozelka, J.; Legendre, F.; Reeder, F.; Chottard, J. C. *Coord Chem Rev.* **1999**, *190-192*, 61.

(173) Fichtinger-Schepman, A. M. J.; Lohman, P. H. M.; Reedijk, J. *Nucleic Acids Res.* **1982**, *10*, 5345.

(174) Monjardet-Bas, V.; Elizondo-Riojas, M. A.; Chottard, J. C.; Kozelka, J. *Angew Chem Int Ed Engl.* **2002**, *41*, 2998.

(175) Reeder, F.; Gonnet, F.; Kozelka, J.; Chottard, J. C. *Chem Eur J.* **1996**, *2*, 1068.

(176) Kjellström, J.; Elmroth, S. K. C. *Chem Comm.* **1997**, 1701.

(177) Sykfont Snygg, Å.; Brindell, M.; Stochel, G.; Elmroth, S. K. C. *Dalton Trans.* **2005**, 1221.

(178) Cohen, G. L.; Bauer, W. R.; Barton, J. K.; Lippard, S. J. *Science.* **1979**, *203*, 1014.

(179) Macquet, J. P.; Butour, J. L. *Biochimie.* **1978**, *60*, 901.

(180) Rice, J. A.; Crothers, D. M.; Pinto, A. L.; Lippard, S. J. *Proc Natl Acad Sci U S A.* **1988**, *85*, 4158.

(181) M., T. P.; C., R. A.; A., F. C.; J., L. S. *Nature.* **1995**, *377*, 649.

(182) Kozelka, J.; Archer, S.; Petsko, G. A.; Lippard, S. J.; Quigley, G. J. *Biopolymers.* **1987**, *26*, 1245.

(183) Takahara, P. M.; Frederick, C. A.; Lippard, S. J. *J Am Chem Soc.* **1996**, *118*, 12309−12321.

(184) Johnson, N. P.; Mazard, A. M.; Escalier, J.; Macquet, J. P. *J Am Chem Soc.* **1985**, *107*, 6376.

(185) Caradonna, J. P.; Lippard, S. J. *Inorg Chem.* **1988**, *27*, 1454.

(186) Osborn, M. F.; White, J. D.; Haley, M. M.; DeRose, V. J. *ACS Chem Bio.* **2014**, *9*, 2404.

(187) Chapman, E. G.; Hostetter, A. A.; Osborn, M. F.; Miller, A. L.; DeRose, V. J. *Binding of Kinetically Inert Metal Ions to RNA: the Case of Platinum(II)*; RSC publishing, 2011.

(188) Reedijk, J. *Proc Natl Acad Sci U S A.* **2003**, *100*, 3611.

(189) Hagrman, D.; Goodisman, J.; Souid, A.-K. *J Pharmacol Exp Ther.* **2004**, *308*, 658.

(190) Chen, Y.; Guo, Z.; Parkinson, J. A.; Sadler, P. J. *Dalton Trans.* **1998**, 3577.

(191) Lovejoy, K. S.; Serova, M.; Bieche, I.; Emami, S.; D'Incalci, M.; Broggini, M.; Erba, E.; Gespach, C.; Cvitkovic, E.; Faivre, S.; Raymond, E.; Lippard, S. J. *Mol Cancer Ther.* **2011**, *10*, 1709.

(192) Chin, K.; Sharp, K. A.; Honig, B.; Pyle, A. M. *Nat Struct Biol.* **1999**, *6*, 1055.

(193) Cate, J. H.; Doudna, J. A. *Structure.* **1996**, *4*, 1221.

(194) Legendre, F.; Bas, V.; Kozelka, J.; Chottard, J. C. *Chemistry.* **2000**, *6*, 2002.

(195) Sykfont, Å.; Ericson, A.; Elmroth, S. K. C. *Chem Comm.* **2001**, 1190.

(196) Koo, H.-S.; Wu, H.-M.; Crothers, D. M. *Nature.* **1986**, *320*, 501.

(197) Koo, H. S.; Drak , J.; Rice, J. A.; Crothers, D. M. *Biochemistry.* **1990**, *29*, 4227.

(198) Levene, S. D.; Wu, H. M.; Crothers, D. M. *Biochemistry.* **1986**, *25*, 3988.

(199) Urata, H.; Akagi, M. *Biochem Biophys Res Commun.* **1989**, *161*, 819.

(200) Spingler, B.; Whittington, D. A.; Lippard, S. J. *Inorg Chem.* **2001**, *40*, 5596.

(201) Utku, S.; Özçelik, A. B.; Gümüş, F.; Yılmaz, Ş.; Arsoy, T.; Açık, L.; Çelebi Keskin, A. *J Pharm Pharmacol.* **2014**, *66*, 1593.

(202) Woese, C. R.; Magrum, L. J.; Gupta, R.; Siegel, R. B.; Stahl, D. A.; Kop, J.; Crawford, N.; Brosius, J.; Gutell, R.; Hogan, J. J.; Noller, H. F. *Nucleic Acids Res.* **1980**, *8*, 2275.

(203) Muralikrishna, P.; Wickstrom, E. *Biochemistry.* **1989**, *28*, 7505.

(204) Dibrov, S. M.; Parsons, J.; Hermann, T. *Nucleic Acids Res.* **2010**, *38*, 4458.

(205) Yusupov, M. M.; Yusupova, G. Z.; Baucom, A.; Lieberman, K.; Earnest, T. N.; Cate, J. H. D.; Noller, H. F. *Science.* **2001**, *292*, 883.

(206) Wilson, D. N.; Schluenzen, F.; Harms, J. M.; Yoshida, T.; Ohkubo, T.; Albrecht, R.; Buerger, J.; Kobayashi, Y.; Fucini, P. *EMBO J.* **2005**, *24*, 251.

(207) Dunkle, J. A.; Xiong, L.; Mankin, A. S.; Cate, J. H. D. *Proc Natl Acad Sci U S A.* **2010**, *107*, 17152.

(208) Rijal, K. Ph.D. Dissertation, Wayne State University, 2011.

(209) Varani, G.; McClain, W. H. *EMBO Rep.* **2000**, *1*, 18.

(210) Costa, M.; Michel, F.; Westhof, E. *EMBO J.* **2000**, *19*, 5007.

(211) Han, J.; Gao, X.; Liu, R.; Yang, J.; Zhang, M.; Mi, Y.; Shi, Y.; Gao, Q. *Chem Biol Drug Des.* **2015**, *87*, 867.

(212) Fanning, J.; Biddle, W. C.; Goldrosen, M.; Crickard, K.; Crickard, U.; Piver, M. S.; Foon, K. A. *Gynecol Oncol.* **1990**, *39*, 119.

(213) van Meerloo, J.; Kaspers, G. J. L.; Cloos, J. In *Cancer Cell Culture: Methods and Protocols*; Cree, I. A., Ed.; Humana Press: Totowa, NJ, 2011, p 237.

(214) Hall, W. A.; Huang, J.; Michael Li, Y.; Vallera, D. A. In *Brain Metastases from Primary Tumors*; Hayat, M. A., Ed.; Academic Press: San Diego, 2014, p 157.

(215) Stepanenko, A. A.; Dmitrenko, V. V. *Gene.* **2015**, *574*, 193.

(216) Silva, H.; Barra, C. V.; Rocha, F. V.; Frézard, F.; Lopes, M. T. P.; Fontes, A. P. S. *J Braz Chem Soc.* **2010**, *21*, 1961.

(217) Huang, R.; Sun, Y.; Gao, Q.; Wang, Q.; Sun, B. *Anticancer Drugs.* **2015**, *9*, 957.

(218) Navanesan, S.; Wahab, N. A.; Manickam, S.; Sim, K. S. *BMC Complement Altern Med.* **2015**, *15*, 186.

(219) Ambrosini, G.; Sambol, E. B.; Carvajal, D.; Vassilev, L. T.; Singer, S.; Schwartz, G. K. *Oncogene.* **2006**, *26*, 3473.

(220) Imrali, A.; Mao, X.; Yeste-Velasco, M.; Shamash, J.; Lu, Y. *Am J Cancer Res.* **2016**, *6*, 1772.

(221) Lamichhane, N.; Dewkar, G. K.; Sundaresan, G.; Wang, L.; Jose, P.; Otabashi, M.; Morelle, J. L.; Farrell, N.; Zweit, J. *J Nucl Med.* **2017**, *58*, 1997.

(222) Štarha, P.; Trávníček, Z.; Dvořák, Z.; Radošová-Muchová, T.; Prachařová, J.; Vančo, J.; Kašpárková, J. *PLOS ONE.* **2015**, *10*, e0123595.

(223) Witham, J.; Valenti, M.; De Haven Brandon, A.; Vidot, S.; Eccles, S.; B Kaye, S.; Richardson, A. *Clin cancer res.* **2008**, *13*, 7191.

(224) Štarha, P.; Vančo, J.; Trávníček, Z.; Hošek, J.; Klusáková, J.; Dvořák, Z. *PLOS ONE.* **2016**, *11*, e0165062.

(225) Park, G. Y.; Wilson, J. J.; Song, Y.; Lippard, S. J. *Proc Natl Acad Sci U S A.* **2012**, *109*, 11987.

(226) Warburg, O. *Science.* **1956**, *123*, 309.

(227) Liberti, M. V.; Locasale, J. W. *Trends Biochem Sci.* **2016**, *41*, 211.

(228) Braunschweiger, P. G.; Basrur, V. S.; Cameron, D.; Sharpe, L.; Santos, O.; Perras, J. P.; Sevin, B. U.; Markoe, A. M. *Biotherapy.* **1997**, *10*, 129.

(229) Egger, A. E.; Rappel, C.; Jakupec, M. A.; Hartinger, C. G.; Heffeter, P.; Keppler, B. K. *J Anal At Spectrom.* **2009**, *24*, 51.

(230) Pyle, A. *J. Biol. Inorg. Chem.* **2002**, *7*, 679.

(231) Baker, N. A.; Sept, D.; Joseph, S.; Holst, M. J.; McCammon, J. A. *Proc Natl Acad Sci U S A.* **2001**, *98*, 10037.

(232) Battiste, J. L.; Mao, H.; Rao, N. S.; Tan, R.; Muhandiram, D. R.; Kay, L. E.; Frankel, A. D.; Williamson, J. R. *Science.* **1996**, *273*, 1547.

(233) Tao, J.; Frankel, A. D. *Proc Natl Acad Sci U S A.* **1993**, *90*, 1571.

(234) Hostetter, A. A.; Osborn, M. F.; DeRose, V. J. *ACS Chem Biol.* **2012**, *7*, 218.

(235) Draper, D. E. *RNA.* **2004**, *10*, 335.

(236) Misra, V. K.; Draper, D. E. *J. Mol. Biol.* **2000**, *299*, 813.

(237) Casiano-Negroni, A.; Sun, X.; Al-Hashimi, H. M. *Biochemistry* **2007**, *46*, 6525.

(238) Mohanty, U.; Spasic, A.; Kim, H. D.; Chu, S. *J. Phys. Chem. B* **2005**, *109*, 21369.

(239) Woodson, S. A. *Curr. Opin. Chem. Biol.* **2005**, *9*, 104.

(240) Tan, Z.-J.; Chen, S.-J. *Biophys. J.* **2011**, *101*, 176.

(241) Mascotti, D. P.; Lohman, T. M. *Biochemistry* **1997**, *36*, 7272.

(242) García-García, C.; Draper, D. E. *J. Mol. Biol.* **2003**, *331*, 75.

(243) Casiano-Negroni, A.; Sun, X.; Al-Hashimi, H. M. *Biochemistry.* **2007**, *46*, 6525.

(244) Hendrix, M.; Priestley, E. S.; Joyce, G. F.; Wong, C.-H. *J Am Chem Soc.* **1997**, *119*, 3641.

(245) Kulik, M.; Goral, A. M.; Jasiński, M.; Dominiak, P. M.; Trylska, J. *Biophys J.* **2015**, *108*, 655.

(246) Sharp, K. A.; Honig, B.; Harvey, S. C. *Biochemistry.* **1990**, *29*, 340.

(247) Bakin, A.; Ofengand, J. *Biochemistry* **1993**, *32*, 9754.

(248) Abeysirigunawardena, S. C.; Chow, C. S. *RNA* **2008**, *14*, 782.

(249) Sakakibara, Y.; Chow, C. S. *ACS Chem. Biol.* **2012**, *7*, 871.

(250) Sakakibara, Y.; Chow, C. S. *J. Am. Chem. Soc.* **2011**, *133*, 8396.

(251) Greenbaum, N. In *Fine-Tuning of RNA Functions by Modification and Editing*; Grosjean, H., Ed.; Springer Berlin Heidelberg: 2005; Vol. 12, p 205.

(252) Mikkelsen, N. E.; Johansson, K.; Virtanen, A.; Kirsebom, L. A. *Nat Struct Mol Biol.* **2001**, *8*, 510.

(253) Sakakibara, Y., Wayne State University 2012.

(254) Sakakibara, Y.; Abeysirigunawardena, S. C.; Duc Anne-Cécile, E.; Dremann, D. N.; Chow, C. S. *Angew Chem Int Ed.* **2012**, *51*, 12095.

(255) Dilruba, S.; Kalayda, G. V. *Cancer Chemother Pharmacol.* **2016**, *77*, 1103.

ABSTRACT

INSIGHTS INTO NUCLEIC ACID-PLATINUM(II) COMPOUND INTERACTIONS AND STRUCTURAL IMPACTS

by

SUPUNI THALALLA GAMAGE

May 2019

Advisor: Dr. Christine S. Chow

Major: Chemistry (Biochemistry)

Degree: Doctor of Philosophy

With the discovery of cisplatin in the 1960s, it has been widely studied as a precursor for anticancer drug development. Despite its effectiveness against certain cancers, clinical usage of cisplatin is restricted by a number of side effects and resistance. In the past decade, scientists have been exploring biologically important ligands such as sugar derivatives in the hope of overcoming such challenges. Attachment of a sugar moiety could facilitate lower accumulation of platinum drugs in the body as well as enhance cellular uptake. In this study, a carbohydrate-linked cisplatin analog, *cis*-dichlorido[(2-*β*-D-glucopyranosidyl)propane-1,3-diammine]platinum (**5**) has been studied. The aim was to evaluate the impact of the carbohydrate moiety on the reaction kinetics with nucleosides, target site identification, structural impacts on oligonucleotides, and selective cancer cell targeting. All of the experiments in this thesis work were carried out in comparison to the parent compound cisplatin. Compound **5** was synthesized and a reactivity study was carried out with deoxy-/ribonucleosides and oligonucleotides using high performance liquid chromatography (HPLC) and liquid chromatography mass spectrometry (LC-MS). A series of gel-based kinetic experiment

was carried out comparing **5** and cisplatin with DNA and RNA oligos, with mono- and bis-activated complexes. A salt dependence kinetic study was also carried out to understand the contribution of electrostatics on the reactivity. A study was done to analyze the effects of compound **5** on DNA duplex structure by measuring the bending angles. Furthermore, probing studies on ribosomal RNA (rRNA) showed compound **5** localization on rRNA. The potency of the compound was assessed by MTT assays. Overall, mono-activated compound **5** showed preferred binding to G over dG, which is opposite of the preference of cisplatin for dG. A similar trend was observed for mono-activated **5** at the oligonucleotide level, in which RNA binding was preferred over DNA. However, in all the experiments, the reaction rate for mono- or bis-activated **5** was lower (≥2.5-fold) than that of aquated cisplatin. Data from the kinetic experiments suggest that the bulky carbohydrate ligand may play a role in reducing the reactivity of compound **5**. Salt dependence kinetic data suggested the RNA binding preference of **5** may come from its ability to form additional hydrogen-bonding interactions with the target compared to cisplatin. Therefore, glycoconjugation alters target specificity of the platinum compound. Furthermore, compound **5** formed platinum adducts that bend the DNA structure in a manner similar to cisplatin. Cell-based assays showed that **5** has selectivity towards glucose transporter (GLUT) overexpressing cancer cells (DU145) over normal cells (RWPE1). Overall, these findings support the potential of using glycoconjugated platinum complexes as lead compounds for anticancer drug development with controlled activity and target selectivity.

Electrostatics play an important role in RNA-ligand interactions. Positively charged drug molecules and other ligands are attracted to the negatively charged RNA.

Monovalent and divalent ions affect the electrostatic properties and influence these interactions; however, few methods exist to study these interactions in solution. This work focused on the use of cationic transition metal complexes as tools to study the electrostatic contributions of drug-RNA interactions. More specifically, positively charged mono-activated cisplatin and small model rRNA constructs were employed. The rates of the platination were determined by using gel shift analysis in the presence of different aminoglycosides. The rates of platination with RNA were shown to decrease in the presence of aminoglycosides, suggesting a competition between cisplatin and aminoglycosides to bind to the RNA. This work demonstrated the utility of monoaquated cisplatin kinetics as a tool to study RNA-aminoglycoside interactions. Overall, these findings are important for providing details on drug-RNA interactions, improving cationic drugs for nucleic acids, identifying unique RNA drug targets, and developing tools to investigate RNA microenvironments.

AUTOBIOGRAPHICAL STATEMENT

SUPUNI THALALLA GAMAGE

ADVISOR: Dr. Christine S. Chow

THESIS TITLE: INSIGHTS INTO NUCLEIC ACID-PLATINUM(II) COMPOUND INTERACTIONS AND STRUCTURAL IMPACTS

EDUCATION

- **Ph.D.; Biological Chemistry, 2019 May, Wayne State University, Detroit, MI, USA**
- **B.S. (First Class Honors); Chemical Biology, 2011, University of Colombo, Sri Lanka**

PUBLICATIONS

1. Muthunayake NS, Colangelo W, Thalalla Gamage S, Cunningham PR, Chow C, *In vivo* expression and ribosome mapping of peptide antibiotics in bacteria. Manuscript in preparation

2. Thalalla Gamage S, Dedduwa-Mudalige G, Elmroth SKC, Chow C, Electrostatics and salt-dependent cisplatin kinetics with ribosomal RNA hairpins reveal cisplatin as an electrostatic probe. Manuscript in preparation